

UC Santa Cruz

UC Santa Cruz Electronic Theses and Dissertations

Title

Kinetic, Mechanistic, and Structural Investigations of Human Lipoxygenases

Permalink

<https://escholarship.org/uc/item/0bw1m8nk>

Author

van Hoorebeke, Christopher Anthony

Publication Date

2022

Peer reviewed|Thesis/dissertation

UNIVERSITY OF CALIFORNIA
SANTA CRUZ

KINETIC, MECHANISTIC, AND STRUCTURAL INVESTIGATIONS OF
HUMAN LIPOXYGENASES

A dissertation submitted in partial satisfaction
of the requirements for the degree of

DOCTOR OF PHILOSOPHY

in

CHEMISTRY

by

Christopher A. van Hoorebeke

September 2022

The Dissertation of Christopher A. van Hoorebeke
is approved by:

Professor Michael Stone, Chair

Professor Theodore Holman

Professor Timothy Johnstone

Peter Biehl
Vice Provost and Dean of Graduate Studies

Copyright © by
Christopher A. van Hoorebeke
2022

Table of Contents

List of Figures.....	iv
List of Tables.....	v
List of Schemes.....	vi
Abstract.....	vii
Acknowledgements.....	ix
Chapter 1 Introduction.....	1
Chapter 2 Fatty acids negatively regulate platelet function through formation of noncanonical 15-lipoxygenase-derived eicosanoids.....	19
Chapter 3 Kinetic and mechanistic investigations of a lipoxygenase activator reveal isoform specificity and V-type activation.....	63
Chapter 4 Structural basis for altered positional specificity of 15-Lipoxygenase-1 with 5S-HETE and 7S-HDHA and the implications for the biosynthesis of Resolvin E4.....	99

List of Figures

Chapter 1

Figure 1.1.....	14
-----------------	----

Chapter 2

Figure 2.1.....	48
Figure 2.2.....	49
Figure 2.3.....	50
Figure 2.4.....	51
Figure 2.5.....	52
Figure 2.6.....	53
Figure 2.7.....	54

Chapter 3

Figure 3.1.....	82
Figure 3.2.....	82
Figure 3.3.....	83
Figure 3.4.....	84
Figure 3.5.....	85
Figure 3.6.....	88
Figure S3.1.....	89
Figure S3.2.....	90
Figure S3.3.....	90
Figure S3.4.....	91
Figure S3.5.....	92

Chapter 4

Figure 4.1.....	123
Figure 4.2.....	123
Figure 4.3.....	124
Figure 4.4.....	128
Figure 4.5.....	131
Figure S4.1.....	132

List of Tables

Chapter 1

Table 1.1.....	14
Table 1.2.....	14

Chapter 2

Table 2.1.....	44
Table 2.2.....	44
Table 2.3.....	45
Table 2.4.....	45

Chapter 3

Table 3.1.....	82
Table 3.2.....	83
Table 3.3.....	84
Table 3.4.....	85
Table 3.5.....	86

Chapter 4

Table 4.1.....	124
Table 4.2.....	125
Table 4.3.....	125
Table 4.4.....	125
Table 4.5.....	126
Table 4.6.....	126
Table 4.7.....	127
Table 4.8.....	128
Table 4.9.....	129
Table 4.10.....	129
Table 4.11.....	130

List of Schemes

Chapter 1

Scheme 1.1.....14

Chapter 3

Scheme 3.1.....87

Abstract
KINETIC, MECHANISTIC, AND STRUCTURAL INVESTIGATIONS OF
HUMAN LIPOXYGENASES

Christopher van Hoorebeke

The research contained in this dissertation examines the kinetic, mechanistic, and structural basis of human lipoxygenase (LOX) catalysis. LOX are found throughout the plant and animals kingdoms, and in humans LOX are involved in inflammatory signaling. Through this involvement in the inflammatory process and the ability to oxidize membrane bound polyunsaturated fatty acids (PUFA), LOX have been implicated in a variety of cancers and disease states. The impact of substrate saturation on platelet 12-LOX kinetics and mechanism was investigated in Chapter 2. The platelet signaling pathways and implications on platelet aggregation of these substrates were determined. Additionally, the novel allosteric effect of 15S-HpEPE on 12-LOX mechanism was probed. Chapter 3 scrutinized a previously discovered lipoxygenase activator. This dissertation works shows that the activator is LOX isoform specific, with only h15-LOX-1 being kinetically activated in the presence of the compound. Furthermore, the activator was found to activate the catalysis of shorter PUFA substrates, AA and LA, but not that of the longer SPM precursor, DHA. The implications of this finding has consequences on the potential therapeutic development of the activating compound. The effect on enzyme kinetics and mechanism was assayed, and a V-type activation was observed. Chapter 4 builds off of a previous discovery in our lab that demonstrated the altered positional specificity of h15-LOX-1 when reacting with the metabolites of 5-LOX. In this

chapter, site-directed mutagenesis was performed on key active site residues, with the kinetic and mechanistic implications of those residues determined experimentally. Additionally, the consequence of the altered positional specificity with regards to the biosynthesis of the potent SPM, Resolvin E₄, was examined.

Acknowledgements

I would like to begin by thanking my PhD advisor, Professor Theodore Holman, for believing in me back when I was an undergraduate researcher. You gave me the confidence to enter graduate school and it was an honor to earn my PhD under your leadership. You fostered an environment where I learned the skills that will allow me to provide for my family, and for that I am forever grateful. Next, I would like to thank my PhD dissertation committee members, Professors Michael Stone (Chair) and Timothy Johnstone, for the thoughtful insight and project management advice.

Next, I would like to thank all of my fellow graduate students in the Chemistry/CB3 programs. Although you are all busy with your own projects, you were always willing to help me and offer a fresh perspective. I am going to miss you Brother Pete. I have been blessed to share the Holman lab with great scientist and I am thankful for everything they have taught me, especially Steve, Josh, Ansari, and Michelle. Meesh, you have been a great lab mate and an even better friend. Thank you for always being there and for bringing me pastries that you usually end up eating the majority of.

Finally, I would like to thank my family. To my amazing fiancée, Jasmine: I am so lucky to have had you by my side for this entire journey. Your love and support has helped drive me to this point and given me the motivation to stick with it. Thank you for putting up with me during the COVID lockdown, I know I can be hard to handle at times. Taylor, thank you for being the best brother a brother could have. I

know I always have someone I can reach out to when times are tough. Last but not least I need to acknowledge my mother, Melodee. You sacrificed so much to give Taylor and I the education you thought would allow us to live a better life and you motivated me to pursue this PhD. Thank you for all of your love and support.

Chapter 1

INTRODUCTION

1.1 Lipoxygenase

Lipoxygenases (LOX) are a family of non-heme iron containing enzymes that are found in great abundance throughout the animal and plant kingdom¹, and have recently been characterized in certain bacteria². LOX primarily catalyze the dioxygenation of polyunsaturated fatty acids (PUFA) containing a 1,4 cis-cis pentadiene moiety¹. Arachidonic acid (AA, C₂₀ Δ₄, n-6) and linoleic acid (LA, C₁₈ Δ₂, n-6) are the most abundant and common LOX PUFA substrates in mammals and humans. The human genome encompasses six known operative LOX genes¹ (ALOXE3, ALOX5, ALOX12B, ALOX12, ALOX15, ALOX15B) encoding for the six different LOX isoforms (eLOX3, h5-LOX, h12R-LOX, h12-LOX, h15-LOX-1, h15-LOX-2, respectively). LOX isoforms are named based on the location (carbon number) of the enzymatic molecular oxygen insertion with the canonical substrate, AA (**Figure 1.1**). The primary LOX reaction involves the abstraction of a bis-allylic hydrogen from the previously mentioned 1,4 cis-cis pentadiene moiety. Following hydrogen abstraction and local radical rearrangement, molecular oxygen, believed to have traveled through an oxygen channel, is inserted two carbons away from the site of abstraction, thus generating a hydroperoxide product (HpETE). The hydroperoxide products generated are in the *S* chirality except for the h12R-LOX isoform which creates a product in the *R* chirality. One of the major difficulties in studying LOX is that a single isoform can react with a multitude of substrates,

leading to a variety of products. While h5-LOX reacts with AA to form 100% 5S-HpETE product, h12-LOX and h15-LOX-1 metabolize AA to create mixtures of 12S-HpETE and 15S-HpETE, with h12-LOX making 95% 12S-HETE (5% 15S-HETE) and h15-LOX-1 making 90% 15S-HETE (10% 12S-HETE). This gets further complicated by the fact that the LOX isoforms can react with their own products and the LOX products of other isoforms to create. Furthermore, the fidelity of the LOX reactions with the canonical substrate AA is eroded when longer substrates, such as docosahexaenoic acid (DHA, C₂₂Δ₆, n-3), are metabolized and a variety of products are formed³. The naming of LOX is based on C₂₀ PUFA and when longer or shorter substrates are used the products are oxygenated at differing locations. h15-LOX-1 reacts with the C₁₈ PUFA LA to form mostly the 13S-HpODE product and the C₂₂ PUFA DHA to form a mixture of primarily 17S-HpDHA and 14S-HpDHA, with the 17-product being the most abundant, and minor amounts of 11- and 20S-HpDHA. Therefore a more comprehensive understanding of LOX nomenclature and the products formed should be centered around the position of primary oxygenation relative to the methyl-end, with h5-LOX oxygenating at the w-16 position, h12-LOX oxygenating at the w-9 position, and h15-LOX-1 oxygenating at the w-6 position. While there is high sequence conservation (85% similar, 74% identical) between h15-LOX-1 and the main lipoxygenase found in mice, referred to as 12/15-LOX⁴, there are major catalytic differences between the two species which

complicates the translational research and therapeutic testing. The mouse equivalent of h15-LOX-1 metabolizes AA into a mixture of 12S-HpETE and 15S-HpETE, with 12S-HpETE being the major product. Molecules that have been found to be potent inhibitors of h15-LOX-1 have at times failed to inhibit the mouse 12/15-LOX.

1.2 Lipoxygenase expression and genes

The tissue expression and cellular localization of these human LOX genes has been extensively studied¹ (**Table 1.1**). ALOX5, located on chromosome 10, is expressed in high abundance in neutrophils, dendritic cells, macrophages, as well as other immune cells and is believed to be mostly localized to the nucleus. While *in vitro* experiments have shown h5-LOX is active in the absence of five-lipoxygenase activating protein (FLAP), FLAP is necessary for the *in vivo* activity of h5-LOX⁵. Found on chromosome 17, ALOX12⁶, as the enzyme name (platelet-type h12-LOX) suggest, is highly expressed in platelets and has been found in certain endothelial cells. Similar to ALOX12, the A15LOX and A15LOXB⁷ genes are also located on chromosome 17. While both of the h15-LOX genes have been found to be expressed in macrophages, ALOX15B is constitutively expressed and the ALOX15 expression is dependent on IL-4 and IL-13 signaling⁸. ALOX15 expression has also been seen in eosinophils and has been implicated in various cancers and neurological conditions⁹. While less extensively studied,

ALOX15B has been found to be expressed primarily in epithelial cells including skin and hair roots¹⁰. Like ALOX15, ALOX15B is believed to be upregulated a variety of cancers. The less studied ALOXE3 and ALOX12B genes are co-clustered with ALOX15B on chromosome 17, and are expressed in the epithelial cells. With regards to human sequence identity/similarity (**Table 1.2**), h15-LOX-1 and h12-LOX are the most identical and similar at 65% and 79%, respectively. Surprisingly, although they both primarily abstract a w-8 hydrogen, h15-LOX-1 and h15-LOX-2 have relatively low sequence identity at 37%. The two most widely researched animal lipoxygenases are rabbit 15-LOX, r15-LOX¹¹, and mouse 12/15-LOX. r15-LOX has the shares the most identical and similar residues to h15-LOX-1 at 81% and 95%, respectively. The majority of the work in this dissertation is centered on h5-LOX, h12-LOX, h15-LOX-1, and h15-LOX-2 so the remaining focus will be targeted towards them.

1.3 Lipoxygenase Catalysis/Mechanism

The primary catalytic cycle of human LOX is centered around a four reaction mechanism¹. It is necessary for the non-heme coordinated iron to be in the Fe³⁺ (ferric) state. This activated LOX iron stereoselectively abstracts the pro-s hydrogen from bis-allylic methylene, thereby generating an inactive, ferrous enzyme and a carbon fatty acid radical. Following a radical rearrangement that spans two carbons, molecular oxygen reacts with the

carbon radical resulting in a peroxy-radical on the terminal oxygen. This peroxy-radical is rapidly reduced by the ferrous iron leaving a hydroperoxy fatty acid and a regenerated ferric enzyme. It should be noted that the cellular environment is largely reducing, with glutathione peroxidase and other antioxidants quickly reducing the hydroperoxy fatty acid (HpETE) to a hydroxy fatty acid (HETE). Through kinetic and mechanistic experimentation it has been shown that the stereoselective abstraction of the hydrogen atom is a proton-coupled electron transfer reaction (PCET) and is the catalytic rate-limiting step¹². The localization of molecular oxygen in the active site has been studied extensively¹³⁻¹⁴. The antarafacial addition of oxygen relative to hydrogen abstraction coupled with structural studies of soybean 15-lipoxygenase (sLO) suggest the presence of an oxygen channel from the surface of the protein to a specific location in the protein active site. Site-directed mutagenesis studies coupled with kinetic experiments with sLO have provided compelling evidence for the presence of an oxygen channel, where minor fluctuations in protein structure enable the diffusion of O₂ to the active site. Although there is a lack of oxygen channel based studies for human LOX, the work done with sLO highlighted a number of key residues that defined the oxygen channel¹⁵. Interestingly, there is high conservation of these residues in both h15-LOX-1 and h12-LOX, providing an avenue of investigation for the future.

As previously mentioned, one of the complicating factors in the understanding of LOX catalysis comes from the fact that multiple human LOX can re-react with some of their initial products and the oxylipin products of other LOX and related oxygenase's (COX, CYP450), forming dioxylipins and epoxy-lipins. Kinetic experimentation has shown these reactions to be far less catalytically efficient and the binding affinity of these secondary substrates is drastically lower¹⁶. This secondary catalytic cycle is substrate dependent as the requirement for a bis-allylic hydrogen persists. The secondary catalysis by h5-LOX has been examined experimentally as the end products are leukotrienes A and B, potent inflammatory mediators¹⁷. h5-LOX reacts with AA, abstracting a hydrogen from the seventh carbon (relative to carboxy-head) to form 5S-HpETE, h5-LOX then reacts with 5-HpETE by abstracting a hydrogen from the tenth carbon. The radical from this carbon rearranges to the sixth carbon (now neighboring the hydroperoxy-carbon), and the overlap of anti-bonding and bonding orbitals with the peroxide facilitates the homolytic cleavage of the oxygen-oxygen bond, generating an epoxide between the fifth and sixth carbons. One of the chapters in this thesis is focused on the secondary catalytic cycle of h12-LOX and h15-LOX-1 with 15-oxylipins, the omega-3 PUFA EPA product 15S-HpEPE in particular. Both of these enzymes have been shown to react with 15S-HpEPE for form a variety of dioxylipins as they are capable of C10 hydrogen abstraction. Following hydrogen abstraction, the radical rearrangement can lead to: i) molecular

oxygenation at C8, yielding a diperoxylin (8,15-diHpEPE), ii) molecular oxygenation at C14, yielding another diperoxylin (14,15-diHpEPE), iii) 14,15-epoxylin formation whose non-enzymatic hydrolysis yields a dioxylin (8,15-diHEPE). The implications of these findings will be explored in Chapter 2.

1.4 Lipoxygenase Structure

Across the animal and plant kingdom, the structure of LOX is formed from a single polypeptide chain. Spanning 662-676 amino acids, these enzymes have a mass of ~75 kDa. While most of the human LOX are believed to exist as monomers, recent evidence has indicated that h12-LOX exist as a homo-dimer or tetramer¹⁸. This polypeptide chain folds into a two domain structure which are covalently connected through an intrinsically disordered loop¹⁹. The smaller, N-terminal domain is referred to as the polycystin-1, lipoxygenase, alpha toxin (PLAT) domain. It consists of eight antiparallel strands, together known as a β -barrel, although the size of the PLAT domains varies slightly between different animal and plant species. Conserved among other proteins, particularly human lipases, the PLAT domain is believed to be necessary for cytosolic LOX to interact with membrane and micelle bound substrates²⁰. Studies have shown that site-directed mutagenesis targeting the PLAT domain hinders the ability of LOX to bind to cellular membranes. The longer, catalytically active C-terminal domain consists of 18-22 helices, which

contains the largely hydrophobic active site, as well as the coordinated iron. The catalytic domain is required for substrate recognition and turnover. The “triad hypothesis” has been proposed for defining the LOX active site²¹. This hypothesis can be explained through examination of the structure-activity relationship of h12-LOX and h15-LOX-1. The first part of the triad is made up by positively charged arginine residues, R402 and R404, on the surface of the LOX structure. These positively charged residues are believed to interact with the negatively charged carboxylate head of the PUFA substrate and supports the methyl-tail first model of substrate entry into the active site. Early research noted the importance of these residues for catalytic activity, although more recent results have cast uncertainty on those findings. The second segment of the triad occurs at the curved point of the LOX active site. Here a bulky, aromatic residue, F414, and L407 are believed to facilitate positioning in part through pi-pi stacking with the double-bond system found in PUFA. Our lab has shown through SDM that catalytic efficiency and substrate affinity can be negatively affected through the removal of aromatic residues. Interestingly, the catalytic efficiency and substrate affinity was recovered through the creation of a F414W mutant, further highlighting the importance of the pi orbital interactions²². The final portion of the triad hypothesis is found at the “bottom” of the active site. Here hydrophobic residues in the 417 and 418 positions and F352 line the end of active site and control the depth of substrate insertion²³. The 417 residue is an isoleucine and

alanine in h15-LOX-1 and h12-LOX, respectively. It is believed that the less bulky alanine residue for h12-LOX facilitates a deeper substrate positioning, placing the C10 carbon in proximity to the active site iron, promoting the creation of 12S-HETE. The residues for iron coordination are highly conserved among animal and plant LOX. In mammals, the iron is coordinated by a water molecule, four histidine residues, and the carboxylate of the C-terminal isoleucine. To date, there has been challenges with the crystallization and structure determination of human LOX. While crystal structures exist for both h15-LOX-2²⁴ and h5-LOX²⁵, the h5-LOX construct was significantly mutated, casting doubt on the applicability of the structure model. Numerous attempts have been made at crystallization of h15-LOX-1 and h12-LOX. Although there has been a h12-LOX structure²⁶ added to the PDB, the structure was never published and there are doubts if the protein used was catalytically active. Due to the high sequence homology of h15-LOX-1 and r15-LOX, the rabbit structure²⁷ has been used to generate *in silico* structural models for the human ortholog and has been successfully utilized for the design of potent, selective inhibitors.

1.5 Lipoxygenase Allostery

Allosteric modification of enzymes occurs commonly throughout biological systems and is one of the main ways through which cellular integrity is sustained. Regulation through allostery is thought to be imparted

by conformational changes in protein structure that effect substrate affinity or through the polymerization or dissociation of subunits²⁸. Human LOX have been found to undergo a range of varying modes of allosteric modulation. h5-LOX was the first human LOX be identified as having allosteric regulators. ATP and calcium, Ca²⁺, have been found to increase the catalytic efficiency (5-fold activation) of h5-LOX, both *in vitro* and *in vivo*²⁹. The N-terminal PLAT domain is negatively charged and the binding of Ca²⁺ neutralizes this negative charge, enabling the association of the PLAT domain with cellular membrane-bound lipids. The allosteric regulation by ATP was found to be non-specific as AMP and ADP were both found cause similar responses. Allosteric regulation of hLOX by LOX products and substrate mimics has been observed by many studies. h15-LOX-1 and h15-LOX-2 have both been found to be allosterically regulated by their main LA metabolite, 13S-HODE³⁰. The presence of 13-HODE modifies the specificity of the h15-LOX enzymes for AA and LA, the two most abundant w-6 PUFA in the body. Additionally, the substrate mimic, oleyl sulfate, has been shown to allosterically regulate h15-LOX-1 through a decrease in the kinetic isotope effect³¹. The major h12-LOX and minor h15-LOX-1 AA product, 12S-HETE, exhibited a similar mode of allostery to that of 13S-HODE when interacting with h15-LOX-1. The presence of 12S-HETE not only altered the AA/LA substrate specificity, but was also found to allosterically activate the rate-limiting C-H bond abstraction. This was determined to independent of iron

oxidation was the hydroperoxy product, 12S-HpETE, elicited a similar response³². Recent work by the Holman lab has shed additional light on modes of product feedback allostery, including novel data presented in Chapter 2. The ω-3 PUFA products, 15S-HpEPE, 14S-HpDHA, and 17S-HpDHA, have been found to be negative allosteric modulators of h12-LOX and h15-LOX-1^{3,16,33}. By varying the concentration of those products individually, the ratio of secondary products formed through oxygenation and dehydration differs. The presence of product based allostery suggest a complex network of LOX regulation. Chapter 3 of this thesis explores the allosteric activation of h15-LOX-1 by a recently discovered small molecule. This h15-LOX-1 activator was found to be specific for that LOX isozyme and the site of interaction is independent of previously known allosteric regulators.

1.6 Lipoxygenase and Platelets

Cardiovascular disease (CVD) is the leading cause of death in the USA, comprising of roughly 25-33% of all annual deaths³⁴. Platelets play a major role in the regulation of homeostasis and thrombosis. Excessive, uncontrolled platelet aggregation is responsible for the progression of some CVD. While known antiplatelet therapeutics exist and have been successful in treating patients, the side effects can be serious in nature. Heparin, one of the most widely used antiplatelet drugs, has been found to induce thrombocytopenia in certain cases. While platelets contain a LOX, h12-LOX,

that is capable of metabolizing a variety of PUFA which can activate and deactivate platelet aggregation, exogenous PUFA metabolites from extracellular sources can also regulate platelet activation. While w-3 and w-6 PUFA are generally thought to be “anti-inflammatory” and “inflammatory” signaling molecules, respectively, the picture isn’t as clear with platelets. Both w-3 and w-6 metabolites have been shown to exhibit anti-aggregatory effects on platelets, although through differing signaling pathways and at varying potencies³⁵. Chapter 2 examines the platelet effect, signaling pathway, and h12-LOX metabolization of 3 separate C20 PUFA metabolites, 15S-HETE, 15S-HETrE, and 15S-HEPE. While these are the primary products of h15-LOX-1 and h15-LOX-2, their endogenous levels in platelets indicated the presence of a different PUFA metabolizing enzyme.

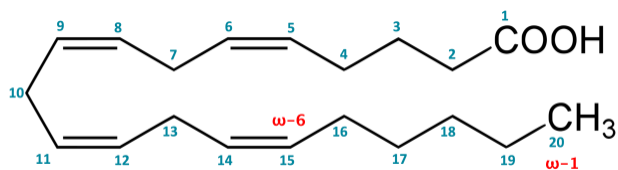
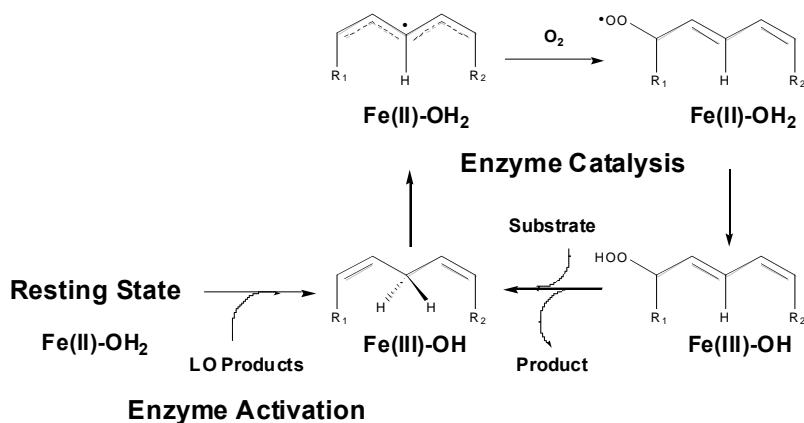
1.7 Figures, Tables and Schemes

Gene	Enzyme	Expression tissue
ALOX5	h5-LOX	Macrophages, neutrophils
ALOX12	h12-LOX	Platelets
ALOX12B	h12R-LOX	Epithelial (skin)
ALOX15	h15-LOX-1	Macrophages, eosinophils
ALOX15B	h15-LOX-2	Macrophages, epithelial
ALOXE3	eLOX3	Epithelial (skin)

Table 1.1 LOX gene expression tissue

	5-LOX	12-LOX	12R-LOX	15-LOX-2	eLOX3
15-LOX-1	40, 60	65, 79	34, 53	37, 55	36, 52
eLOX3	39, 56	36, 53	54, 71	51, 66	
15-LOX-2	42, 62	37, 56	46, 66		
12R-LOX	40, 58	36, 55			
12-LOX	41, 60				

Table 1.2 % Identical, % Similarity. 15-LOX-1: P16050, 5-LOX: P09917, 12-LOX: P18054, 12R-LOX: O75342, 15-LOX-2: O15296, eLOX3: Q9BYJ1.



1.8 References

- [1] Brash, A. R. (1999) Lipoxygenases: Occurrence, Functions, Catalysis and Acquisition of Substrate, *J. Biol. Chem.* 274, 23679-23682.
- [2] Vance, R. E., Hong, S., Gronert, K., Serhan, C. N., and Mekalanos, J. J. (2004) The opportunistic pathogen *Pseudomonas aeruginosa* carries a secretable arachidonate 15-lipoxygenase, *Proc Natl Acad Sci U S A* 101, 2135-2139.
- [3] Perry, S. C., Kalyanaraman, C., Tourdot, B. E., Conrad, W. S., Akinkugbe, O., Freedman, J. C., Holinstat, M., Jacobson, M. P., & Holman, T. R. (2020). 15-Lipoxygenase-1 biosynthesis of 7S,14S-diHDHA implicates 15-lipoxygenase-2 in biosynthesis of resolvin D5. *Journal of lipid research*, 61(7), 1087–1103.
- [4] Gronert, K., Maheshwari, N., Khan, N., Hassan, I. R., Dunn, M., & Schwartzman, M. L. (2005). A role for the mouse 12/15-lipoxygenase pathway in promoting epithelial wound healing and host defense. *Journal of Biological Chemistry*, 280(15), 15267-15278.
- [5] Evans, J. F., Ferguson, A. D., Mosley, R. T., & Hutchinson, J. H. (2008). What's all the FLAP about?: 5-lipoxygenase-activating protein inhibitors for inflammatory diseases. *Trends in pharmacological sciences*, 29(2), 72-78.
- [6] Nugteren, D. H. (1975). Arachidonate lipoxygenase in blood platelets. *Biochimica et Biophysica Acta (BBA)-Lipids and Lipid Metabolism*, 380(2), 299-307.
- [7] Brash, A. R., Boeglin, W. E., and Chang, M. S. (1997) Discovery of a second 15S-lipoxygenase in humans, *Proc Natl Acad Sci U S A* 94, 6148-6152.
- [8] Wittwer, J., & Hersberger, M. (2007). The two faces of the 15-lipoxygenase in atherosclerosis. *Prostaglandins, Leukotrienes and Essential fatty acids*, 77(2), 67-77.
- [9] Singh, N. K., & Rao, G. N. (2019). Emerging role of 12/15-Lipoxygenase (ALOX15) in human pathologies. *Progress in lipid research*, 73, 28-45.
- [10] Lee, D. J., Lee, J., Ha, J., Park, K. C., Ortonne, J. P., & Kang, H. Y. (2012). Defective barrier function in melasma skin. *Journal of the European Academy of Dermatology and Venereology*, 26(12), 1533-1537.

- [11] Schewe, T., Halangk, W., Hiebsch, C., and Rapoport, S. M. (1975) A lipoxygenase in rabbit reticulocytes which attacks phospholipids and intact mitochondria, *Febs Lett* 60, 149-152.
- [12] Soudackov, A. V., & Hammes-Schiffer, S. (2016). Proton-coupled electron transfer reactions: analytical rate constants and case study of kinetic isotope effects in lipoxygenase. *Faraday discussions*, 195, 171-189.
- [13] Schneider, C., Pratt, D. A., Porter, N. A., & Brash, A. R. (2007). Control of oxygenation in lipoxygenase and cyclooxygenase catalysis. *Chemistry & biology*, 14(5), 473-488.
- [14] Saam, J., Ivanov, I., Walther, M., Holzhütter, H. G., & Kuhn, H. (2007). Molecular dioxygen enters the active site of 12/15-lipoxygenase via dynamic oxygen access channels. *Proceedings of the National Academy of Sciences*, 104(33), 13319-13324.
- [15] Collazo, L., & Klinman, J. P. (2016). Control of the position of oxygen delivery in soybean lipoxygenase-1 by amino acid side chains within a gas migration channel. *Journal of Biological Chemistry*, 291(17), 9052-9059.
- [16] Freedman, C., Tran, A., Tourdot, B. E., Kalyanaraman, C., Perry, S., Holinstat, M., Jacobson, M. P., and Holman, T. R. (2020) Biosynthesis of the Maresin Intermediate, 13S,14S-Epoxy-DHA, by Human 15-Lipoxygenase and 12-Lipoxygenase and Its Regulation through Negative Allosteric Modulators, *Biochemistry* 59, 1832-1844.
- [17] Rådmark, O., Werz, O., Steinhilber, D., & Samuelsson, B. (2015). 5-Lipoxygenase, a key enzyme for leukotriene biosynthesis in health and disease. *Biochimica et Biophysica Acta (BBA)-Molecular and Cell Biology of Lipids*, 1851(4), 331-339.
- [18] Tsai, W.C., Aleem, A.M., Whittington, C., Cortopassi, W.A., Kalyanaraman, C., Baroz, A., Iavarone, A.T., Skrzypczak-Jankun, E., Jacobson, M.P., Offenbacher, A.R. and Holman, T. (2021). Mutagenesis, hydrogen–deuterium exchange, and molecular docking investigations establish the dimeric interface of human platelet-type 12-lipoxygenase. *Biochemistry*, 60(10), pp.802-812.
- [19] Nelson, M. J., & Seitz, S. P. (1994). The structure and function of lipoxygenase. *Current opinion in structural biology*, 4(6), 878-884.
- [20] Newcomer, M. E., & Brash, A. R. (2015). The structural basis for specificity in lipoxygenase catalysis. *Protein Science*, 24(3), 298-309.

- [21] Vogel, R., Jansen, C., Roffeis, J., Reddanna, P., Forsell, P., Claesson, H.E., Kuhn, H. and Walther, M. (2010). Applicability of the triad concept for the positional specificity of mammalian lipoxygenases. *Journal of Biological Chemistry*, 285(8), pp.5369-5376.
- [22] Sloane, D. L., Leung, R., Craik, C. S., & Sigal, E. (1991). A primary determinant for lipoxygenase positional specificity. *Nature*, 354(6349), 149-152.
- [23] Sloane, D. L., Leung, R., Barnett, J., Craik, C. S., & Sigal, E. (1995). Conversion of human 15-lipoxygenase to an efficient 12-lipoxygenase: the side-chain geometry of amino acids 417 and 418 determine positional specificity. *Protein Engineering, Design and Selection*, 8(3), 275-282.
- [24] Kobe, M. J., Neau, D. B., Mitchell, C. E., Bartlett, S. G., & Newcomer, M. E. (2014). The structure of human 15-lipoxygenase-2 with a substrate mimic. *Journal of Biological Chemistry*, 289(12), 8562-8569.
- [25] Gilbert, N. C., Bartlett, S. G., Waight, M. T., Neau, D. B., Boeglin, W. E., Brash, A. R., & Newcomer, M. E. (2011). The structure of human 5-lipoxygenase. *Science*, 331(6014), 217-219.
- [26] PDB entry: 3D3L
- [27] Choi, J., Chon, J. K., Kim, S., & Shin, W. (2008). Conformational flexibility in mammalian 15S-lipoxygenase: reinterpretation of the crystallographic data. *Proteins: Structure, Function, and Bioinformatics*, 70(3), 1023-1032.
- [28] Laskowski, R. A., Gerick, F., & Thornton, J. M. (2009). The structural basis of allosteric regulation in proteins. *FEBS letters*, 583(11), 1692-1698.
- [29] Smyrniotis, C. J., Barbour, S. R., Xia, Z., Hixon, M. S., & Holman, T. R. (2014). ATP allosterically activates the human 5-lipoxygenase molecular mechanism of arachidonic acid and 5 (S)-hydroperoxy-6 (E), 8 (Z), 11 (Z), 14 (Z)-eicosatetraenoic acid. *Biochemistry*, 53(27), 4407-4419.
- [30] Wecksler, A. T., Kenyon, V., Garcia, N. K., Deschamps, J. D., Van Der Donk, W. A., & Holman, T. R. (2009). Kinetic and structural investigations of the allosteric site in human epithelial 15-lipoxygenase-2. *Biochemistry*, 48(36), 8721-8730.
- [31] Mogul, R., Johansen, E., & Holman, T. R. (2000). Oleyl sulfate reveals allosteric inhibition of soybean lipoxygenase-1 and human 15-lipoxygenase. *Biochemistry*, 39(16), 4801-4807.

- [32] Joshi, N., Hoobler, E. K., Perry, S., Diaz, G., Fox, B., and Holman, T. R. (2013) Kinetic and structural investigations into the allosteric and pH effect on the substrate specificity of human epithelial 15-lipoxygenase-2, *Biochemistry* 52, 8026-8035.
- [33] Tsai, W. C., Kalyanaraman, C., Yamaguchi, A., Holinstat, M., Jacobson, M. P., and Holman, T. R. (2021) In Vitro Biosynthetic Pathway Investigations of Neuroprotectin D1 (NPD1) and Protectin DX (PDX) by Human 12-Lipoxygenase, 15-Lipoxygenase-1, and 15-Lipoxygenase-2, *Biochemistry* 60, 1741-1754.
- [34] Mehta, N. K., Abrams, L. R., & Myrskylä, M. (2020). US life expectancy stalls due to cardiovascular disease, not drug deaths. *Proceedings of the National Academy of Sciences*, 117(13), 6998-7000.
- [35] Yeung, J., Hawley, M., & Holinstat, M. (2017). The expansive role of oxylipins on platelet biology. *Journal of Molecular Medicine*, 95(6), 575-588.

Chapter 2

FATTY ACIDS NEGATIVELY REGULATE PLATELET FUNCTION THROUGH FORMATION OF NONCANONICAL 15-LIPOXYGENASE- DERIVED EICOSANOIDS

2.1 Abstract

The antiplatelet effect of polyunsaturated fatty acids is primarily attributed to its metabolism to bioactive metabolites by oxygenases, such as lipoxygenases (LOX). Platelets have demonstrated the ability to generate 15-LOX-derived metabolites (15-oxylipins); however, whether 15-LOX is in the platelet or is required for the formation of 15-oxylipins remains unclear. This study seeks to elucidate whether 15-LOX is required for the formation of 15-oxylipins in the platelet and determine their mechanistic effects on platelet reactivity. In this study, 15-HETrE, 15-HETE and 15-HEPE attenuated collagen-induced platelet aggregation and 15-HETrE inhibited platelet aggregation induced by multiple agonists. The observed anti-aggregatory effect was due to inhibition of intracellular signaling including $\alpha\text{IIb}\beta\text{3}$ and protein kinase C activities, calcium mobilization and granule secretion. While 15-HETrE inhibited platelets partially through activation of PPAR β , 15-HETE inhibited platelets partially through activation of PPAR α . A reduction in 12-LOX activity was observed following *in vitro* catalysis with arachidonic acid in the presence of 15-HETrE, 15-HETE or 15-HEPE. Additionally, a 15-oxylipin-dependent attenuation of 12-HETE level was observed in platelets following *ex vivo* treatment with 15-HETrE, 15-HETE or 15-HEPE. Platelets treated with DGLA formed 15-HETrE and collagen-induced platelet aggregation was attenuated only in the presence of ML355 or aspirin, but not in the presence of 15-LOX-1 or 15-LOX-2 inhibitors. Expression of 15-LOX-1, but not 15-LOX-2, was decreased in leukocyte-depleted platelets compared to non-depleted platelets. Taken together, these findings suggest that 15-oxylipins regulate platelet

reactivity; however, platelet expression of 15-LOX-1 is low suggesting 15-oxylipins may be formed in the platelet through a 15-LOX-independent pathway.

2.2 Introduction

Long-chain polyunsaturated fatty acids (PUFAs) are shown to be protective against cardiovascular diseases^{53,66}; however, the mechanism of this effect is not well understood. PUFAs have been shown to regulate and alter platelet function through their metabolism to bioactive oxylipins by the two main oxygenases, cyclooxygenase (COX) and lipoxygenase (LOX)¹. Platelets express COX-1, whose inhibition by non-steroidal anti-inflammatory drugs (NSAIDs) is thought to be a primary reason for the observed decrease in platelet reactivity^{42,66}. Regarding the role of lipoxygenases in platelets, 12-LOX is highly expressed and plays an important role in regulating platelet activation^{2,67}. However, the presence of 15-LOX in the platelet and whether it is required for the formation of 15-LOX-derived oxylipins (15-oxylipins) remains unclear.

Although platelets have been demonstrated to generate 15-oxylipins, such as 15(S)-hydroxyeicosatetraenoic acid (15-HETE) from arachidonic acid (AA) and 15(S)-hydroxyeicosatrienoic acid (15-HETrE) from dihomo- γ -linolenic acid (DGLA), the source of these molecules is poorly defined^{24,63}. Lipoxygenases could potentially generate these molecules; however, studies have indicated that these 15-oxylipins are generated by COX^{16,66}. Interestingly, the role of these 15-oxylipins in platelet biology is also controversial. While 15-HETrE, 15-HETE and 15(S)-hydroxyeicosapentaenoic

(15-HEPE), from eicosapentaenoic acid (EPA), have been shown to inhibit platelet reactivity^{16,57}, other studies have observed a pro-aggregatory effect of 15-HETE on platelet function^{45,61}. With respect to their mechanism of action, oxylipins can inhibit platelet function by increasing cyclic adenosine monophosphate (cAMP) levels via Gas-coupled receptors, or binding intracellular nuclear receptor, such as peroxisome proliferator-activated receptors (PPARs)^{52,66}. Although 15-HETE has been reported to interact with PPARs in other cell types^{25,45}, the mechanism underlying the effects of 15-HETE on platelet reactivity is not well understood. Given these contradictory and poorly defined results, a better understanding of the 15-oxylipins effects on platelet activity is warranted. This study helps to elucidate the mechanism of 15-oxylipin formation in platelets and determine the effects of 15-HETrE, 15-HETE and 15-HEPE on the regulation of platelet reactivity.

2.3 Methods

Isolation of human platelets

All research involving human subjects was approved by the University of Michigan Institutional Review Board. Prior to blood collection, written informed consent was obtained from all subjects in this study. Blood was collected into vacutainers containing sodium citrate (Becton, Dickinson and Company (BD), Franklin Lakes, NJ) and centrifuged for 10 minutes at 200g to obtain platelet rich plasma. Acid citrate dextrose (2.5% sodium citrate tribasic, 1.5% citric acid, 2.0% D-glucose) and apyrase (0.02 U/ml) were added to the platelet rich plasma, which was then centrifuged for 10 minutes at 2000g. Platelets were resuspended in Tyrode's buffer (10 mM

HEPES, 12 mM NaHCO₃, 127 mM NaCl, 5 mM KCl, 0.5 mM NaH₂PO₄, 1 mM MgCl₂, and 5 mM glucose) and adjusted to 3 x 10⁸ platelets/ml, unless otherwise stated.

Leukocyte-depletion of platelets

Washed platelets (5 x 10⁸ platelets/ml) were incubated with magnetic CD45 MicroBeads (10 µl/ml) (Miltenyi Biotec Inc., Auburn, CA) for 30 minutes. Following incubation, platelets were treated with EDTA (2.5 mM) and filtered through a magnetic-activated cell sorting separation column that selectively captured CD45 positive cells. Platelets were pelleted from the column flow-through by centrifugation following treatment with acid citrate dextrose and apyrase, as described above.

Quantification of platelet-derived 15-oxylipins

Leukocyte-depleted platelets were incubated with 10 µM DGLA (dimethyl sulfoxide (DMSO) as control) for 10 minutes at 37°C, pelleted at 1000g for 1 min, and the supernatant was frozen. Subsequently, 13S-hydroxy-9Z,11E-octadecadienoic-9,10,12,13-d₄ acid (d₄-13HODE) (20 ng) was added to the thawed supernatant and oxylipins were extracted with 1.5 mL dichloromethane, reduced with 20 µl of trimethylphosphite, and dried under a stream of N₂. Samples were resuspended in 50 µl of methanol (MeOH) containing 10 ng of d₈-12HETE. Prior to chromatography, 100 µl of 0.1% formic acid in water were added to samples, and 90 µl were injected for analysis. UPLC-MS/MS was performed to monitor the oxylipin production, as previously described⁵², with the addition of the following m/z transitions: 15-HETE: 319→219, 15-HETrE: 321→221, 14,15-diHETE: 335→205, 8,15-diHETE: 335→155. Quantitation was performed with a 15-HETE standard curve. Quantitation of 14,15-

diHETE was based on the relative ionization efficiency of it to 15-HETE as the standard (0.98 +/-0.2).

Production and isolation of 15-oxylipins

The synthesis of 15-HETrE, 15-HETE, and 15-HEPE were performed as previously described^{48,71}. Briefly, 15S-hydroperoxy-8Z,11Z,13E-eicosatrienoic acid (15-HpETrE), 15S-hydroperoxy-5Z,8Z,11Z,13E-eicosatetraenoic acid (15-HpETE), and 15S-hydroperoxy-5Z,8Z,11Z,13E,17Z-eicosapentaenoic acid (15-HpEPE) were synthesized by reaction of DGLA, AA or EPA, respectively, (25-50 μ M) with soybean lipoxygenase-1. The hydroperoxide products, 15-HpETrE, 15-HpETE, and 15-HpEPE were reduced to the alcohols, 15-HETrE, 15-HETE, and 15-HEPE with trimethylphosphite. The 15-oxylipins were then purified by HPLC using a C18 HAISIL 250 \times 10 mm semiprep column isocratically in a mobile phase containing 54.5:44.5:1 mixture of acetonitrile, water, and formic acid, respectively.

Platelet aggregation and dense granule secretion

A Chrono-log Model 700D lumi-aggregometer was used to measure platelet aggregation and ATP release under stirring conditions (1100 rpm) at 37°C for six minutes, following the addition of collagen (Chrono-log, Havertown, PA), thrombin (Enzyme Research Laboratories, South Bend, IN), AA (Cayman Chemical Company, Ann Arbor, MI), or ADP (Sigma-Aldrich, St. Louis, MO).

Protein kinase C substrate phosphorylation

Platelets were incubated with metabolite prior to stimulation with collagen for 5 minutes in an aggregometer. Reactions were stopped with the addition of 5X

Laemmli sample buffer, boiled, and separated on a SDS-PAGE gel. Western blots were performed with antibodies to GAPDH (Santa Cruz Biotechnology, Santa Cruz, CA) and protein kinase C (PKC) substrate (Cell Signaling Technology, Danvers, MA).

Quantification of calcium mobilization and α IIB β 3 activation via flow cytometry

Washed platelets (1.0×10^6 platelets/ml) were incubated with DMSO, 15-HETrE or 15-HETE ($10 \mu\text{M}$) for 10 minutes at 37°C . Platelets were then treated for 5 minutes with either Fluo-4-AM ($0.5 \mu\text{g}$; Thermo Fisher Scientific, Waltham, MA) or PAC-1 (BD Pharmingen, Franklin Lakes, NJ), an antibody that binds the active conformation of α IIB β 3. Platelets, supplemented with CaCl_2 (1 mM), were stimulated with convulxin (2.5 ng/ml , purchased from Dr. Kenneth J. Clemetson, Theodor Kocher Institute, University of Berne, Bern, Switzerland) and the mean fluorescence intensity of the sample was continuously measured on an Accuri C6 flow cytometer (BD Biosciences).

α -granule secretion

Human platelets treated with metabolite for 10 minutes were stimulated with collagen ($5 \mu\text{g/ml}$) for 5 minutes under stirring conditions in the presence of the tetrapeptide Arg-Gly-Asp-Ser (RGDS; 2 mM ; Sigma-Aldrich, St. Louis, MO) to prevent platelet aggregation. A PE-conjugated P-selectin antibody (BD Pharmingen, Franklin Lakes, NJ) was added to the stimulated platelets for 10 minutes and P-selectin surface expression was quantified by flow cytometry.

Vasodilator-stimulated phosphoprotein phosphorylation

Platelets were incubated with oxylipins (10 μ M), forskolin (5 μ M), or DMSO for 10 minutes prior to the addition of 5X Laemmli sample buffer (Tris 1.5 M, pH 6.8; 10% sodium dodecyl sulfate, 50% glycerol, 25% β -mercaptoethanol, 0.6% bromophenol blue). Samples were boiled and then separated on a SDS-PAGE gel. Western blots were performed with antibodies to phosphorylated (pS157) and total vasodilator-stimulated phosphoprotein (VASP) (Santa Cruz Biotechnology, Santa Cruz, CA).

15-LOX-1 and 15-LOX-2 expression in platelets

To leukocyte-depleted platelets, non-depleted platelets, 15-LOX-1, 15-LOX-2 and 12-LOX enzymes were added 5X Laemmli sample buffer and samples were boiled and then separated on a SDS-PAGE gel. Western blots were performed with antibodies to 15-LOX-1 (Abcam, Cambridge, UK) or 15-LOX-2 (Abcam, Cambridge, UK), and b-actin (Cell Signaling Technology, Danvers, MA).

Thromboxane B₂ (TXB₂) and 12-HETE formation

Platelets pretreated with 15-HETrE or 15-HETE (10 μ M), were stimulated with collagen (5 μ g/ml) for 5 minutes in an aggregometer. Platelets were pelleted by centrifugation at 1000g for 1 min and the supernatant was transferred to a new tube. The supernatant was immediately placed on dry ice. Thromboxane B₂ (TXB₂) and 12(S)-hydroxyeicosatetraenoic acid (12-HETE) were quantified by UPLC-MS/MS, as described above.

Mass spectrometry analysis of 12-LOX enzymatic products from 15-oxylipin substrates

Briefly, 12-LOX (60 pmoles) was reacted with 10 μ M of each 15-oxylin, quenched, extracted three times, reduced with trimethylphosphite, and evaporated under a stream of nitrogen gas. Reactions were analyzed via LC-MS/MS. The chromatography system was coupled to a Thermo-Electron LTQ LC-MS/MS for mass analysis. All analyses were performed in negative ionization mode at the normal resolution setting. MS² was performed in a targeted manner with a mass list containing the following m/z ratios \pm 0.5: 317.5 (HEPEs), 319.5 (HETEs), 321.5 (HETrEs), 331.5 (diHEPEs), 335.5 (diHETEs), 337.4 (diHETrEs), triHEPEs (349.5), 351.5 (triHETEs), and 353.5 (triHETrEs).

Kinetic analysis of AA, DGLA, EPA, and corresponding 15-oxylin with 12-LOX

Overexpression and purification of human 12-LOX was performed as previously described¹⁹. 12-LOX steady-state kinetic reactions were constantly stirred at ambient temperature, in a 1 cm² quartz cuvette containing 2 mL of 25 mM HEPES, pH 8 with DGLA, AA, EPA, 15-HpETrE, 15-HpETE, or 15-HpEPE. Substrate concentrations were varied from 0.25 μ M to 10 μ M for the PUFA reactions or 0.5 μ M to 25 μ M for the 15-oxylin reactions. Concentrations of PUFA were determined by measuring the amount of 15-oxylin produced from complete reaction with soybean lipoxygenase-1 (sLO-1). Concentrations of 5S-HETE, 5S-HpETE, 7S-HDHA, and 7S-HpDHA were determined by measuring the absorbance at 234 nm. Reactions were initiated by the addition of h15-LOX-1 (~20-60 nmoles) and were monitored on a Perkin-Elmer Lambda 45 UV/VIS spectrophotometer. Product formation was

determined by the increase in absorbance at 234 nm for 15-oxylipins ($\epsilon_{234} = 27,000 \text{ M}^{-1} \text{ cm}^{-1}$), 270 nm for di-oxylipins ($\epsilon_{270} = 37,000 \text{ M}^{-1} \text{ cm}^{-1}$)^{8,44}. KaleidaGraph (Synergy) was used to fit initial rates, as well as the second order derivatives (k_{cat}/K_M) to the Michaelis-Menten equation for the calculation of kinetic parameters.

Determination of IC₅₀ of 15-HETrE, 15-HETE, and 15-HEPE against 12-LOX

Purified 12-LOX was added to 10 μM AA in 2 mL of 25 mM HEPES, pH 8.0, in the presence of the control (MeOH) or oxylipin. IC₅₀ values were obtained by determining the enzymatic rate at various 15-HETrE, 15-HETE, and 15-HEPE concentrations and plotting the rates against 15-HETrE, 15-HETE, and 15-HEPE concentrations, followed by a hyperbolic saturation curve fit via KaleidaGraph (Synergy).

Statistical analysis

Two-tailed paired *t* test, one- and two-way analysis of variance (ANOVA) were performed with Prism 9 (GraphPad Software, La Jolla, CA) to analyze the data. The statistical test used in each assay is reported in the figure legend. Data represent mean values \pm standard error of the mean (SEM).

2.4 Results

15-Oxylipins inhibit agonist-induced platelet aggregation

While micromolar levels of 15-HETrE were previously reported to inhibit thromboxane receptor-mediated platelet aggregation¹⁶, it was unknown whether 15-HETrE inhibited platelet activation through other receptors such as PPARs, GPVI, or

P2Y₁₂. Washed human platelets were treated with increasing concentrations of 15-HETrE, 15-HETE or 15-HEPE prior to stimulation with collagen, the GPVI and α 2 β 1 agonist, to determine whether the 15-oxylipins inhibited collagen-mediated platelet aggregation. 15-HETrE, 15-HETE, and 15-HEPE all inhibited platelet aggregation in response to collagen (0.25 μ g/ml), with maximal inhibition of aggregation achieved at 10 μ M (**Figure 2.1A**). Collagen-stimulated platelets were also incubated with 12(S)-hydroxyeicosatetraenoic acid (12-HETrE) to determine the relative potency of 15-oxylipins-dependent inhibition of aggregation compared to previously identified antiplatelet monohydroxylated oxylipins^{52,59,60,68}. The three monohydroxylated 15-oxylipins (15-HETrE, 15-HETE or 15-HEPE) inhibited collagen-mediated platelet aggregation with similar potency to each other and to that of 12-HETrE (**Figure 2.1A**).

Our previous studies have demonstrated that 12-HETrE, a 12-LOX-derived oxylipin from DGLA, inhibits platelet aggregation induced by multiple agonists^{19,52}. In order to determine the potency of 15-oxylipins at inhibiting platelet aggregation in response to common platelet agonists, aggregation was measured in 15-HETrE-treated platelets stimulated with increasing concentrations of collagen, thrombin, ADP, or AA. 15-HETrE was effective at inhibiting low concentration of all agonists tested; however, higher doses of collagen, AA, and thrombin were able to overcome the inhibitory effects of 15-HETrE (**Figure 2.1B-E**). Aggregation induced by high doses of ADP (20 μ M) remained inhibited by 15-HETrE (**Figure 2.1D**).

15-Oxylipins inhibit intracellular platelet signaling

Since the 12-LOX-derived oxylipin from AA, 12-HETE, plays a critical role enhancing platelet activation^{43,75}, but 12-HETrE inhibits platelet reactivity and clot formation^{19,52}, we focused on elucidating the mechanism by which either 15-HETrE or 15-HETE inhibit platelet activation. To assess whether 15-HETrE or 15-HETE attenuated platelet aggregation through modulation of intracellular signaling, Ca²⁺ mobilization, integrin activation, PKC activation and granule secretion were evaluated in GPVI-stimulated platelets treated with 15-HETE or 15-HETrE. Ca²⁺ mobilization, a key regulator of integrin α IIB β 3 activation, was evaluated in platelets treated with oxylipins in real-time by flow cytometry to determine if Ca²⁺ mobilization was inhibited in the presence of 15-HETE and 15-HETrE. Collagen poorly activates platelets in the static conditions used to measure Ca²⁺ mobilization and integrin activation on a flow cytometer³². Therefore, convulxin (CVX), a snake venom toxin was used to stimulate GPVI for real-time flow cytometer experiments. Pretreatment of platelets with 15-HETrE or 15-HETE (10 μ M) resulted in a decrease in Ca²⁺ mobilization following stimulation with CVX compared to control-treated platelets (**Figure 2.2A**). Since Ca²⁺ mobilization is required for activation of the integrin α IIB β 3, 15-HETrE and 15-HETE were assessed for their ability to attenuate α IIB β 3 activation. 15-HETrE- or 15-HETE-treated platelets were stimulated with CVX (2.5 ng/ml) and activation was measured using flow cytometry in the presence of PAC-1, an antibody that recognizes the active conformation of α IIB β 3. Compared to DMSO, treatment of platelets with 15-HETrE or 15-HETE inhibited α IIB β 3 activation in CVX-stimulated platelets (**Figure 2.2B**).

Since the activation of conventional isoforms of PKC are dependent on Ca^{2+} (Harper and Poole 2010), the ability of 15-HETrE and 15-HETE to inhibit PKC in platelets was tested. At low concentrations of collagen (0.5 $\mu\text{g/ml}$), 15-HETrE- and 15-HETE-treated platelets showed a reduced level of PKC substrate phosphorylation compared to control (**Figure 2.2C**). However, there was no difference in PKC activation between control- and oxylipin-treated platelets at higher concentrations of collagen (5 $\mu\text{g/ml}$) (**Figure 2.2C**). Agonist-dependent granule release was also assessed as a measurement of platelet activation including both dense and α -granules. To evaluate whether 15-HETrE or 15-HETE affect dense granule secretion, platelets were stimulated with increasing concentrations of collagen in the presence of 15-HETrE, 15-HETE, or control (DMSO). Collagen-stimulated platelets incubated with 15-HETE or 15-HETrE released less ATP, a marker of dense granule secretion, than platelets treated with DMSO (**Figure 2.2D**). To determine if 15-HETrE or 15-HETE inhibited α -granule secretion, platelets were stimulated with collagen (5 $\mu\text{g/ml}$) in the presence of 15-HETrE or 15-HETE, and surface expression of P-selectin was measured by flow cytometer¹⁵. Platelets treated with 15-HETrE or 15-HETE had a decrease in P-selectin surface expression compared to control-treated platelets (**Figure 2.2E**).

15-HETrE and 15-HETE inhibit platelet activation via unique PPARs

Independent of direct effects on oxygenases, oxylipins have additionally been proposed to reduce platelet activation through either the initiation of $\text{G}\alpha_s$ -coupled receptor signaling or stimulation of PPARs⁵³. The inhibitory effects of the $\text{G}\alpha_s$ signaling pathway proceed through cAMP-dependent PKA activation⁴⁷. In platelets,

the major substrate of PKA is VASP serine 157 (S157)⁹. To determine if 15-HETrE or 15-HETE regulate platelet function in this manner, VASP phosphorylation was measured in platelets treated with oxylipins (10 μ M) to assess their ability to initiate $G\alpha_s$ signaling. VASP (S157) phosphorylation did not increase in platelets incubated with 15-HETrE or 15-HETE compared to either DMSO or 12-HETE, a negative control (**Figure 2.3A**). As expected, platelets treated with either forskolin, a direct adenylyl cyclase agonist, or 12-HETrE, a 12-LOX oxylipin that signals through a $G\alpha_s$ -coupled receptor⁶⁸, had enhanced VASP phosphorylation (**Figure 2.3A**).

Platelets express all three PPAR isoforms (a, b, and g) and activation of any of these isoforms inhibit platelet function through a non-genomic mechanism^{3,28}. Since 15-HETrE and 15-HETE have been shown to activate PPARs in other cell types^{34,50} we sought to determine if either 15-HETrE or 15-HETE inhibits platelet aggregation in a PPAR-dependent manner in platelets. Platelets were incubated with the previously characterized inhibitors of PPARa (GW6471; 10 μ M), PPARb (GSK3787; 10 μ M), or PPARg (GW9662; 10 μ M), prior to treatment with 15-HETrE or 15-HETE and subsequent collagen stimulation^{3,4,11,33}. Inhibition of PPARb, but not PPARa or PPARg, reversed the antiplatelet effects of low concentrations of 15-HETrE (2.5 μ M) in collagen-stimulated platelets (**Figure 2.3A**). In contrast, inhibition of PPARa, but not PPARb or PPARg, reversed the ability of low concentrations of 15-HETE (2.5 μ M) to inhibit collagen-induced aggregation (**Figure 2.3B**). None of the PPAR antagonists tested were able to reverse the inhibitory effects of higher concentrations of 15-HETrE or 15-HETE (5 μ M).

Oxylin inhibition of 12-LOX activity in both *ex vivo* and *in vitro* conditions

Previous studies have demonstrated that the antiplatelet effects of 15-HETE were due in part to its ability to selectively inhibit COX⁴⁹, 12-LOX^{31,57,60}, or both⁵⁹. To evaluate whether 15-HETrE or 15-HETE inhibit platelet activation via inhibiting COX or 12-LOX, the levels of their respective AA-derived metabolite, TXB₂ and 12-HETE, were quantified in the releasate of collagen-stimulated platelets. Since Ca²⁺ mobilization is required for TXB₂ and 12-HETE formation¹⁸, high concentration of collagen (5 µg/ml) were used that caused similar levels of Ca²⁺ mobilization. Platelets incubated with 15-HETrE (10 µM) prior to collagen stimulation decreased 12-HETE formation by 44±11% (**Figure 2.4A**) but had no effect on the formation of TXB₂ (**Figure 2.4B**), compared to vehicle-treated platelets. Treatment of platelets with 15-HETE (10 µM) prior to collagen stimulation had a 97±1% decrease in 12-HETE generation (**Figure 2.4A**), with no effect on TXB₂ formation (**Figure 2.4B**), compared to vehicle-treated platelets. In comparison, platelets incubated with 15-HEPE (10 µM) prior to collagen stimulation had an 89±1% decrease in 12-HETE formation (**Figure 2.4A**), with no effect on TXB₂ formation (**Figure 2.4B**) compared to vehicle-treated platelets, indicating that 15-HEPE was more similar to 15-HETE with respect to a platelet response than that of 15-HETrE. Together this data indicates that while 15-HETrE and 15-HEPE can inhibit 12-HETE production, 15-HETE inhibits 12-HETE production more effectively than either 15-HETrE or 15-HEPE.

The aforementioned data indicates that treatment of platelets with 15-HETE, 15-HEPE or 15-HETrE diminished the ability of platelets to produce 12-HETE,

however, the mechanism is unknown. It is possible that these 15-oxylipins could directly inhibit 12-LOX. Therefore, the formation of 12-HETE was measured *in vitro* following the incubation of AA with recombinant 12-LOX in the presence of 15-HETrE, 15-HETE or 15-HEPE to determine if they directly inhibit 12-LOX. Similar to the data obtained with platelets (**Figure 2.4**), 15-HETE ($IC_{50} = 46 \pm 19 \mu M$) was a more potent inhibitor of purified 12-LOX than 15-HETrE ($IC_{50} = 105 \pm 55 \mu M$) or 15-HEPE ($IC_{50} = 142 \pm 11 \mu M$), however, the low potency of these 15-oxylipins indicate no direct inhibition of 12-LOX in the platelet.

12-LOX product profile and kinetics with C20 PUFAs and 15-oxylipins substrates

15-HpETE was previously shown to be converted into 8,15- and 14,15-diHETEs^{10,63} and 8,15-diHETE were capable of inhibiting ADP-induced platelet aggregation⁶; however, 15-HpETE was a poor substrate for 12-LOX. In this study, we demonstrate that 12-LOX poorly converts 15-HpETrE and 15-HpEPE to their 8,15- and 14,15-products, with only ~1% being produced before enzymatic inactivation occurs. Of the small amount of di-oxylipins produced, roughly twice as much of the 14,15-product was made relative to the 8,15-product for the three 15-oxylipins investigated (**Table 2.1**). The 8,15-product is due to the degradation of the 14,15-epoxide, while the 14,15-product is due to oxygenation^{27,29}. This mechanism was confirmed by the increase in the 8,15-product upon lowering of the O₂ concentration (**Table 2.1**). It should be noted that the reaction of 12-LOX with the alcohol form of the 15-oxylipins was significantly reduced, consistent with the formation of the epoxide product, which requires the hydroperoxide moiety.

The kinetics of 12-LOX reacting with the three PUFA substrates, DGLA, AA and EPA, revealed similar kinetic values (**Table 2.2**). The kinetics of the corresponding hydroperoxide 15-oxylipins of these three PUFAs also revealed similar values (*vide supra*), indicating that for both the PUFAs and the 15-oxylipins, the double bond configuration had little effect on kinetics, given that all of these 6 substrates are 20 carbons in length. However, it should be noted that the kinetic rates of the hydroperoxide 15-oxylipins were approximately 10-fold less than that of the PUFA substrates, which agrees with previous results with other oxylin substrates^{13,37,54}.

***Ex vivo* platelet incubation with 15-oxylipins**

The results above indicate that 12-LOX reacts slowly with 15-oxylipins under *in vitro* conditions and therefore, the 15-oxylipins were incubated with platelets in order to determine the reactivity of 12-LOX under *ex vivo* conditions. Specifically, the formation of the di-oxylipins from the 15-oxylipin were measured in platelets incubated with 15-HpETE, 15-HpETrE or 15-HpEPE and their reduced alcohol species, all at 10 mM. The first observation is that the total di-oxylin produced from all three of the hydroperoxide 15-oxylipins is comparable, approximately 100 ng per 1×10^9 platelets and is consistent with amount of di-oxylin produced when 14(S)-hydroperoxydedocosahexaenoic acid (14-HpDHA) was added to platelets¹³. Second, only 1/10 of the reduced alcohol oxylin was produced compared to the hydroperoxide oxylipins, which is consistent with the *in vitro* kinetics, where the alcohol oxylipins were observed to be poorer substrates than the hydroperoxides, consistent with generation of the epoxide product. Finally, both the alcohol and hydroperoxy oxylipins

produced a majority of the 8,15- product (**Table 2.3**), suggesting that the alcohol oxylipin may be an oxygenation product.

12-LOX Allosteric and hypoxic regulation of epoxidation

Oxylipins have been previously determined to dose-dependently affect the ratio of di-oxygenation:epoxidation products^{13,54}, due to allosteric regulation of enzyme mechanism. In order to determine if 15(S)-hydroperoxyeicosapentaenoic acid (15-HpEPE) could also affected the ratio of LOX products, the product profile was assessed in solutions ranging from 1 to 20 mM of 15-HpEPE. Increased concentrations of 15-HpEPE reduced epoxide formation from 84% at 1 mM 15-HpEPE to 58% at 20 mM (**Table 2.4**), indicating that 15-HpEPE is also a 12-LOX allosteric regulator that affects secondary product formation.

The 12-HETrE/15-HETrE ratio in platelets treated with DGLA

12-HETrE and 15-HETrE are antiplatelet oxylipins derived from DGLA that have independently been shown to be produced by DGLA-treated platelets^{12,63,68}. Our group has already demonstrated that supplementation with DGLA increased 12-HETrE formation in the platelet⁶⁸. In order to determine whether platelets were able to form 15-oxylipins, the levels of 12-HETrE and 15-HETrE in the releasate of platelets treated with DGLA (10 μ M) were quantified by mass spectrometry to determine their ratio of formation from a common sample. Since leukocytes are a common contaminate of isolated platelets and a potential source of 15-HETrE, washed human platelets were leukocyte-depleted by magnetic-activated cell sorting^{56,57}. The purity of the leukocyte-depleted platelets was quantified by flow cytometry using leukocyte (CD45) and

platelet (GPIIb α) specific antibodies. The leukocyte-depleted platelets contained 40 ± 11.34 (mean \pm SEM; n= 7) leukocytes per million platelets as detected by flow cytometry (**Figure 2.5A**). Leukocyte-depleted platelets treated with DGLA produced approximately four times as much 12-HETrE (588 ± 352 ng/ml) as 15-HETrE (139 ± 54 ng/ml) for a ratio of 4.2 to 1 (**Figure 2.5B**).

15-LOX expression in human platelets

In this study, we demonstrated that leukocyte-depleted platelets treated with DGLA prior to agonist-induced activation generated 15-HETrE (**Figure 2.5A**); however, it is unclear if 15-LOX or COX-1 produced this 15-oxylin. To assess whether 15-LOX is expressed in platelets, both leukocyte-depleted and non-depleted platelets were probed with 15-LOX-1 or 15-LOX-2 antibodies. As a control, the purified 15-LOX-1, 15-LOX-2, and 12-LOX enzymes^{5,23,41} were tested and as expected, the 15-LOX-1 and 15-LOX-2 antibodies selectively detected the corresponding 15-LOX isozymes, but not the alternate 15-LOX isozyme, nor the 12-LOX enzyme. While 15-LOX-1 expression decreased in leukocyte-depleted platelets compared to non-depleted platelets (**Figure 2.6A**), the expression of 15-LOX-2 did not differ between leukocyte-depleted platelets and non-depleted platelets (**Figure 2.6B**).

Leukocyte-depleted platelets were treated with the 15-LOX-1 selective inhibitor, ML351³⁹, or the 15-LOX-2 selective inhibitor, NCGC00356800²¹, and collagen-induced platelet aggregation were assessed (**Figure 2.6C**). Platelets were also treated with the 12-LOX selective inhibitor, ML355, and with aspirin (ASA), as controls. Agonist-induced platelet aggregation was inhibited following treatment with

ML355 or ASA. However, inhibition of only 15-LOX-1 or 15-LOX-2 did not affect collagen-induced platelet aggregation.

2.5 Discussion

Lipoxygenases (LOXs) are enzymes that catalyze the oxygenation of PUFAs, forming bioactive fatty acids (oxylipins)^{26,35}. LOXs (5-, 12-, and 15-LOX) are expressed in a number of cells and they each produce oxylipins which regulate platelet activity, hemostasis and thrombosis^{66,67}. Regarding the expression of lipoxygenases in platelets, 5-LOX is not expressed in these cells, whereas 12-LOX is highly expressed^{14,66} and its derived oxylipins are known to regulate platelet reactivity^{64,65}. Whether 15-LOX is expressed in platelets has been an ongoing question in the field. While the formation of 15-oxylipins in platelets have already been shown, these studies are not in agreement regarding the role of 15-LOX⁶³ or COX-1^{16,40} in the formation of 15-oxylipins in platelets.

In this study we demonstrated that micromolar levels of 15-HETE, 15-HETrE or 15-HEPE attenuated collagen-induced platelet aggregation. Although several studies reported the 15-HETE and 15-HEPE effects on platelet function^{45,58,59,60}, the effects of 15-HETrE on platelet activity are still not well understood. We have shown that 15-HETrE at micromolar levels attenuated aggregation initiated by low doses of multiple agonists including collagen, thrombin, ADP and AA (**Figure 2.1**). While we demonstrate that the 15-oxylipins have an antiaggregatory effect on platelets, treatment with 15-LOX-1 or 15-LOX-2 inhibitors did not rescue agonist-induced platelet aggregation (**Figure 2.6C**). Since 12-HETE and thromboxane A₂ (TXA₂), the 12-LOX-

derived and the COX-1-derived oxylipins from AA, respectively, have been demonstrated to potentiate platelet activation and aggregation^{30,38}, as expected, inhibition of platelet aggregation was observed following treatment with ML355 or ASA.

The ability of 15-oxylipins to inhibit platelet aggregation suggests that these oxylipins impinge on a common signaling event downstream of receptor activation in the platelet aggregation pathway. Since the 12-LOX-derived oxylipins from AA and DGLA, 12-HETrE and 12-HETE, respectively, play a critical role in regulating platelet reactivity^{38,43,52}, we focused on how 15-HETE and 15-HETrE were regulating platelet signaling following GPVI stimulation. We have shown that both 15-HETE and 15-HETrE inhibited the activation of common signaling events including Ca²⁺ mobilization, and activation of integrin α Ibb3 (**Figure 2.2**). Interestingly, while some 12-LOX oxylipins such as 12-HETrE have been previously shown by our group to inhibit platelet function through activation of the prostacyclin receptor on the surface of the platelet resulting in activation of G_s, formation of cAMP, and activation of PKA, neither 15-HETrE nor 15-HETE resulted in VASP phosphorylation by PKA, suggesting these oxylipins inhibit platelet function in a prostacyclin receptor-independent manner (**Figure 2.3**).

While several key biochemical steps such as calcium mobilization, PKC activation, and integrin activation were shown in the current study to be similarly regulated by 15-HETE and 15-HETrE, the proximal regulatory steps preceding these central biochemical regulators were identified as unique to each of the metabolites

studied. Previously, our group showed that docosapentaenoic acid (DPA) w-6-derived oxylipins activate PPARs in the platelet⁶⁵ and others demonstrated that 15-oxylipins activate PPARs in other cells^{34,46}. In this study, we have shown for the first time that the 15-oxylipins, 15-HETrE and 15-HETE, signal through activation of PPARs in the platelet. While 15-HETrE was found to be a specific agonist for PPARb, 15-HETE appear to function at least partially through the activation of PPARa (**Figure 2.5**). PPAR antagonists reversed the inhibitory effects of lower concentrations of 15-HETE and 15-HETrE, however PPAR inhibitors could not reverse higher concentrations of these oxylipins. These data suggest that 15-HETE and 15-HETrE function predominantly through PPARs, but that at higher concentrations they signal through other compensatory signaling pathways in the platelet independent of PPAR signaling.

A number of monohydroxylated oxylipins have antiplatelet activity; however, how the structure of these oxylipins regulates their mechanism of action remains poorly understood⁶⁶. Independent discoveries demonstrated that 19(S)-hydroxyeicosatetraenoic acid (19-HETE)⁵⁵ and 12-HETrE⁵² both inhibit platelet activation by signaling through the prostacyclin receptor, but the activity of other oxylipins warranted a further investigation into the structure-activity relationship of antiplatelet monohydroxylated oxylipins. A number of physical attributes of monohydroxylated oxylipins have been shown to influence their functionality, such carbon length, double bond configuration, and position/stereochemistry of oxygenation. HETEs and HETrEs both have 20 carbon backbones and double bonds at the 8, 10, and 14 carbons, but HETEs contain an additional double bond at the 5th

carbon. 12-HETE and 12-HETrE have been shown to have opposite effects on platelet activity, suggesting the double bond configuration may be a major contributor to monohydroxylated oxylipin function⁶⁸. Notably, in contrast to the opposite effects observed with 12-HETE and 12-HETrE, this study found that 15-HETE and 15-HETrE have similar but unique functionality. This data suggests that the difference in a single double bond does not change the overall inhibitory effect in platelet function of these 15-oxylipins, as observed with 12-HETE and 12-HETrE, but rather shifts the isoform of PPAR that is activated.

Oxylipin inhibition of platelet function through negative feedback on the production of pro-aggregatory oxylipins has been previously shown⁶⁰. In agreement with previous studies^{31,57,58}, we observe that 15-oxylipins were shown in the current study to partially inhibit 12-HETE formation, which helps explain the inability of PPAR inhibitors to fully reverse 15-oxylipins' antiplatelet effects. Notably, the 15-oxylipins showed a differential ability to inhibit 12-LOX, with platelets treated with 15-HETE, 15-HETrE or 15-HEPE having a 90%, 40%, and 89% decrease in 12-LOX product formation, respectively (**Figure 2.4**). However, the COX-derived product of AA, TXB₂, was not decreased in platelets treated with either 15-HETE, 15-HETrE or 15-HEPE, which suggests that these 15-oxylipins are selectively lowering 12-LOX activity, without lowering the availability of the substrate, AA (**Figure 2.4**).

Previously, our group has demonstrated that treatment with DGLA increased levels of the 12-LOX-derived oxylipin, 12-HETrE, in platelets⁶⁸. In accordance with previous findings^{16,63}, we observe 15-HETrE was detected in the releasate of leukocyte-

depleted platelets treated with DGLA (**Figure 2.5**), suggesting that platelets have the ability to generate 15-oxylipins, but the expression of 15-LOX in platelets remains unclear. Mammalian tissues have two forms of 15-LOX isoforms, reticulocyte 15-LOX (15-LOX-1, gene ALOX15) and epithelial 15-LOX-2 (15-LOX-2, gene ALOX15B), with the tissue distribution of 15-LOX-2 being more limited when compared to that of 15-LOX-1^{7,46}. While 15-LOX-2 is predominantly found in the skin, prostate, lung, and cornea, 15-LOX-1 is expressed in eosinophils, leukocytes, reticulocytes, macrophages, dendritic, and epithelial cells^{20,22}. In agreement with those observations, antibodies for 15-LOX-1 or 15-LOX-2 demonstrated that platelets may express low levels of 15-LOX-1, but do not express 15-LOX-2 (**Figure 2.6**).

Although we demonstrated that 15-LOX-1 might be expressed in platelets at low levels, suggesting that 15-LOX-1 may be involved in the formation of the 15-oxylipins in platelets, based on the significant difference observed on the enzyme's expression between leukocyte-depleted and non-depleted platelets, it is reasonable to consider that platelets have 15-LOX-1 at low concentration or the 15-oxylipins might be formed through a 15-LOX-independent pathway. In fact, previous studies have suggested that 15-oxylipins are produced in a COX-dependent manner in platelets^{16,40,56} and demonstrated that recombinant COX has the ability to metabolize AA into 15(S)-HETE *in vitro*⁵¹. Regardless of the source of the 15-oxylipins, this study suggests that platelets not only form 15-oxylipins, but that they have antiplatelet effects. Hence, it is possible that under physiologic conditions, 15-oxylipins may play an important regulatory role in the onset and stability of the blood clot in the blood

vessel. 15-oxylipins could prevent newly recruited platelets from becoming active at the site of injury, which might regulate the formation of the clot and further attenuate or reduce the thrombotic risk. Furthermore, based on our findings and the fact that 15-LOX-1 is highly expressed in leukocytes⁶⁶, it is reasonable to consider that in whole blood, platelet reactivity might be partially regulated by a transcellular mechanism between platelets and leukocytes through the formation of 15-oxylipins. Therefore, this leukocyte-platelet interaction could regulate clot formation and thus have clinical implication in atherothrombotic diseases through inhibition of platelet activity and thrombosis.

2.6 Tables

Table 2.1 Product profile of h12LOX and 15-oxylipins

h12LOX + substrate	8,15-product (%)	14,15-product (%)
15-HpETrE	77 ± 1	23 ± 1
15-HpETE	66 ± 2	35 ± 2
15-HpEPE	70 ± 1	30 ± 2
15-HpEPE (low O ₂)	83 ± 3	17 ± 3

Table 2.2 12-LOX kinetics with PUFAs and 15-oxylipins

Enzyme + substrate	k_{cat} (s⁻¹)	k_M (μM)	k_{cat}/k_M (s⁻¹μM⁻¹)
DGLA	12 ± 0.3	2.5 ± 0.2	4.9 ± 0.3
AA	11 ± 0.2	0.49 ± 0.07	22 ± 3
EPA	9 ± 0.5	1 ± 0.2	8.7 ± 1.2
15-HpETrE	0.96 ± 0.05	11 ± 1	0.086 ± 0.004
15-HpETE	1.5 ± 0.05	5.8 ± 0.4	0.26 ± 0.001
15-HpEPE	0.93 ± 0.06	9.2 ± 1	0.10 ± 0.008

Table 2.3 Product distribution from reacting platelets with 15-HEPE and 15-HpEPE.

Platelets + substrate	Non-enzymatic (8,15) product (%)	Dioxygenation(8,15/14,15)-product (%)
15S-HEPE	12.6 ± 1.1	87.4 ± 1.1
15S-HpEPE	75.4 ± 0.8	24.6 ± 0.8

Table 2.4 Allosteric effect of 12-LOX with 15-HpEPE

12-LOX + 15-HpEPE	1 µM	2 µM	5 µM	10 µM	15 µM	20 µM
% 8,15-diHEPE	84%	75%	70%	67%	65%	58%

2.7 Figures

Legends

Figure 2.1: 15-HETrE inhibits platelet aggregation independent of the agonist tested. **A)** Washed human platelets (n= 5-8) were treated with increasing concentrations of 12-HETrE, 15-HETrE, 15-HETE or 15-HEPE and then stimulated with collagen (0.25 µg/ml). Data represents mean ± S.E.M. One-way ANOVA statistical analysis with Dunnett's multiple comparison post-test was performed between DMSO and oxylipins. **B)** Washed human platelets (n= 4-6) were treated with increasing concentrations of 12-HETrE, 15-HETrE, 15-HETE or 15-HEPE and then stimulated with increasing concentrations of collagen. Data represents mean ± S.E.M. One-way ANOVA statistical analysis with Dunnett's multiple comparison post-test was performed between DMSO and 15-oxylipins. Washed human platelets were treated with 15-HETrE (10 µM) or vehicle (DMSO) for 10 minutes and then stimulated with increasing concentrations of **C)** thrombin (n=6), **D)** ADP (n=6) or **E)** AA (n=6) in an aggregometer. Data represent mean ± SEM of the maximum aggregation. Two-way ANOVA statistical analysis was performed between DMSO and 15-HETrE with Dunnett's multiple comparison post-test (**p* <0.05, ***p* <0.01, ****p* <0.001)

Figure 2.2: 15-HETE and 15-HETrE inhibit intracellular platelet signaling. **A)** Platelets (n=4) were treated with a 15-HETE or 15-HETrE (10 μ M) and Fluo-4-AM, a cell-permeable, calcium-sensitive dye, then stimulated with convulxin (CVX; 2.5 ng/ml), and Ca^{2+} mobilization was analyzed by flow cytometry in real-time. **B)** Platelets (n=9) that had been treated with 15-HETE or 15-HETrE (10 μ M) were stimulated with CVX (2.5 ng/ml) in the presence of FITC-conjugated PAC-1, an antibody specific to the active conformation of α IIb β 3, and analyzed by flow cytometry in real-time. Two-way ANOVA. **C)** Collagen-stimulated platelets (n=5) pretreated with either 15-HETE (10 μ M) or 15-HETrE (10 μ M) were lysed, and Western blots were performed with antibodies to the phospho-serine PKC substrate motif and GAPDH. Two-tailed paired *t* test. **D)** ATP secretion, a marker of dense granule secretion, was measured from platelets (n= 4-5) incubated with 15-HETE or 15-HETrE (10 μ M) in a lumi-aggregometer in the presence of increasing concentrations of collagen. Two-way ANOVA with Dunnett's multiple comparison post-test. **E)** P-selectin surface expression, a marker of α -granule secretion, was quantified in collagen-stimulated platelets (n=4) treated with 15-HETE or 15-HETrE (10 μ M) by flow cytometry using a PE-conjugated P-selectin antibody. Data represent mean \pm SEM. Two-tailed paired *t* test. **p*<0.05, ***p*<0.01, ****p*<0.001.

Figure 2.3: 15-HETE and 15-HETrE inhibit platelet activation via distinct mechanisms. **A)** The lysates of platelets (n=3-4) treated with forskolin, a direct adenylyl cyclase agonist, oxylipins (10 μ M) or DMSO were separated on a 10% SDS-PAGE gel and Western blots were performed with antibodies to phospho- and total VASP. **B)** Platelets were incubated with PPAR α (GW6471; 10 μ M; n= 3-6), PPAR β (GW3787; 10 μ M; n= 3-6), or PPAR γ (GW9662; 10 μ M; n=3-6) antagonist, prior to the treatment with 15-LOX oxylipin, and then stimulated with collagen (0.25-1 μ g/ml). Data represent mean \pm SEM. Two-tailed paired *t* test.

Figure 2.4: 15-oxylipins inhibit 12-LOX activity. The levels of **A)** 12-HETE and **B)** TXB₂ were quantified in the lysate of collagen-stimulated (5 μ g/ml) platelets (n= 5) pretreated with 15-HETE (10 μ M), 15-HETrE (10 μ M) or 15-HETE (10 μ M). Two-tailed paired *t* test. Data represent mean \pm SEM. ****p*<0.001.

Figure 2.5: Leukocyte-depleted platelets produce 15-HETrE. **A)** Leukocyte-depleted platelets were stained with antibodies specific to platelets (GPIb α) and leukocytes (CD45), and analyzed by flow cytometry to quantify the number of residual polymorphonuclear leukocytes (PMNs) (CD45-positive, GPIb α -negative cells) in each sample. **B)** The levels of 12-HETrE and 15-HETrE were measured in the releasate of leukocyte-depleted platelets (n=3) treated with DGLA (10 μ M). Data represent mean \pm SEM.

Figure 2.6: 15-LOX-1 might be expressed in platelets, but not 15-LOX-2. The lysates of leukocyte depleted platelets (n=3) and non-depleted platelets (n=1), 15-LOX-1, 15-LOX-2 and 12-LOX enzymes were separated on a 10% SDS-PAGE gel and Western blots were performed with antibodies to **A)** 15-LOX-1 or **B)** 15-LOX-2. An antibody to b-actin was used as loading control. Leukocyte-depleted platelets were treated with 15-LOX-1 inhibitor (ML351, 10mM), 15-LOX-2 inhibitor (NCGC00356800, 10mM) or/and 12-LOX inhibitor (ML355, 20mM), or aspirin (ASA, 100mM) for 10min for ML351, NCGC00356800 or ML355 and 40min for ASA, prior stimulation with 2 mg/ml of collagen and **C)** platelet aggregation (n=6) were assessed. Data represent mean \pm SEM. Two-tailed paired *t* test. **p*<0.05, ***p*<0.01, ****p*<0.001, *****p*<0.0001.

Figure 2.7: Schematic overview of the mechanism underlying the inhibitory effect of 15-oxylipins on platelet reactivity. In platelets, 15-LOX-1 or COX-1 might metabolize free DGLA and AA into 15-HETrE and 15-HETE, respectively. Both oxylipins acts partially through activation of PPARs, impinging intracellular signaling and inhibiting 12-LOX activity, which lead to inhibition of platelet activation in response to collagen.

Figure 2.1

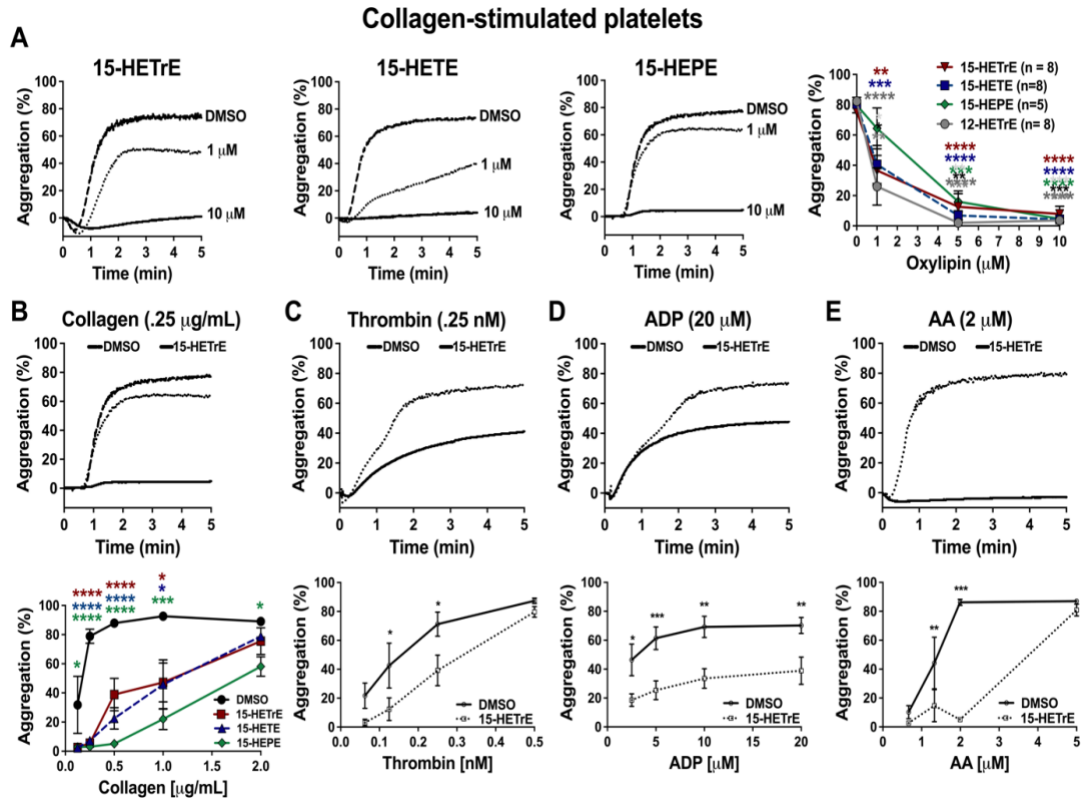


Figure 2.2

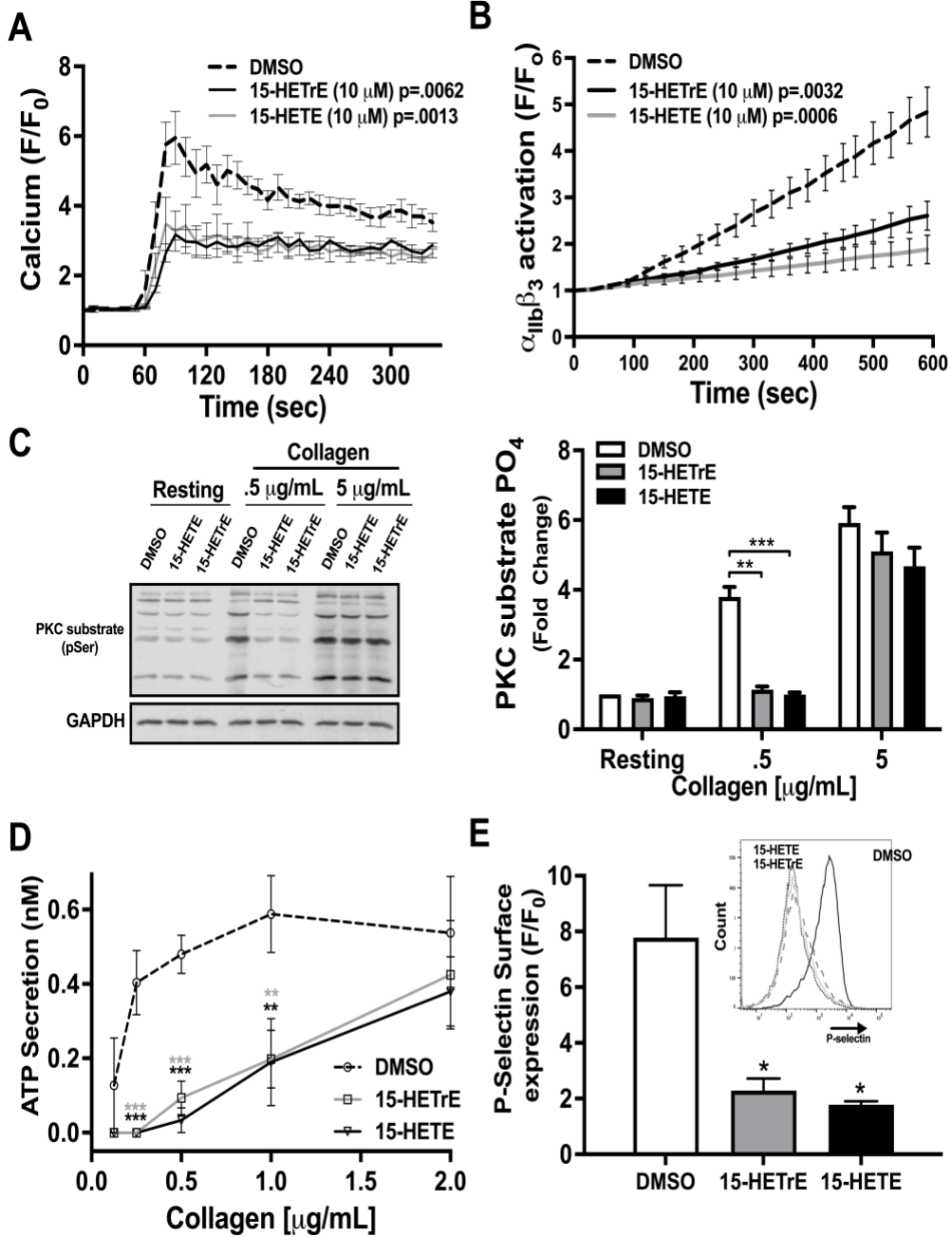


Figure 2.3

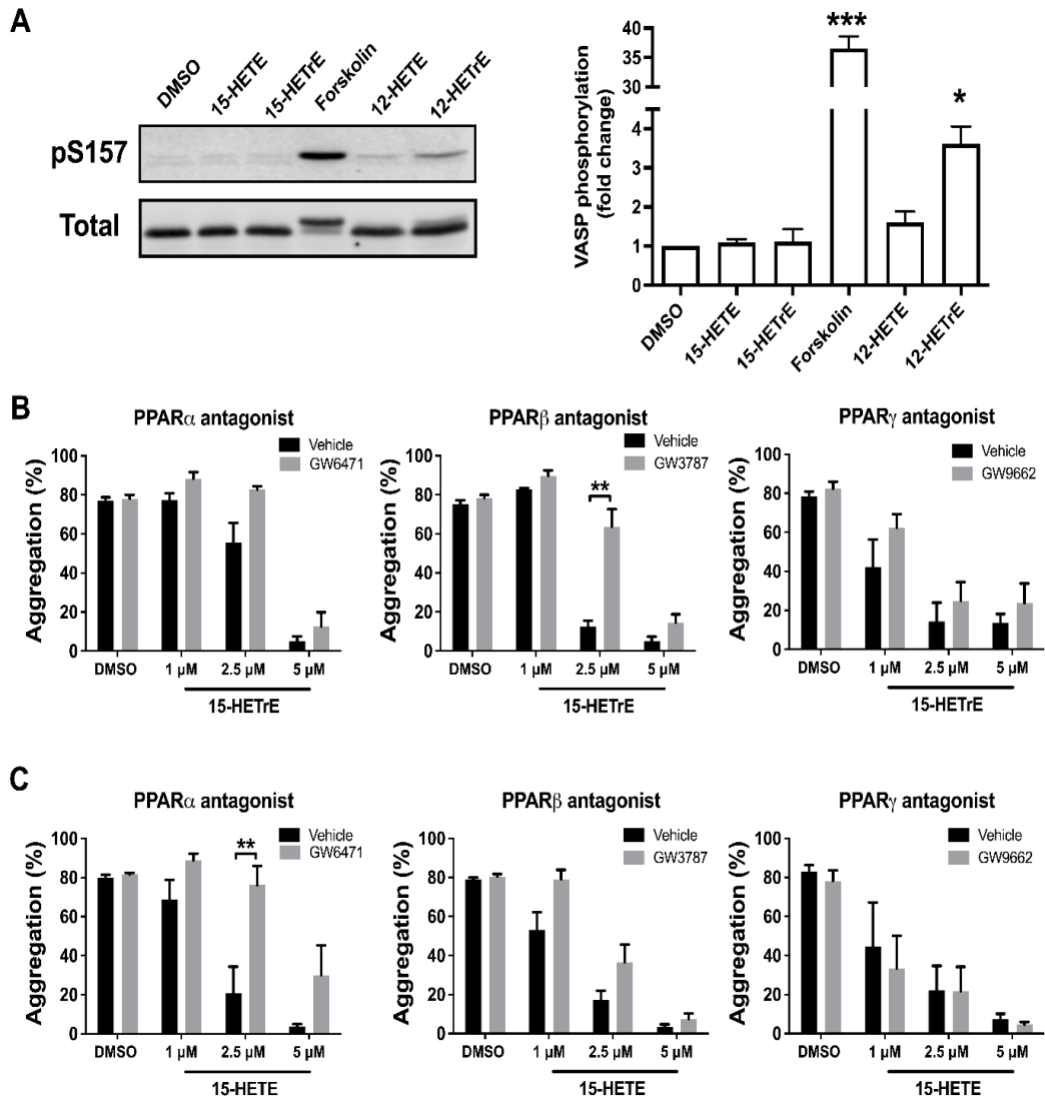


Figure 2.4

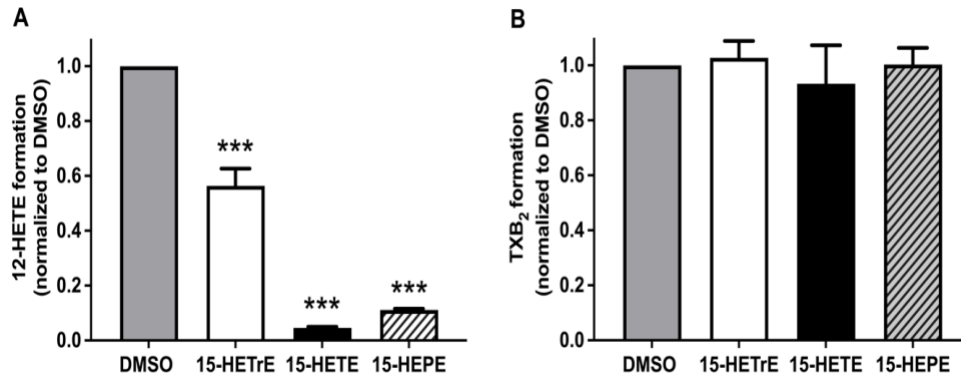


Figure 2.5

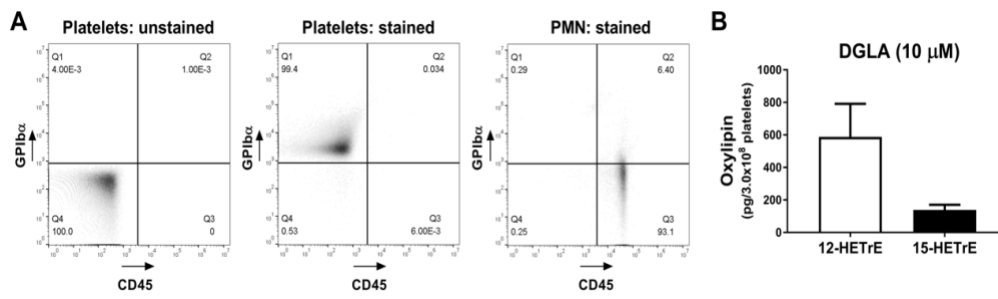


Figure 2.6

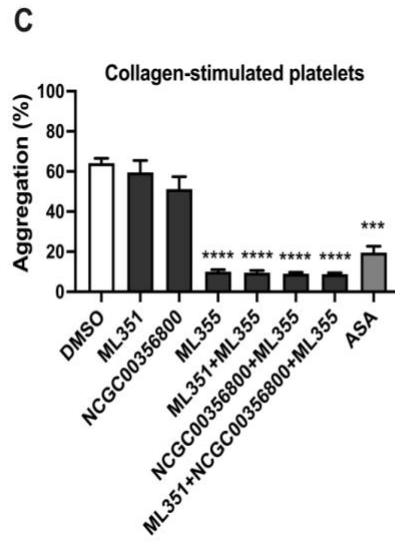
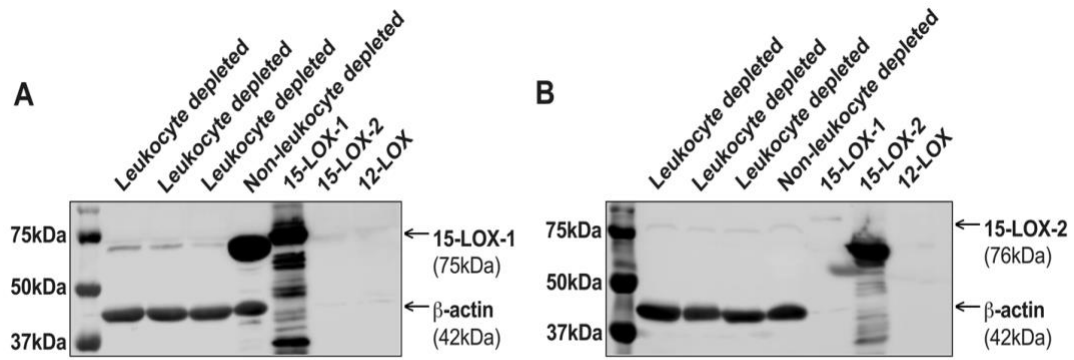
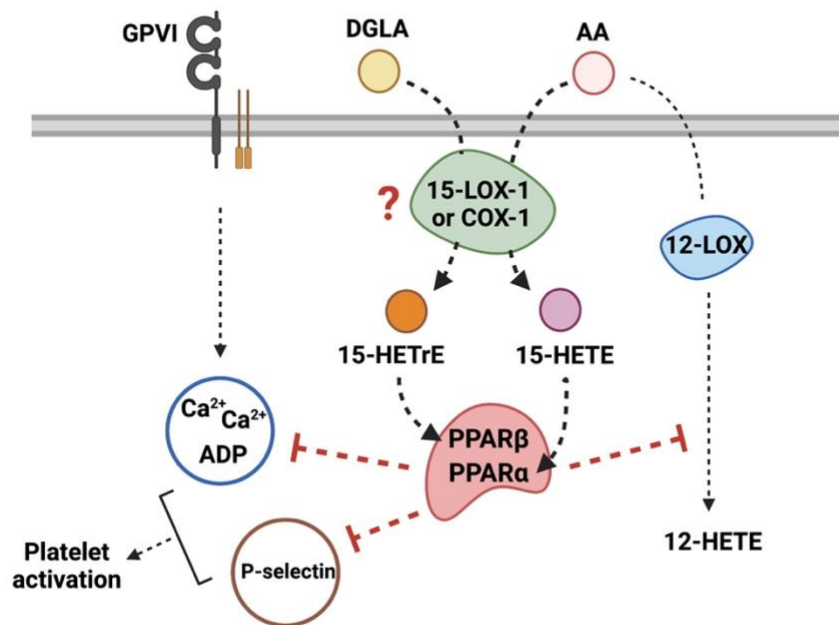


Figure 2.7



2.8 References

- [1] Adili, R., M. Hawley and M. Holinstat (2018). "Regulation of platelet function and thrombosis by omega-3 and omega-6 polyunsaturated fatty acids." *Prostaglandins Other Lipid Mediat* **139**: 10-18.
- [2] Adili, R., B. E. Tourdot, K. Mast, J. Yeung, J. C. Freedman, A. Green, D. K. Luci, A. Jadhav, A. Simeonov, D. J. Maloney, T. R. Holman and M. Holinstat (2017). "First Selective 12-LOX Inhibitor, ML355, Impairs Thrombus Formation and Vessel Occlusion In Vivo With Minimal Effects on Hemostasis." *Arterioscler Thromb Vasc Biol* **37**(10): 1828-1839.
- [3] Ali, F. Y., P. C. Armstrong, A. R. Dhanji, A. T. Tucker, M. J. Paul-Clark, J. A. Mitchell and T. D. Warner (2009). "Antiplatelet actions of statins and fibrates are mediated by PPARs." *Arterioscler Thromb Vasc Biol* **29**(5): 706-711.
- [4] Ali, F. Y., S. J. Davidson, L. A. Moraes, S. L. Traves, M. Paul-Clark, D. Bishop-Bailey, T. D. Warner and J. A. Mitchell (2006). "Role of nuclear receptor signaling in platelets: antithrombotic effects of PPARbeta." *Faseb j* **20**(2): 326-328.
- [5] Amagata, T., S. Whitman, T. A. Johnson, C. C. Stessman, C. P. Loo, E. Lobkovsky, J. Clardy, P. Crews and T. R. Holman (2003). "Exploring sponge-derived terpenoids for their potency and selectivity against 12-human, 15-human, and 15-soybean lipoxygenases." *J Nat Prod* **66**(2): 230-235.
- [6] Bild, G. S., S. G. Bhat, B. Axelrod and P. G. Iatridis (1978). "Inhibition of aggregation of human platelets by 8,15-dihydroperoxides of 5,9,11,13-eicosatetraenoic and 9,11,13-eicosatrienoic acids." *Prostaglandins* **16**(5): 795-801.
- [7] Brash, A. R., W. E. Boeglin and M. S. Chang (1997). "Discovery of a second 15S-lipoxygenase in humans." *Proc Natl Acad Sci U S A* **94**(12): 6148-6152.
- [8] Butovich, I. A. (2006). "A one-step method of 10,17-dihydro(pero)xydocosa-hexa-4Z,7Z,11E,13Z,15E,19Z-enoic acid synthesis by soybean lipoxygenase." *J Lipid Res* **47**(4): 854-863.
- [9] Butt, E., K. Abel, M. Krieger, D. Palm, V. Hoppe, J. Hoppe and U. Walter (1994). "cAMP- and cGMP-dependent protein kinase phosphorylation sites of the focal

adhesion vasodilator-stimulated phosphoprotein (VASP) in vitro and in intact human platelets." *J Biol Chem* **269**(20): 14509-14517.

[10] Dadaian, M. and P. Westlund (1999). "Albumin modifies the metabolism of hydroxyeicosatetraenoic acids via 12-lipoxygenase in human platelets." *J Lipid Res* **40**(5): 940-947.

[11] Du, H., H. Hu, H. Zheng, J. Hao, J. Yang and W. Cui (2014). "Effects of peroxisome proliferator-activated receptor γ in simvastatin antiplatelet activity: influences on cAMP and mitogen-activated protein kinases." *Thromb Res* **134**(1): 111-120.

[12] Falardeau, P., M. Hamberg and B. Samuelsson (1976). "Metabolism of 8,11,14-eicosatrienoic acid in human platelets." *Biochim Biophys Acta* **441**(2): 193-200.

[13] Freedman, C., A. Tran, B. E. Tourdot, C. Kalyanaraman, S. Perry, M. Holinstat, M. P. Jacobson and T. R. Holman (2020). "Biosynthesis of the Maresin Intermediate, 13S,14S-Epoxy-DHA, by Human 15-Lipoxygenase and 12-Lipoxygenase and Its Regulation through Negative Allosteric Modulators." *Biochemistry* **59**(19): 1832-1844.

[14] Funk, C. D., L. Furci and G. A. FitzGerald (1990). "Molecular cloning, primary structure, and expression of the human platelet/erythrocyte cell 12-lipoxygenase." *Proc Natl Acad Sci U S A* **87**(15): 5638-5642.

[15] Furie, B., B. C. Furie and R. Flaumenhaft (2001). "A journey with platelet P-selectin: the molecular basis of granule secretion, signalling and cell adhesion." *Thromb Haemost* **86**(1): 214-221.

[16] Guichardant, M., S. Natchayan-Durbin and M. Lagarde (1988). "Occurrence of the 15-hydroxy derivative of dihomogammalinolenic acid in human platelets and its biological effect." *Biochim Biophys Acta* **962**(1): 149-154.

[17] Harper, M. T. and A. W. Poole (2010). "Diverse functions of protein kinase C isoforms in platelet activation and thrombus formation." *J Thromb Haemost* **8**(3): 454-462.

- [18] Holinstat, M., O. Boutaud, P. L. Apopa, J. Vesci, M. Bala, J. A. Oates and H. E. Hamm (2011). "Protease-activated receptor signaling in platelets activates cytosolic phospholipase A2 α differently for cyclooxygenase-1 and 12-lipoxygenase catalysis." *Arterioscler Thromb Vasc Biol* **31**(2): 435-442.
- [19] Ikei, K. N., J. Yeung, P. L. Apopa, J. Ceja, J. Vesci, T. R. Holman and M. Holinstat (2012). "Investigations of human platelet-type 12-lipoxygenase: role of lipoxygenase products in platelet activation." *J Lipid Res* **53**(12): 2546-2559.
- [20] Ivanov, I., H. Kuhn and D. Heydeck (2015). "Structural and functional biology of arachidonic acid 15-lipoxygenase-1 (ALOX15)." *Gene* **573**(1): 1-32.
- [21] Jameson, J. B., 2nd, A. Kantz, L. Schultz, C. Kalyanaraman, M. P. Jacobson, D. J. Maloney, A. Jadhav, A. Simeonov and T. R. Holman (2014). "A high throughput screen identifies potent and selective inhibitors to human epithelial 15-lipoxygenase-2." *PLoS One* **9**(8): e104094.
- [22] Jiang, W. G., G. Watkins, A. Douglas-Jones and R. E. Mansel (2006). "Reduction of isoforms of 15-lipoxygenase (15-LOX)-1 and 15-LOX-2 in human breast cancer." *Prostaglandins Leukot Essent Fatty Acids* **74**(4): 235-245.
- [23] Joshi, N., E. K. Hoobler, S. Perry, G. Diaz, B. Fox and T. R. Holman (2013). "Kinetic and structural investigations into the allosteric and pH effect on the substrate specificity of human epithelial 15-lipoxygenase-2." *Biochemistry* **52**(45): 8026-8035.
- [24] Kim, H. Y., J. W. Karanian and N. Salem, Jr. (1990). "Formation of 15-lipoxygenase product from docosahexaenoic acid (22:6w3) by human platelets." *Prostaglandins* **40**(5): 539-549.
- [25] Kozak, K. R., R. A. Gupta, J. S. Moody, C. Ji, W. E. Boeglin, R. N. DuBois, A. R. Brash and L. J. Marnett (2002). "15-Lipoxygenase metabolism of 2-arachidonylglycerol. Generation of a peroxisome proliferator-activated receptor alpha agonist." *J Biol Chem* **277**(26): 23278-23286.
- [26] Kuhn, H., M. Walther and R. J. Kuban (2002). "Mammalian arachidonate 15-lipoxygenases structure, function, and biological implications." *Prostaglandins Other Lipid Mediat* **68-69**: 263-290.

- [27] Kutzner, L., K. Goloshchapova, K. M. Rund, M. Jübermann, M. Blum, M. Rothe, S. F. Kirsch, W. H. Schunck, H. Kühn and N. H. Schebb (2020). "Human lipoxygenase isoforms form complex patterns of double and triple oxygenated compounds from eicosapentaenoic acid." *Biochim Biophys Acta Mol Cell Biol Lipids* **1865**(12): 158806.
- [28] Lannan, K. L., J. Sahler, N. Kim, S. L. Spinelli, S. B. Maggirwar, O. Garraud, F. Cognasse, N. Blumberg and R. P. Phipps (2015). "Breaking the mold: transcription factors in the anucleate platelet and platelet-derived microparticles." *Front Immunol* **6**: 48.
- [29] Maas, R. L. and A. R. Brash (1983). "Evidence for a lipoxygenase mechanism in the biosynthesis of epoxide and dihydroxy leukotrienes from 15(S)-hydroperoxyicosatetraenoic acid by human platelets and porcine leukocytes." *Proc Natl Acad Sci U S A* **80**(10): 2884-2888.
- [30] Maskrey, B. H., G. F. Rushworth, M. H. Law, A. T. Treweeke, J. Wei, S. J. Leslie, I. L. Megson and P. D. Whitfield (2014). "12-hydroxyicosatetraenoic acid is associated with variability in aspirin-induced platelet inhibition." *J Inflamm (Lond)* **11**(1): 33.
- [31] Mitchell, P. D., C. Hallam, P. E. Hemsley, G. H. Lord and D. Wilkinson (1984). "Inhibition of platelet 12-lipoxygenase by hydroxy-fatty acids." *Biochemical Society Transactions* **12**(5): 839-841.
- [32] Moers, A., N. Wettschureck, S. Grüner, B. Nieswandt and S. Offermanns (2004). "Unresponsiveness of platelets lacking both Galpha(q) and Galpha(13). Implications for collagen-induced platelet activation." *J Biol Chem* **279**(44): 45354-45359.
- [33] Moraes, L. A., M. Spyridon, W. J. Kaiser, C. I. Jones, T. Sage, R. E. Atherton and J. M. Gibbins (2010). "Non-genomic effects of PPARgamma ligands: inhibition of GPVI-stimulated platelet activation." *J Thromb Haemost* **8**(3): 577-587.
- [34] Naruhn, S., W. Meissner, T. Adhikary, K. Kaddatz, T. Klein, B. Watzer, S. Müller-Brüsselbach and R. Müller (2010). "15-hydroxyicosatetraenoic acid is a preferential peroxisome proliferator-activated receptor beta/delta agonist." *Mol Pharmacol* **77**(2): 171-184.

- [35] Orafaie, A., M. Mousavian, H. Orafai and H. Sadeghian (2020). "An overview of lipoxygenase inhibitors with approach of in vivo studies." *Prostaglandins Other Lipid Mediat* **148**: 106411.
- [36] Paul, B. Z., J. Jin and S. P. Kunapuli (2004). "Preparation of mRNA and cDNA libraries from platelets and megakaryocytes." *Methods Mol Biol* **273**: 435-454.
- [37] Perry, S. C., C. Kalyanaraman, B. E. Tourdot, W. S. Conrad, O. Akinkugbe, J. C. Freedman, M. Holinstat, M. P. Jacobson and T. R. Holman (2020). "15-Lipoxygenase-1 biosynthesis of 7S,14S-diHDHA implicates 15-lipoxygenase-2 in biosynthesis of resolvin D5." *J Lipid Res* **61**(7): 1087-1103.
- [38] Porro, B., P. Songia, I. Squellerio, E. Tremoli and V. Cavalca (2014). "Analysis, physiological and clinical significance of 12-HETE: a neglected platelet-derived 12-lipoxygenase product." *J Chromatogr B Analyt Technol Biomed Life Sci* **964**: 26-40.
- [39] Rai, G., N. Joshi, S. Perry, A. Yasgar, L. Schultz, J. E. Jung, Y. Liu, Y. Terasaki, G. Diaz, V. Kenyon, A. Jadhav, A. Simeonov, K. van Leyen, T. R. Holman and D. J. Maloney (2010). Discovery of ML351, a Potent and Selective Inhibitor of Human 15-Lipoxygenase-1. Probe Reports from the NIH Molecular Libraries Program. Bethesda (MD), National Center for Biotechnology Information (US).
- [40] Rauzi, F., N. S. Kirkby, M. L. Edin, J. Whiteford, D. C. Zeldin, J. A. Mitchell and T. D. Warner (2016). "Aspirin inhibits the production of proangiogenic 15(S)-HETE by platelet cyclooxygenase-1." *Faseb j* **30**(12): 4256-4266.
- [41] Robinson, S. J., E. K. Hoobler, M. Riener, S. T. Loveridge, K. Tenney, F. A. Valeriote, T. R. Holman and P. Crews (2009). "Using enzyme assays to evaluate the structure and bioactivity of sponge-derived meroterpenes." *J Nat Prod* **72**(10): 1857-1863.
- [42] Schrör, K. (1997). "Aspirin and platelets: the antiplatelet action of aspirin and its role in thrombosis treatment and prophylaxis." *Semin Thromb Hemost* **23**(4): 349-356.
- [43] Sekiya, F., J. Takagi, T. Usui, K. Kawajiri, Y. Kobayashi, F. Sato and Y. Saito (1991). "12S-hydroxyeicosatetraenoic acid plays a central role in the regulation of platelet activation." *Biochem Biophys Res Commun* **179**(1): 345-351.

[44] Serhan, C. N., J. Dalli, S. Karamnov, A. Choi, C. K. Park, Z. Z. Xu, R. R. Ji, M. Zhu and N. A. Petasis (2012). "Macrophage proresolving mediator maresin 1 stimulates tissue regeneration and controls pain." *Faseb Journal* **26**(4): 1755-1765.

[45] Setty, B. N. and M. J. Stuart (1986). "15-Hydroxy-5,8,11,13-eicosatetraenoic acid inhibits human vascular cyclooxygenase. Potential role in diabetic vascular disease." *J Clin Invest* **77**(1): 202-211.

[46] Shappell, S. B., D. S. Keeney, J. Zhang, R. Page, S. J. Olson and A. R. Brash (2001). "15-Lipoxygenase-2 expression in benign and neoplastic sebaceous glands and other cutaneous adnexa." *J Invest Dermatol* **117**(1): 36-43.

[47] Smolenski, A. (2012). "Novel roles of cAMP/cGMP-dependent signaling in platelets." *J Thromb Haemost* **10**(2): 167-176.

[48] Smyrniotis, C. J., S. R. Barbour, Z. Xia, M. S. Hixon and T. R. Holman (2014). "ATP allosterically activates the human 5-lipoxygenase molecular mechanism of arachidonic acid and 5(S)-hydroperoxy-6(E),8(Z),11(Z),14(Z)-eicosatetraenoic acid." *Biochemistry* **53**(27): 4407-4419.

[49] Spector, A. A., J. A. Gordon and S. A. Moore (1988). "Hydroxyeicosatetraenoic acids (HETEs)." *Progress in Lipid Research* **27**(4): 271-323.

[50] Thuillier, P., A. R. Brash, J. P. Kehrer, J. B. Stimmel, L. M. Leesnitzer, P. Yang, R. A. Newman and S. M. Fischer (2002). "Inhibition of peroxisome proliferator-activated receptor (PPAR)-mediated keratinocyte differentiation by lipoxygenase inhibitors." *Biochem J* **366**(Pt 3): 901-910.

[51] Thuresson, E. D., K. M. Lakkides and W. L. Smith (2000). "Different catalytically competent arrangements of arachidonic acid within the cyclooxygenase active site of prostaglandin endoperoxide H synthase-1 lead to the formation of different oxygenated products." *J Biol Chem* **275**(12): 8501-8507.

[52] Tourdot, B. E., R. Adili, Z. R. Isingizwe, M. Ebrahim, J. C. Freedman, T. R. Holman and M. Holinstat (2017). "12-HETRe inhibits platelet reactivity and thrombosis in part through the prostacyclin receptor." *Blood Adv* **1**(15): 1124-1131.

- [53] Tourdot, B. E., I. Ahmed and M. Holinstat (2014). "The emerging role of oxylipins in thrombosis and diabetes." *Front Pharmacol* **4**: 176.
- [54] Tsai, W. C., C. Kalyanaraman, A. Yamaguchi, M. Holinstat, M. P. Jacobson and T. R. Holman (2021). "In Vitro Biosynthetic Pathway Investigations of Neuroprotectin D1 (NPD1) and Protectin DX (PDX) by Human 12-Lipoxygenase, 15-Lipoxygenase-1, and 15-Lipoxygenase-2." *Biochemistry* **60**(22): 1741-1754.
- [55] Tunaru, S., R. Chennupati, R. M. Nüsing and S. Offermanns (2016). "Arachidonic Acid Metabolite 19(S)-HETE Induces Vasorelaxation and Platelet Inhibition by Activating Prostacyclin (IP) Receptor." *PLoS One* **11**(9): e0163633.
- [56] Turnbull, R. E., K. N. Sander, J. Turnbull, D. A. Barrett and A. H. Goodall (2022). "Profiling oxylipins released from human platelets activated through the GPVI collagen receptor." *Prostaglandins Other Lipid Mediat* **158**: 106607.
- [57] Vanderhoek, J. Y. and J. M. Bailey (1984). "Activation of a 15-lipoxygenase/leukotriene pathway in human polymorphonuclear leukocytes by the anti-inflammatory agent ibuprofen." *J Biol Chem* **259**(11): 6752-6756.
- [58] Vanderhoek, J. Y., N. W. Schoene and P. P. Pham (1991). "Inhibitory potencies of fish oil hydroxy fatty acids on cellular lipoxygenases and platelet aggregation." *Biochem Pharmacol* **42**(4): 959-962.
- [59] Vedelago, H. R. and V. G. Mahadevappa (1988). "Differential effects of 15-HPETE on arachidonic acid metabolism in collagen-stimulated human platelets." *Biochem Biophys Res Commun* **150**(1): 177-184.
- [60] Vericel, E. and M. Lagarde (1980). "15-Hydroperoxyeicosatetraenoic acid inhibits human platelet aggregation." *Lipids* **15**(6): 472-474.
- [61] Vijil, C., C. Hermansson, A. Jeppsson, G. Bergström and L. M. Hultén (2014). "Arachidonate 15-lipoxygenase enzyme products increase platelet aggregation and thrombin generation." *PLoS One* **9**(2): e88546.

[62] Wecksler, A. T., V. Kenyon, N. K. Garcia, J. D. Deschamps, W. A. van der Donk and T. R. Holman (2009). "Kinetic and structural investigations of the allosteric site in human epithelial 15-lipoxygenase-2." *Biochemistry* **48**(36): 8721-8730.

[63] Wong, P. Y., P. Westlund, M. Hamberg, E. Granström, P. H. Chao and B. Samuelsson (1985). "15-Lipoxygenase in human platelets." *J Biol Chem* **260**(16): 9162-9165.

[64] Yamaguchi, A., L. Stanger, C. J. Freedman, M. Standley, T. Hoang, R. Adili, W. C. Tsai, C. van Hoorebeke, T. R. Holman and M. Holinstat (2021). "DHA 12-LOX-derived oxylipins regulate platelet activation and thrombus formation through a PKA-dependent signaling pathway." *J Thromb Haemost* **19**(3): 839-851.

[65] Yeung, J., R. Adili, A. Yamaguchi, C. J. Freedman, A. Chen, R. Shami, A. Das, T. R. Holman and M. Holinstat (2020). "Omega-6 DPA and its 12-lipoxygenase-oxidized lipids regulate platelet reactivity in a nongenomic PPAR α -dependent manner." *Blood Adv* **4**(18): 4522-4537.

[66] Yeung, J., M. Hawley and M. Holinstat (2017). "The expansive role of oxylipins on platelet biology." *J Mol Med (Berl)* **95**(6): 575-588.

[67] Yeung, J. and M. Holinstat (2011). "12-lipoxygenase: a potential target for novel anti-platelet therapeutics." *Cardiovasc Hematol Agents Med Chem* **9**(3): 154-164.

[68] Yeung, J., B. E. Tourdot, R. Adili, A. R. Green, C. J. Freedman, P. Fernandez-Perez, J. Yu, T. R. Holman and M. Holinstat (2016). "12(S)-HETrE, a 12-Lipoxygenase Oxylipin of Dihomo- γ -Linolenic Acid, Inhibits Thrombosis via G α s Signaling in Platelets." *Arterioscler Thromb Vasc Biol* **36**(10): 2068-2077.

Chapter 3

KINETIC AND MECHANISTIC INVESTIGATIONS OF A LIPOXYGENASE ACTIVATOR REVEAL ISOFORM SPECIFICITY AND V-TYPE ACTIVATION

3.1 Abstract

Regulation of lipoxygenase (LOX) activity is of great interest due to the involvement of the various LOX isoforms in the inflammatory process and hence many diseases. The bulk of investigations have centered around the discovery and design of inhibitors. However, the emerging understanding of the role of h15-LOX-1 in the resolution of inflammation provides rationale for the development of activators as well. While previous inquiries have discovered and characterized allosteric regulation that occurred independent of the active site, these allosteric molecules were similar to the substrate and/or product in their composition. The current work further characterizes a previously discovered small molecule activator, PKUMDL_MH_1001 (**1**), which activates h15-LOX-1. Structural characterization of **1** identifies it as a mixture of *cis*- and *trans*-diastereomers, with kinetic analysis indicating similar potency between the two, *cis*-**1** and *trans*-**1**. **1** activates catalysis with arachidonic acid ($AC_{50} = 7.8 \pm 1 \text{ mM}$, $A_{\text{max}} = 240\%$) and linoleic acid ($AC_{50} = 5.3 \pm 0.7 \text{ mM}$, $A_{\text{max}} = 98\%$), but not docosahexaenoic acid (DHA) or mono-oxylipins. Steady-state kinetics demonstrated V-type activation for **1**, with a *b* value of 2.2 ± 0.4 and an K_x of $16 \pm 1 \text{ mM}$. Finally, the mechanism of activation was not due to decreasing substrate inhibition, nor did **1** affect inhibitor or allosteric effector activity, indicating a unique binding site for **1**. Future work will be aimed at the design and development of a small molecule activator that is capable of activating h15-LOX-1 when reacting with DHA and other omega-3 fatty acids while not activating reactions with AA and LA.

3.2 Introduction

Lipoxygenases (LOX) are non-heme iron enzymes found throughout the animal¹ and plant kingdoms,^{1, 2} as well as certain bacteria.^{3, 4} They catalyze the dioxygenation of polyunsaturated fatty acids (PUFA) containing at least one *cis*-1,4-pentadiene motif. In humans there are four main isoforms that have been extensively studied: human leukocyte 5-LOX (h5-LOX, ALOX5),⁵ human platelet 12-LOX (h12-LOX, ALOX12),⁶ human reticulocyte 15-LOX-1 (h15-LOX-1, ALOX15),⁷ and human epithelial 15-LOX-2 (h15-LOX-2, ALOX15B).⁸ They are named based on their positional specificity on the canonical substrate, arachidonic acid (AA), with h15-LOX-1 producing 15-hydroperoxyeicosatetraenoic acid (15-HpETE), and so forth. These LOX products, often referred to as oxylipins, are potent signaling mediators involved in a variety of cellular processes and responses, such as inflammation.⁹⁻¹² Acute inflammation is a necessity in response to injury or infection,¹³ with LOX and cyclooxygenase (COX) metabolizing AA and linoleic acid (LA), into pro-inflammatory signaling molecules, such as HETEs, HODEs, prostaglandins, and thromboxanes.¹⁴⁻¹⁸ HETEs can be further metabolized by LOX and/or hydrolase enzymes to produce leukotrienes and eoxins.¹⁹⁻²¹ Membrane-bound fatty acids (i.e. phospholipids) are also metabolized by certain LOXs, such as h15-LOX-1 and h15-LOX-2, leading to the degradation of cellular membranes, which has been implicated in the progression of ferroptosis, a non-apoptotic form of programmed cell death.^{22, 23} LOX is also involved in the resolution of inflammation, with lipoxins, maresins, resolvins, and protectins playing an important role in the

resolution of both acute and chronic inflammation.²⁴⁻²⁷ These molecules are known as specialized pro-resolving mediators (SPM).²⁸

Given the important role of LOXs in both the initiation and resolution of inflammation, it is logical that LOX specific inhibitors would be of great value to understanding their role in biology. The development of isoform-specific LOX inhibitors has provided the drug development field with extensive tools for untangling the complicated inflammatory network^{29, 30} Zileuton, which targets h5-LOX,³¹ is the only FDA approved LOX therapeutic and is used for the treatment of asthma by decreasing the production of the pro-inflammatory molecule, leukotriene.³² Additional potential hLOX therapeutics undergoing further investigations include: a platelet 12-LOX inhibitor, ML355,³³ an h12-LOX inhibitor proposed for the potential treatment of heparin-induced thrombocytopenia (HIT) and type-1 diabetes,³⁴ as well as other inhibitors.³⁵⁻³⁷ The h15-LOX-1 inhibitor, ML351,³⁸ is being investigated for the possible treatment of stroke^{39, 40} and chronic pain.⁴¹ In addition, other low-nM h15-LOX-1 inhibitors have been used to study macrophage inflammation.⁴²⁻⁴⁶ While these inhibitors have proven to be invaluable tools for understanding the role of LOX in cellular processes, our expanded understanding of the pro-resolution role of SPM suggest that molecules that activate LOXs could also help our study of the role of LOX in biology. For example, allosteric regulation of human LOX during certain points of the inflammatory cascade could affect resolution thereby lowering the level of inflammation.

Oxylipins allosterically regulate the activity of human LOX, with 15S-HpEPE, 14S-HpDHA, and 17S-HpDHA altering the oxygenation/dehydration product ratio of h15-LOX-1,^{47, 48} despite having no appreciable effect on the enzyme's overall turnover rate. Furthermore, 12S-HpETE and 13S-HpODE, were shown to affect the substrate specificity between AA and LA, which was independent of the oxidation state of the oxylipin, with 12S-HETE and 13S-HODE causing a similar change in substrate specificity.^{49, 50} Interestingly, there have been no published synthetic small-molecules which allosterically affect LOX catalysis, until recently. Meng, et al.⁵¹ published three small molecules which increased the rate of h15-LOX-1. One activator, PKUMDL_MH_1001 (**1**) (also known as PKUMDL_AAM_101),⁵² displayed moderate potency ($AC_{50} = 6.8 \mu\text{M}$) and a moderate increase in rate (max activation = 85%). Intriguingly, if **1** was added to whole blood, h15-LOX-1 products increased in concentration, indicating cellular activity for this activator. Further molecular dynamic (MD) investigations by this research group examined the activation mechanism of **1** and proposed an exterior AA binding site which prevented substrate inhibition instead of increasing the turnover number.⁵³ Shintoku et al. subsequently utilized **1** to increase h15-LOX-1 activity in cancer cells and accelerate cell death through the ferroptosis.⁵⁴ Taken together, these data support the conclusion that **1** is a small-molecule capable of activating h15-LOX-1, however certain critical biochemical details were lacking, such as assignment of the correct diastereomer, LOX and fatty acid specificity, allosteric site assessment and kinetic assignment of the steady-state mechanism. The current work aims to provide a comprehensive

understanding of the biochemical and kinetic properties imparted on h15-LOX-1 by **1**, so as to define its constraints for use in *in vivo* experiments.

3.3 Methods

Expression and Purification of h5-LOX-1, h12-LOX, h15-LOX-1, and h15-LOX-2.

Overexpression and purification of wild-type (wt) h15-LOX-1 (Uniprot entry P16050),^{55, 56} h12-LOX (Uniprot entry P18054),^{55, 56} h5-LOX (Uniprot entry P09917)⁵⁷ and h15-LOX-2 (Uniprot entry O15296)⁵⁸ was performed as previously described. A nickel-NTA chromatography system at 4 °C was used to purify His-tag labeled h12-LOX, h15-LOX-1, and h15-LOX-2. The purity of h15-LOX-1, h15-LOX-2, and h12-LOX was assessed by sodium dodecyl sulfate-polyacrylamide gel electrophoresis (SDS-PAGE) to be >90%. The metal content was assessed on a Finnigan inductively coupled plasma mass spectrometer (ICP-MS), via comparison with an iron standard solution. Cobalt-EDTA was used as an internal standard. The h5-LOX was not purified due to a dramatic loss of activity and was prepared as an ammonium sulfate precipitate.

Synthesis of **1** (1-[(7*E*)-7-benzylidene-3-phenyl-3*a*,4,5,6-tetrahydro-3*H*-indazol-2-yl]-2-(4-methylpiperazin-1-yl)ethenone) and isolation of diastereotopic pairs.

The diastereotopic mixture of compound **1** was synthesized according to published procedures, with the synthetic step which generates the diastereomers

shown in **Figure 3.1**.⁵⁹ The diastereomeric pairs, *cis*-**1** and *trans*-**1**, were separated via high pressure liquid chromatography (HPLC) on a Higgins Haisil Semi-preparative (5 μ m, 250mm x 10mm) C18 column with a 95:5 to 5:95 gradient of water and ACN, both with 0.1% (v/v) formic acid (FA) over 70 minutes and a flow rate of 2 mL/min.

1 (1-[(7*E*)-7-benzylidene-3-phenyl-3*a*,4,5,6-tetrahydro-3*H*-indazol-2-yl]-2-(4-methylpiperazin-1-yl)ethenone)

¹H NMR (800 MHz, CDCl₃) δ 7.36 (m, 7H), 7.29 (tt, 1H), 7.25 (d, 2H), 7.18 (d, 1H), 4.89 (d, 1H), 3.72 (s, 2H), 3.06 (d bm, 1H), 2.97 (ddd, 1H), 2.78 (bs, 8H), 2.44 (s, 3H), 2.43 (ddd, 1H), 2.21 (ddd, 1H), 1.93 (ddd, 1H), 1.69 (qd, 1H), 1.47 (qt, 1H). ¹³C NMR (500 MHz, d₈-DMSO) δ 168.5, 158.7, 142.2, 135.7, 130.9, 129.7, 129.7, 128.8, 128.6, 127.9, 127.2, 125.7, 67.4, 58.9, 56.3, 54.7, 52.6, 45.8, 29.2, 28.7, 23.7. HRMS *m/z* 429.27 [M⁺H] (calculated for C₂₇H₃₂N₄O, 428.26). See Supporting information, **Figures S3.1-3.3**.

***Cis-Trans* Identification via Molecular Mechanics Computation of 1**

1 has two stereocenters on C12 and C14 that constitute four diastereomers (**Figure 3.1**), which were not characterized previously.⁵⁹ Molecular modeling was utilized to predict the stereochemical configuration of the diastereomers using Chem3D 20.1 (**Table 3.1**). Each diastereomer was analyzed using Chem3D's molecular mechanics (MM2) to minimize energy calculation using a minimum RMS gradient of 0.0100 and running a maximum of 10,000 iterations. Due to the localized

dihedral angles being large enough to differentiate the *cis*- and *trans*-isomers, no other molecular mechanics calculations are required. Furthermore, the dihedral angle measurements between the two hydrogens were recorded to later confirm the *J* value of the hydrogen on C14 by using the Karplus equation. Comparisons between both the *J*-values from each Karplus equation calculation and the experimental NMR data yields the distinction between the *cis* and *trans* isomers of **1**.

LC-MS/MS Analysis of **1**

The structure of the final reaction product (**1**) was verified in part through liquid chromatography coupled with electrospray-ionization tandem mass spectrometry (LC/ESI-MS/MS). Chromatographic separation of the two diastereotopic pairs, *cis*-**1** and *trans*-**1**, was performed on a Dionex UltiMate 3000 UHPLC with a C₁₈ column (MAC-MOD, ACE Excel 5 μm, 250 mm × 4.6 mm). The autosampler was held at 4 °C, and the injection volume was 20 μL. Mobile phase A consisted of H₂O with 0.1% (v/v) FA, and mobile phase B consisted of acetonitrile with 0.1% FA. The flow rate was 1.0 mL/min. The initial condition (5% mobile phase B) was held for 2 min and then ramped up to 95% over 10 min. Mobile phase B was held at 95% for an additional 3 min. The chromatography system was coupled to an Orbitrap Velos Pro (Thermo Scientific) for mass analysis. Analytes were ionized via heated electrospray ionization with 4.0 kV spray voltage and 35, 10, and 0 arbitrary units for sheath, auxiliary, and sweep gas, respectively. The radiofrequency amplitude of the S-Lens was 65%, the probe and capillary temperatures were 45 and 380 °C,

respectively. All analyses were performed in positive ionization mode at the high-resolution setting (100,000). MS² was performed in the ion trap with a normal scan rate at 35% normalized collision energy in a targeted manner with a mass list containing the following *m/z* ratios ± 0.3 : 429.27 (**1**) and its fragments, 329.17, 301.16, 244.1, and 141.10 (Supporting information, **Figure S3.4**).

Specificity of 1 with LOX isozymes and Fatty Acids and Oxylin Substrates

1 was screened to determine its activation specificity against human lipoxygenases. h15-LOX-1 and h15-LOX-2 reactions were performed in 25 mM HEPES (pH 7.5), while h12-LOX reactions were carried out in 25 mM HEPES (pH 8.0). Reactions with the crude, ammonium sulfate precipitated h5-LOX were carried out in 25 mM HEPES (pH 7.3), 0.3 mM CaCl₂, 0.1 mM EDTA, and 0.2 mM ATP. All isoforms were screened at 10 μ M **1**, 10 μ M AA, and 0.01% Triton X-100. 15S-HpETE formation rates were determined by the increase in absorbance at 234 nm ($\epsilon_{234\text{nm}} = 27,000 \text{ M}^{-1} \text{ cm}^{-1}$), with the concentration of AA being determined by measuring the amount of 15S-HpETE produced from the complete reaction with soybean lipoxygenase-1 (sLO-1). Rate enhancement of h15-LOX-1 by **1** was also determined with 15S-HpETE as substrate. Reactions were carried out in 25 mM HEPES (pH 7.5), 0.01% Triton X-100, and 10 μ M for **1**, with concentrations varying for 15S-HpETE (e.g., 5, 10 and 20 μ M). Following the addition of enzyme, substrate turnover was monitored at 270 nm (conjugated triene) for the creation of diHpETEs ($\epsilon_{270\text{nm}} = 37,000 \text{ M}^{-1} \text{ cm}^{-1}$). All reactions were performed in duplicate at ambient temperature under constant stirring. Reactions were initiated by the addition of

enzyme and were monitored on a Perkin-Elmer Lambda 45 UV/VIS spectrophotometer. Simultaneous reactions were run in the absence of **1** for all reactions in order to determine the increase in maximal rate.

Kinetic Analysis of **1 and AC₅₀ Determination with h15-LOX-1**

h15-LOX-1 reactions were performed, at ambient temperature, constantly stirred with a magnetic stir bar in a 1 cm² quartz cuvette containing 2 mL of 25 mM HEPES (pH 7.5), 0.01% Triton X-100, and substrate in the presence and absence of **1**. The AA concentration was varied from 0.74 to 19.3 μM, while the concentration of **1** was held constant (four separate experiments of 0, 5, 20, and 30 μM of **1**). AC₅₀ investigations were performed at 10 μM substrate (AA, DHA, or LA) and concentrations of **1** ranging from 0.5 to 100 μM. The AC₅₀ for the isolated diastereomer pairs were determined. An AC₅₀ assay utilizing the buffer conditions of the discovering lab⁴⁶ was also performed, 100 mM PBS (pH 7.4) and 1% DMSO. *UV KinLab*TM (Perkin Elmer) was used to fit initial rates, and KaleidaGraph (Synergy) was used to determine the kinetic parameter (k_{cat}/K_M) to the Michaelis-Menten equation for the calculation of kinetic parameters. Activation rates were determined by subtracting the rate of the vehicle (DMSO) reaction from the rate of the reaction with **1**. AC₅₀ values were obtained by determining the % change in enzymatic rate, relative to vehicle control, at seven activator concentrations and plotting them against activator concentration. The data was fit using a four-parameter, variable slope analysis normalized with R_{MAX}=100%. Reactions were initiated through the addition

of enzyme (~60 nM final concentration). The data used for the saturation curve fits were performed in triplicate.

h15-LOX-1 Product Profile in the presence of 1

Product profile reactions were carried out in a similar manner as the kinetic reactions detailed above except no Triton X-100 was added. Reactions were quenched with the addition of 3% glacial acetic acid, washed 3x with 2 mL DCM, reduced with a drop of trimethylphosphite, evaporated under a stream of N₂ gas, reconstituted in a 1:1 mixture of ACN and H₂O with 0.1%FA, and injected on a Dionex UltiMate 3000 UHPLC with a C₁₈ column (Phenomenex Kinetex, 1.7 μm, 150 mm × 2.1 mm) coupled to an Orbitrap Velos Pro (Thermo Scientific) for product analysis. Mobile phase A consisted of water with 0.1% (v/v) FA, and mobile phase B consisted of acetonitrile with 0.1% FA. The flow rate was 0.2 mL/min. The initial condition (50% mobile phase B) was held for 1 min and then ramped up to 75% over 16 min. Mobile phase B was held at 75% for an additional 9 min. Analytes were ionized via heated electrospray ionization with -4.0 kV spray voltage and 35, 10, and 0 arbitrary units for sheath, auxiliary, and sweep gas, respectively. The radiofrequency amplitude of the S-Lens was 65%, and the probe and capillary temperatures were 45 and 380 °C, respectively. All analyses were performed in negative ionization mode at the normal resolution setting. MS² was performed at 35% normalized collision energy in a targeted manner with a mass list containing the following *m/z* ratios ±0.1: 319.2 (HETE) and 335.2 (diHETE).

Substrate Inhibition & Lag Phase Investigations in the presence of 1

Initial rate screening was carried out to determine the capacity of **1** to lower the inhibitory effects of high substrate concentrations on h15-LOX-1⁴⁴. The reactions were carried out at ambient temperature, constantly stirred with a magnetic stir bar in a 1 cm² quartz cuvette containing 2 mL of 25 mM HEPES (pH 7.5) and 0.01% Triton X-100. The substrate, DHA and AA, concentrations varied from 25, 50, and 100 μ M while the activator concentration was held constant at 10 μ M. Additional experiments were performed to investigate if the activator altered the affinity of substrates to the ferrous form of h15-LOX-1 as has been previously seen⁴⁴. Reactions were conducted as described for the steady-state experiments above, initiating the assays by adding h15-LOX-1, final concentration of \sim 60 nM, to buffers containing LA, AA, or DHA under substrate limiting conditions (5 μ M). Lag phases, the time difference from reaction initiation to maximal rate, and V_0 , were recorded. Reactions were run in triplicate.

Inhibition Potential of ML351 in the Presence of **1**

The inhibition potential of the selective, potent h15-LOX-1 inhibitor, ML351³⁶, was determined in the presence of **1**. Reaction rates were determined by following the formation of the conjugated diene product, 15-HpETE, at 234 nm with a Perkin-Elmer Lambda 40 UV/Vis spectrophotometer at five inhibitor concentrations with and without 10 μ M of **1** present. All reaction mixtures were 2 mL in volume and constantly stirred using a magnetic stir bar at ambient temperature with the appropriate amount of h15-LOX-1, \sim 60 nM. All reactions were carried out in 25 mM HEPES buffer (pH 7.5), 0.01% Triton X-100 and 10 μ M AA. The concentration of AA was quantitated by allowing the reaction to go to completion with sLO-1. IC_{50} values were obtained by plotting the initial reaction rates against inhibitor concentration,

followed by a hyperbolic saturation curve fit. The data used for the saturation curve fits were performed in triplicate.

Impact of **1 on Allosteric Modulators of h15-LOX-1**

The negative allosteric modulator, 14S-HpDHA was varied from 1 μM to 100 μM in the presence and absence of 10 μM of **1** in order to determine if **1** altered the allosteric effect of 14S-HpDHA. The concentration of 12S-HETE was also varied (0.1 μM to 5 μM), with a 1 μM , 1:1 LA and AA mixture as substrate. **1** (10 μM) was added in order to determine if it altered the allosteric effect of 12S-HETE. The product profile reactions and extractions were carried out as mentioned above. MS² was performed at 35% normalized collision energy in a targeted manner with a mass list containing the following m/z ratios ± 0.1 : 295.2 (HODE), 319.2 (HETE), and 359.2 (diHDHA).

3.4 Results and Discussion

Synthesis and Structural Validation of Activator

The synthesis of **1** was performed as described earlier,⁵⁹ and the structure indicates two stereocenters (**Figure 3.1**), leading to two diastereomeric pairs of enantiomers, *cis*-**1** and *trans*-**1**. LC-MS/MS analysis resolved the two diastereomers, accounting for 14% and 86% of the total area, respectively (**Supporting Information, Figure S3.4**), with MS² fragments being observed for both diastereomers ($m/z = 329, 301, 244$ and 141). The two diastereomers were isolated by preparative HPLC and the stereochemistry and the *J*-couplings of the vicinal protons H33 and H34 were used to determine the relative stereochemistry at these positions

(**Figure 3.2**). The two diastereomers were modeled using Chem3D and their *J*-couplings were predicted using the Karplus relationship as implemented Chem3D. Comparison of the predicted and observed coupling constants revealed the major product to be the *trans* stereoisomer.

Specificity of **1 with LOX isozymes and Fatty Acids and Oxylin Substrates**

1 was screened at 10 and 20 μ M against h5-LOX, h12-LOX, h15-LOX-1, and h15-LOX-2, to determine the specificity of the activator for hLOXs. It was determined that only h15-LOX-1 had an increased rate, 67% at 10 μ M, in the presence of **1** (**Table 3.2**), with the remaining hLOX isoforms displaying mild, dose-independent inhibition, indicating that **1** is a h15-LOX-1 specific activator. With confirmation that **1** selectively activates h15-LOX-1 against AA catalysis, the role of **1** with 15S-HpETE as the substrate was investigated, however, no activation was observed. This indicates that activation by **1** is specific for the reaction of h15-LOX-1 with AA but not the oxylin 15S-HpETE, which may have implications for the use of **1** *in vivo* since h15-LOX-1 must react with oxylin in order to form some SPM. Interestingly, the AC₅₀ for the two isolated diastereomer pairs, *cis*-**1** and *trans*-**1**, were determined to be the same and therefore all subsequent experiments utilized the diastereotopic mixture, **1** (Supporting information, **Figure S3.5**). Considering that the structures of *cis*-**1** and *trans*-**1** are distinct (**Figure 3.1** and **3.2**), this result could suggest the protein binding site is not specific to the stereocenters of **1**. It should be noted that the two enantiomers from each diastereotopic pair were not resolved, so it is possible that there could be potency differences between the enantiomers.

AC₅₀ Determination with h15-LOX-1

Following the determination that **1** was specific for h15-LOX-1, the AC₅₀ with AA, LA and DHA was determined to better understand the substrate specificity of **1**. The reaction of h15-LOX-1 with LA (C18:2 PUFA) and AA (C20:4 PUFA) were activated in the presence of **1** (**Figure 3.3**), with the AC₅₀ for LA being 5.3 +/- 0.7 μM (98 % max activation) and 7.8 +/- 1 μM for AA (240 % max activation). It should be noted that the AC₅₀ value for AA is comparable to that observed by Meng et al.⁴⁴ (AC₅₀ value = 6.8 +/- 0.4 μM, max activation = 85 %), however, these conditions are distinct from that of Meng et al. When we attempted to reproduce their work under the published conditions, a reliable AC₅₀ could not be obtained. As has been published previously,^{36, 60} the absence of stirring can lead to variable rates, which we observed under the conditions of Meng et al.⁴⁴. Gratifyingly, with constant stirring and initiation of the reaction by enzyme addition, an AC₅₀ of 9.7 +/- 1 μM (150 % max activation) at 50 μM AA was obtained with the Meng et al.⁴⁶ buffer conditions (**Table 3.3, Figure 3.4**), which is comparable to the reported value of this publication. Finally, the reaction rate of h15-LOX-1 with DHA, a C22:6 PUFA, was not activated with **1**, up to 100 mM (**Figure 3.3**). These data indicate that the activation of 15-LOX-1 by **1** is dependent on the nature of the PUFA substrate, with C18 and C20 PUFAs being activated, however C22 PUFAs are not. The lack of DHA activation has relevancy concerning **1** as a cellular tool since DHA is one of the main SPM precursors.

Lag Phase and Substrate Inhibition in the presence of 1

Previous studies have suggested that part of the kinetic activation potential of **1** was derived from its ability to lower the effect of substrate inhibition on h15-LOX-1^{46,47}. To further shed light on this hypothesis, lag phase experiments at high substrate concentration were carried out because the lag phase observed for LOX reactions is partially due to substrate binding to the inactive ferrous form⁴⁴. Given this, it was observed that the h15-LOX-1 lag phase was reduced by 140 seconds with activator (25 μ M AA), with a 98% rate increase (**Table 3.4** and **Figure 3.5**). This reduced lag phase and increased rate was decreased slightly with increasing substrate concentration, 50 and 100 μ M AA. With DHA, the lag phase decreased by nearly 200 seconds, with the rate increasing 25% at 100 μ M AA. Taken together, these data indicate that while **1** does lower the affinity of AA and DHA to the ferrous form of h15-LOX-1, this effect does not account for enzyme activation since DHA catalysis is not enhanced.

Inhibitory and Allosteric modulators effect in the presence of 1

ML351 is a selective, potent inhibitor of h15-LOX-1 that targets the active site. The IC₅₀ was determined in the presence of **1**, however no change in IC₅₀ value was observed. This result suggests that any structural changes imparted to h15-LOX-1, as a result of **1** binding, does not change the active site affinity for ML351 in a quantifiable manner.

With respect to allostery, 14S-HpDHA is a known allosteric modulator of h15-LOX-1, where increasing concentrations affects the ratio of diHpDHA products being formed. With the addition of **1**, the allosteric effect of 14S-HpDHA on the

diHpDHA metabolite ratio was unaffected, implying that the allosteric binding of **1** does not compete with that of 14S-HpDHA. 12S-HETE is also an allosteric modulator which regulates the substrate preference of h15-LOX-1 when reacting with AA and LA, however, **1** did not modify the allosteric effect of 12S-HETE, indicating that **1** does not compete for the same binding site as 12S-HETE. Taken together, these data imply that the activation binding site of **1** is distinct from that of both ML351 (i.e. the catalytic site³⁸) and the allosteric effector molecules.^{47, 48, 50} These data support the proposed hypothesis that **1** binds to a novel site on the exterior of 15-LOX-1.⁴⁶

Steady-State Kinetic Analysis of **1**

Given the fact that AC₅₀ values do not account for substrate concentration variations, steady-state kinetics with AA as the substrate were performed with 0, 5, 20 and 30 μM **1** (**Table 3.5, Figure 3.6**). **1** did not affect K_M appreciably, however, it did increase k_{cat} and k_{cat}/K_M , in a hyperbolic, dose dependent manner. This saturation behavior of k_{cat} and k_{cat}/K_M is indicative of hyperbolic inhibition (i.e. partial inhibition), as seen previously with h15-LOX-2.⁵⁸ These data indicate the presence of an allosteric activation binding site that affects the catalysis by changing the microscopic rate constants of h15-LOX-1, as described in Scheme 1. From **Scheme 3.1**, eqs 1-4 allow for the determination of K_x , the strength of binding, a, the change in K_M and b, the change in k_{cat} . As mentioned above, K_M is not affected by **1** indicating that the value of a is 1. If this value for a is inserted into eq. 4, b and K_x can be determined from the fit to be 2.2 +/- 0.4 and 16 +/- 1 μM , respectively (**Figure 3.6**).

These kinetic parameters indicate V-type activation⁶¹ and the formation of a catalytically active ternary complex (X•E•S) between h15-LOX-1 and **1**, consistent with the proposed model of Meng et al.^{51, 53} It should be noted that the b value is consistent with the less accurate AC₅₀ measurement for AA (242% max activation). In addition, the K_x is also similar to the AC₅₀, with only a 2-fold difference.

3.5 Conclusion

LOXs are important players in the inflammatory response of human cells and as such, both inhibitors and allosteric molecules have been developed. Recently, a LOX activator was discovered by Meng et al., **1**, which has the potential of being a valuable tool molecule for probing the cellular activity of LOX, however, its mechanism of action was poorly defined. In the current work, we expand on the work of Meng et al. and have determined the following. The synthesis of **1** allows for the isolation of the cis- and trans-diastereomers, with both having similar activator activity. The trans-diastereomer is the major product and is active against 15-LOX-1, however, it is inactive against 5-LOX, 12-LOX and 15-LOX-2, indicating it is a LOX selective molecule. In addition, it activates 15-LOX-1 for LA and AA catalysis but not DHA catalysis, indicating its activity is dependent on the nature of the fatty acid substrate. It was also observed that **1** reduced substrate inhibition, as suggested by Meng et al. However, since this effect was observed for both AA and DHA, but the rate of DHA is not activated, the reduced substrate inhibition does not account for the activation of 15-LOX-1. The effect of **1** did not compete with the known catalytic and

allosteric effector molecules, indicating its binding site is unique to catalysis and allosteric sites, consistent with the site proposed by Meng et al. Finally, **1** did not affect K_M but did increase the value of k_{cat} , supporting the hypothesis that its binding site is remote from the catalysis site. In total, our data support the hypothesis that **1** is a potent activator that is selective to both its LOX target and its PUFA substrate affect, which supports the cellular work that demonstrated it as a tool molecule which increased the activity of 15-LOX-1 with respect to its LA/AA catalysis.

3.6 Figures

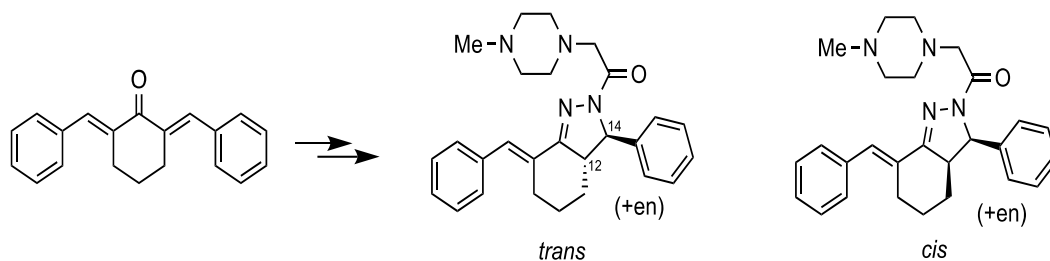


Figure 3.1 Synthetic step which generates the diastereotopic mixture as described by Khalaf et al. (1982).

Calculation	Carbon 12 Configuration	Carbon 14 Configuration	Conformation	Localized Dihedral Angle	Coupling from Karplus Equation (Hz)
1	(S)	(R)	<i>anti-clinal</i>	157.6°	8.87
2	(S)	(S)	<i>syn periplanar</i>	24.1°	7.00
3	(R)	(S)	<i>anti-clinal</i>	-132.8°	5.88
4	(R)	(R)	<i>syn periplanar</i>	-24.6°	6.95

Table 3.1: Results from Chem3D MM2 minimize energy calculations and Karplus Equation.

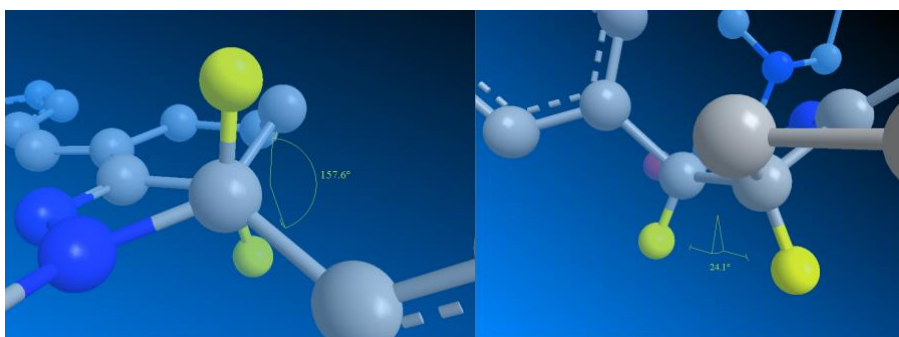


Figure 3.2 Chem3D visualizations of H33 and H34. Left: *trans* visualization of calculation 1.

Right: *cis* visualization of calculation 2.

Enz	0 μ M Activator	10 μ M Activator	20 μ M Activator
h5-LOX	100 (1.5)	78.3 (0.0)	91.3 (0.5)
h12-LOX	100 (1.0)	75.0 (0.0)	83.3 (0.5)
h15-LOX-1	100 (0.5)	167 (0.5)	212 (2.0)
h15-LOX-2	100 (1.0)	74.4 (0.5)	94.9 (0.5)

Table 3.2 Activator Specificity versus h5-LOX, h12-LOX, h15-LOX-1, and h15-LOX-2 with AA as the substrate. Initial rates, measured as dA/sec, are presented as a percentage, with 0 μ M activator reactions set to 100%. The error is displayed in parentheses.

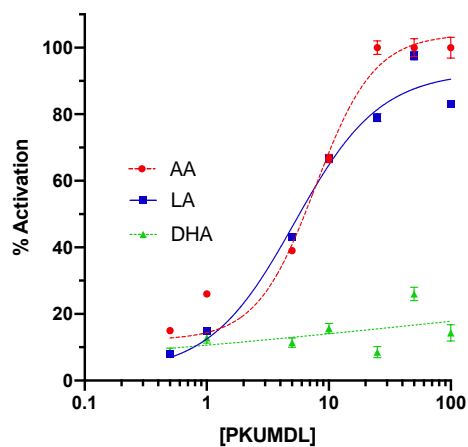


Figure 3.3 1 AC_{50} with LA, AA, and DHA reactions.

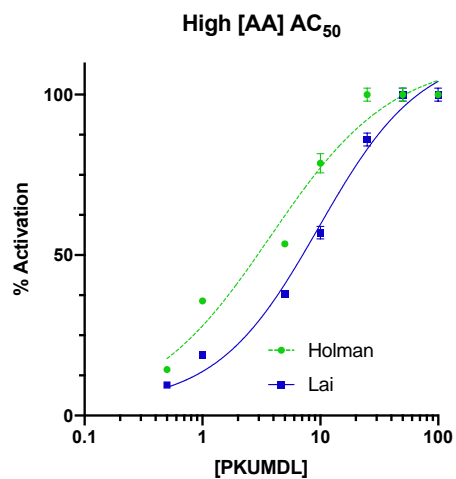


Figure 3.4 High [AA] AC₅₀ using Holman lab and Lai lab buffer conditions.

AC ₅₀ Kinetics	10 μM PUFA	50 μM PUFA	50 μM* PUFA
AA	7.8 (1) μM +240 (20) %	3.8 (0.6) μM +190 (10) %	9.7 (1) μM +150 (7) %
LA	5.3 (0.7) μM +98 (9) %	N/D	N/D
DHA	>100 μM +26 (10) %	N/D	N/D

Table 3.3 AC₅₀ values (mM) and max activation % at different polyunsaturated fatty acid (PUFA) concentrations. N/D = not determined *This AC₅₀ value was determined using the buffer conditions from Lai et al., however with stirring.⁴⁶ The lack of stirring increased the AC₅₀ significantly. The error is displayed in parentheses.

Arachidonic Acid	25 μM	50 μM	100 μM
$\Delta\text{Lag phase (sec)}$	140 (10) s	93 (6) s	110 (20) s
% Rate increase	98 (3) %	71 (7) %	30 (12) %

Docosahexaenoic Acid	25 μM	50 μM	100 μM
$\Delta\text{Lag phase (sec)}$	84 (7) s	150 (20) s	200 (20) s
% Rate increase	19 (10) %	22 (10) %	25 (10) %

Table 3.4 Substrate inhibition determination in the presence of activator. “ $\Delta\text{Lag phase}$ ” is the change in lag phase from reactions with and without activator. Lag phase is the time from initiation of reaction to V_0 . “% rate increase” is the increase in V_0 between reactions with and without activator. The error is displayed in parentheses.

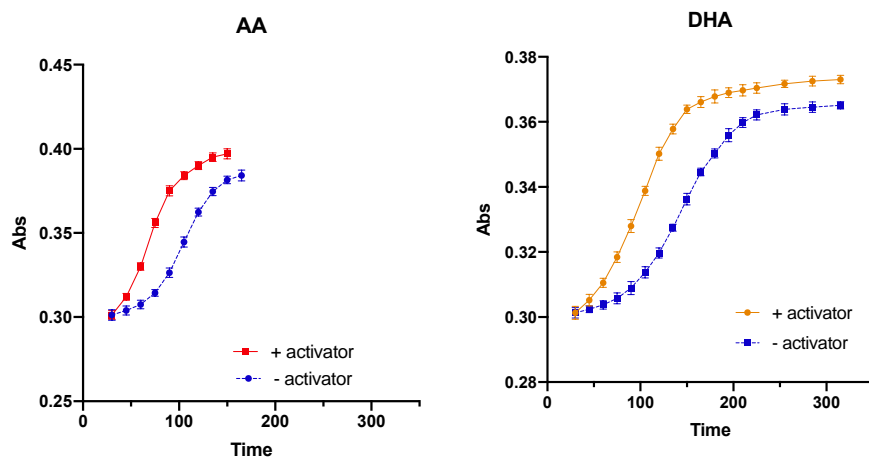
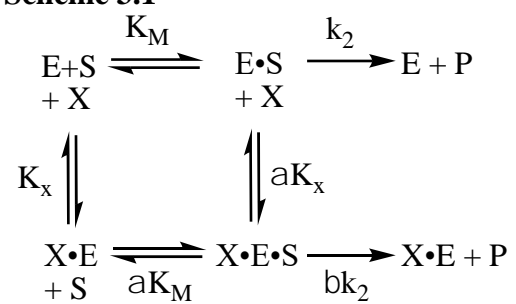


Figure 3.5 Activity plots of AA+h15-LOX-1 (left) and DHA+h15-LOX-1 (right), time is in seconds. Error is shown as bars for each measurement.

Steady-State Kinetics	0 μM	5 μM	20 μM	30 μM
k_{cat} (sec^{-1})	9.1 (0.92)	12 (0.59) (+29%)	15 (0.90) (+65%)	16 (1.1) (+79%)
K_m (μM)	6.3 (2.6)	5.7 (0.75) (-8%)	5.6 (0.91) (-10%)	5.4 (1.3) (-14%)
k_{cat}/K_m ($\text{sec}^{-1}\mu\text{M}^{-1}$)	1.5 (0.021)	2.1 (0.026) (+41%)	2.7 (0.019) (+83%)	3.0 (0.030) (+107%)

Table 3.5. Steady-state kinetic parameters with activator present. k_{cat} is in units of sec^{-1} , K_m is in units of μM and k_{cat}/K_m is in units of $\text{sec}^{-1}\mu\text{M}^{-1}$. Error values are in the parentheses, with % change from control boldened.

Scheme 3.1



Equations:

$$1/v = (\alpha K_M / k_{cat}) * [(X) + K_x] / (\beta[X] + \alpha K_x) * 1/[S]$$

$$+ 1/ k_{cat} * [(X) + \alpha K_x] / (\beta[X] + \alpha K_x) \tag{1}$$

$$K_M \text{ (app)} = (\alpha K_M) * [(X) + K_x] / ([X] + \alpha K_x) \tag{2}$$

$$k_{cat} / K_M = (k_{cat} / \alpha K_M) * (\beta[X] + \alpha K_x) / ([X] + K_x) \tag{3}$$

$$k_{cat} = k_{cat} * (\beta[X] + \alpha K_x) / ([X] + \alpha K_x) \tag{4}$$

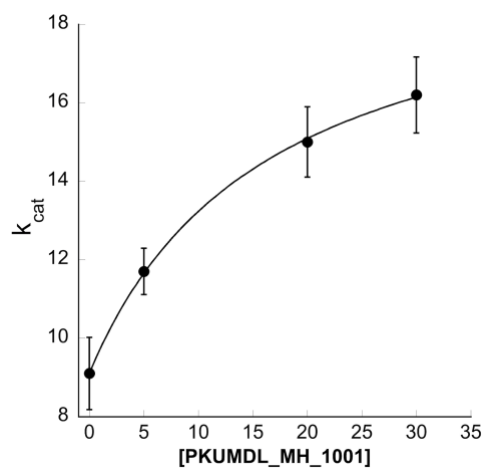


Figure 3.6. k_{cat} apparent is plotted against increasing concentrations of **1** and fit to equation 4, resulting in b and K_x being 2.2 ± 0.4 and 16 ± 1 mM, respectively (a was set to 1).

Figure S3.1. ^1H (800 MHz, in CDCl_3) and ^{13}C (125 MHz, in $d_8\text{-DMSO}$) for PKUMDL_MH_1001.

C Pos.	d_c , type	H Pos.	d_H , J (Hz)	COSY
1	129.7, CH	49	7.36, m	H-48,H-50
2	125.7, CH	50 ^a	7.36, m	H-49,H-51
3	129.7, CH	51	7.36, m	H-50,H-52
4	127.2, CH	52	7.36, m	H-51
5	130.9, C			
6	127.2, CH	48	7.36, m	H-49
7	127.9, CH	47	7.18, d (1.5)	H-54
8	135.7, C			
9	28.7, CH ₂	53	3.06, d bm (15.1)	H-54,H-55,H-56
		54	2.43, ddd (13.0,5.6,2.9)	H-53,H-55,H-56
10	23.7, CH ₂	55	1.47 qt (12.8, 3.8)	H-53,H-54,H-56,H-57,H-58
		56	1.93, ddd (13.7,5.2,2.3)	H-53,H-54,H-55,H-57,H-58
11	29.2, CH ₂	57	2.21, ddd (12.7,4.2,2.2)	H-34,H-55,H-56,H-58
		58	1.69, qd (12.9, 2.9)	H-34,H-55,H-56,H-57
12	56.3, CH	34	2.97, ddd (9.4,6.5,5.8)	H-34,H-57,H-58
13	158.7, C			
14	67.4, CH	33	4.89, d (9.4)	H-34
N15				
N16				
17	142.2, C			
18	128.8, CH	46	7.25, d (7.0)	H-45
19	128.6, CH	45	7.36, m	H-44,H-46
20	125.7, CH	44 ^a	7.29, tt (7,2)	H-43,H-45
21	128.6, CH	43	7.36, m	H-44,H-61
22	128.8, CH	61	7.25, d (7.0)	H-43
23	168.5, C			
24	58.9, CH ₂	59,60	3.72, s	
N25				
O26				
27	52.6, CH ₂	41,42	2.78, bs	
28	54.7, CH ₂	35,36	2.78, bs	
N29				
30	54.7, CH ₂	37,38	2.78, bs	
31	52.6, CH ₂	39,40	2.78, bs	
32	45.8, CH ₃	62,63,64	2.44, s	

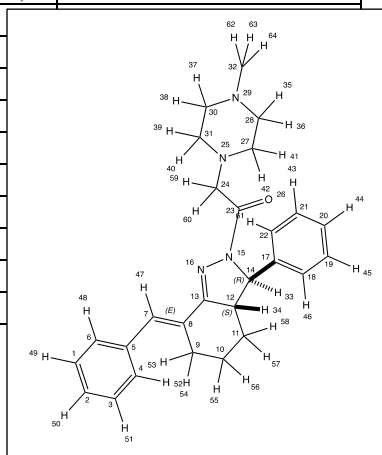


Figure S3.2 ^1H NMR of PKUMDL_MH_1001.

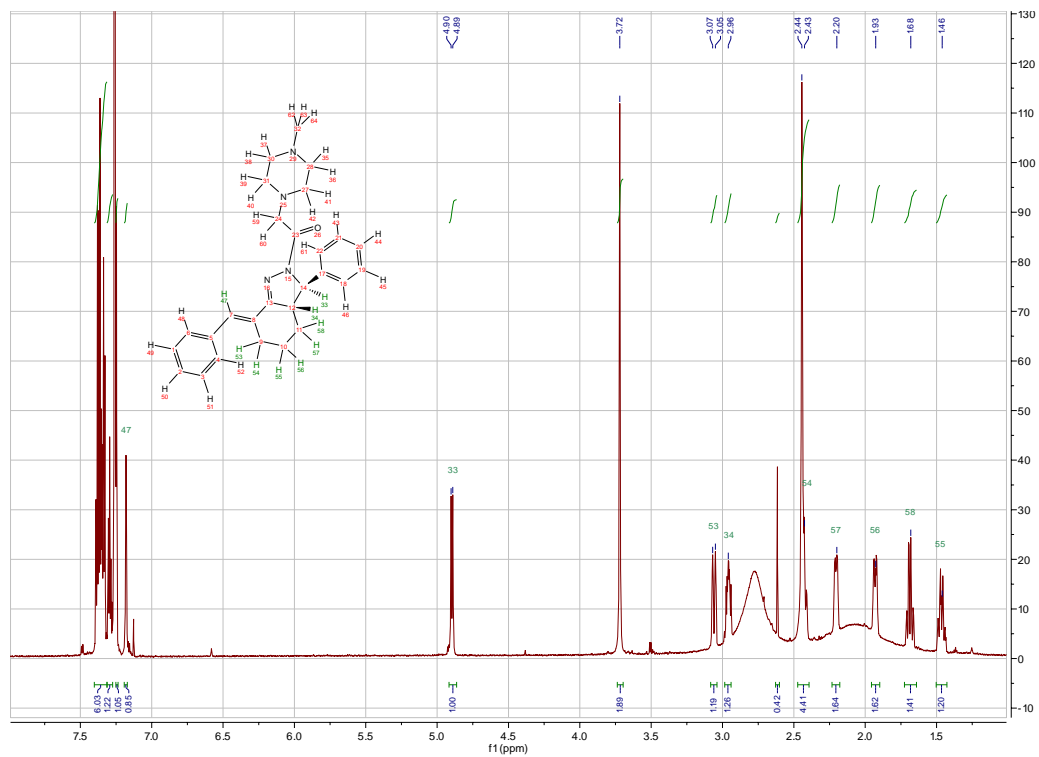


Figure S3.3 ^{13}C NMR of PKUMDL_MH_1001.

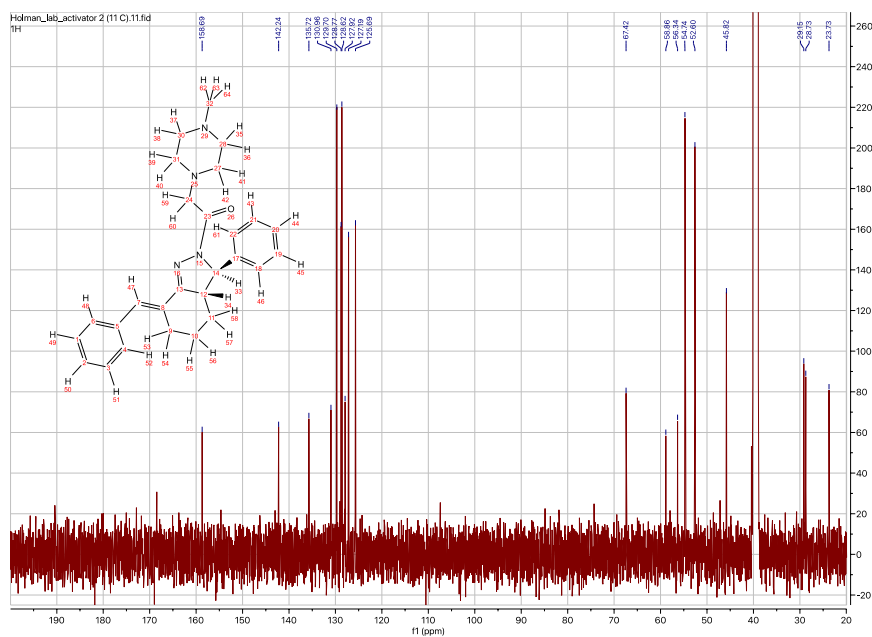
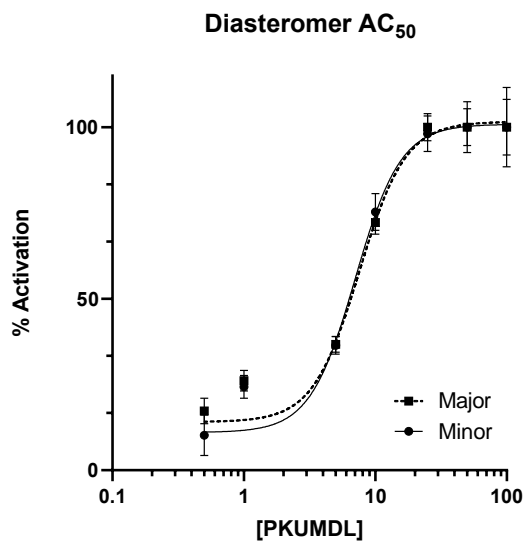


Figure S3.4 AC_{50} of major and minor diastereomer pairs with $[AA] = 10 \mu\text{M}$. Error is shown as bars. Major peak = $7.5 \mu\text{M}$, Minor peak = $7.0 \mu\text{M}$



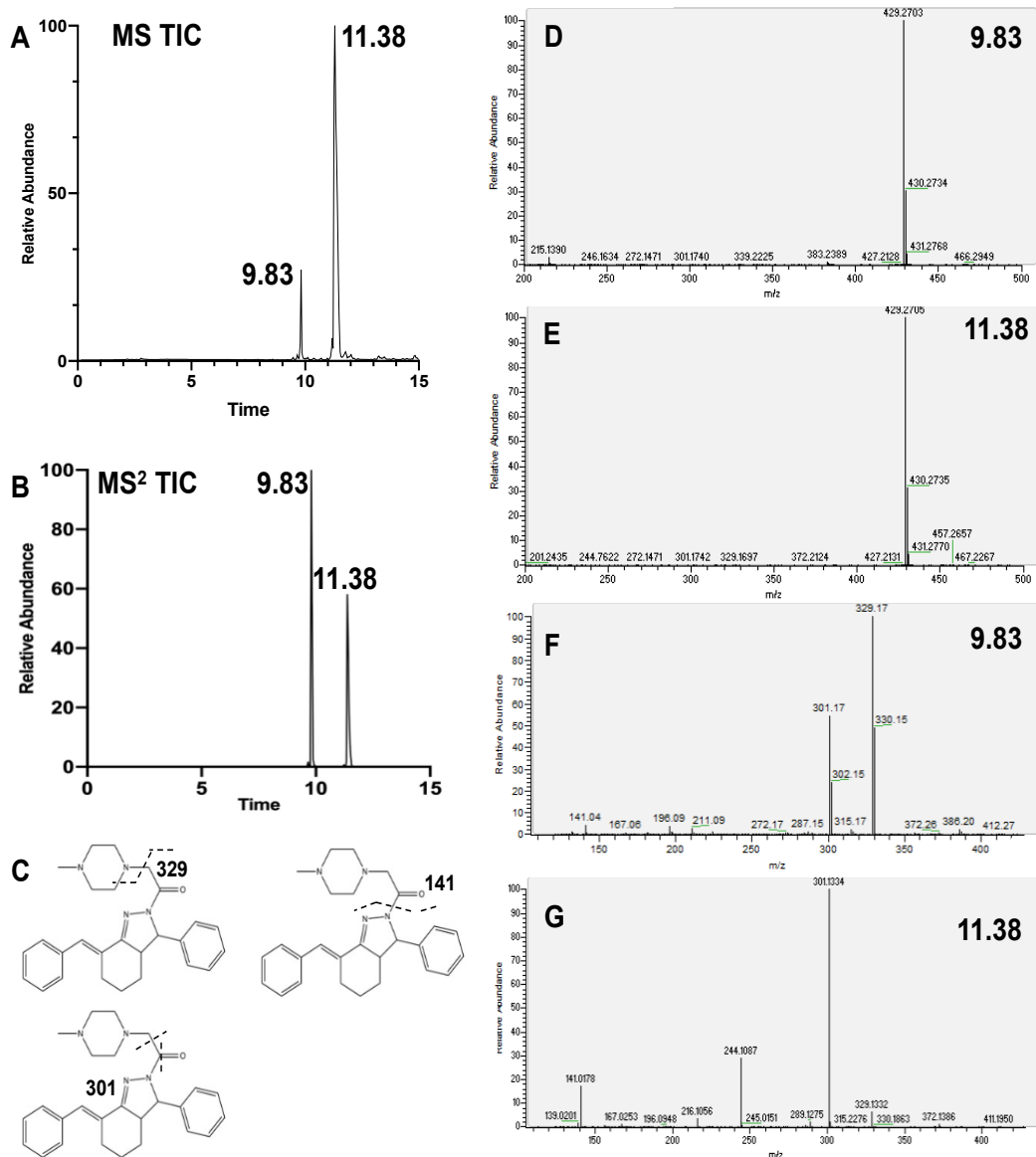


Figure S3.5 LC-MS/MS data for diastereomeric pairs. A) LC-MS TIC trace showing minor “cis” peak at 9.83 min and major “trans” peak at 11.38 min. B) MS² trace with 429.4 mass filter, major and minor peaks align with those in A. C) Fragment identification of MS² data in F and G. D) Parent ion of MS TIC peak at 9.83 min (429.2703). E) Parent ion of MS TIC peak at 11.38 min (429.2705). F and G) MS² fragments for 9.83 min and 11.38 min peaks after the 429.4 mass filter was applied.

3.7 References

- [1] Brash, A. R. (1999) Lipoxygenases: Occurrence, Functions, Catalysis and Acquisition of Substrate, *J. Biol. Chem.* 274, 23679-23682.
- [2] Grechkin, A. (1998) Recent Developments in Biochemistry of the Plant Lipoxygenase Pathway, *Prog. Lipid Res.* 37, 317-352.
- [3] Vance, R. E., Hong, S., Gronert, K., Serhan, C. N., and Mekalanos, J. J. (2004) The opportunistic pathogen *Pseudomonas aeruginosa* carries a secretable arachidonate 15-lipoxygenase, *Proc Natl Acad Sci U S A* 101, 2135-2139.
- [4] Deschamps, J. D., Ogunsola, A. F., Jameson, J. B., 2nd, Yasgar, A., Flitter, B. A., Freedman, C. J., Melvin, J. A., Nguyen, J. V., Maloney, D. J., Jadhav, A., Simeonov, A., Bomberger, J. M., and Holman, T. R. (2016) Biochemical and Cellular Characterization and Inhibitor Discovery of *Pseudomonas aeruginosa* 15 Lipoxygenase, *Biochemistry* 55, 3329-3340.
- [5] Borgeat, P., and Samuelsson, B. (1979) Arachidonic acid metabolism in polymorphonuclear leukocytes: effects of ionophore A23187, *Proc Natl Acad Sci U S A* 76, 2148-2152.
- [6] Hamberg, M., and Samuelsson, B. (1974) Prostaglandin endoperoxides. Novel transformations of arachidonic acid in human platelets, *Proc Natl Acad Sci U S A* 71, 3400-3404.
- [7] Schewe, T., Halangk, W., Hiebsch, C., and Rapoport, S. M. (1975) A lipoxygenase in rabbit reticulocytes which attacks phospholipids and intact mitochondria, *Febs Lett* 60, 149-152.
- [8] Brash, A. R., Boeglin, W. E., and Chang, M. S. (1997) Discovery of a second 15S lipoxygenase in humans, *Proc Natl Acad Sci U S A* 94, 6148-6152.
- [9] Dennis, E. A., and Norris, P. C. (2015) Eicosanoid storm in infection and inflammation, *Nat Rev Immunol* 15, 511-523.
- [10] Nayeem, M. A. (2018) Role of oxylipins in cardiovascular diseases, *Acta Pharmacol Sin* 39, 1142-1154.
- [11] Tourdot, B. E., Ahmed, I., and Holinstat, M. (2014) The emerging role of oxylipins in thrombosis and diabetes, *Front Pharmacol* 4, 176.
- [12] Wasternack, C., and Feussner, I. (2018) The Oxylipin Pathways: Biochemistry and Function, *Annu Rev Plant Biol* 69, 363-386.

- [13] Medzhitov, R. (2008) Origin and physiological roles of inflammation, *Nature* 454, 428-435.
- [14] Edin, M. L., Duval, C., Zhang, G., and Zeldin, D. C. (2020) Role of linoleic acid derived oxylipins in cancer, *Cancer Metastasis Rev* 39, 581-582.
- [15] Vane, J. R. (1971) Inhibition of prostaglandin synthesis as a mechanism of action for aspirin-like drugs, *Nat New Biol* 231, 232-235.
- [16] Zeldin, D. C. (2001) Epoxygenase pathways of arachidonic acid metabolism, *J Biol Chem* 276, 36059-36062.
- [17] Oates, J. A., FitzGerald, G. A., Branch, R. A., Jackson, E. K., Knapp, H. R., and Roberts, L. J., 2nd. (1988) Clinical implications of prostaglandin and thromboxane A₂ formation (1), *N Engl J Med* 319, 689-698.
- [18] Smith, W. L., Marnett, L. J., and DeWitt, D. L. (1991) Prostaglandin and thromboxane biosynthesis, *Pharmacol Ther* 49, 153-179.
- [19] Funk, C. D. (2001) Prostaglandins and leukotrienes: Advances in eicosanoid biology [Review], *Science* 294, 1871-1875.
- [20] Claesson, H. E. (2009) On the biosynthesis and biological role of eoxins and 15 lipoxygenase-1 in airway inflammation and Hodgkin lymphoma, *Prostaglandins & other lipid mediators* 89, 120-125.
- [21] Haeggstrom, J. Z., and Funk, C. D. (2011) Lipoxygenase and leukotriene pathways: biochemistry, biology, and roles in disease, *Chem Rev* 111, 5866-5898.
- [22] Dixon, S. J., Lemberg, K. M., Lamprecht, M. R., Skouta, R., Zaitsev, E. M., Gleason, C. E., Patel, D. N., Bauer, A. J., Cantley, A. M., Yang, W. S., Morrison, B., 3rd, and Stockwell, B. R. (2012) Ferroptosis: an iron-dependent form of nonapoptotic cell death, *Cell* 149, 1060-1072.
- [23] Yang, W. S., and Stockwell, B. R. (2016) Ferroptosis: Death by Lipid Peroxidation, *Trends Cell Biol* 26, 165-176.
- [24] Levy, B. D., Clish, C. B., Schmidt, B., Gronert, K., and Serhan, C. N. (2001) Lipid mediator class switching during acute inflammation: signals in resolution, *Nat Immunol* 2, 612-619.

- [25] Serhan, C. N., and Savill, J. (2005) Resolution of inflammation: the beginning programs the end, *Nat Immunol* 6, 1191-1197.
- [26] Serhan, C. N., Hong, S., Gronert, K., Colgan, S. P., Devchand, P. R., Mirick, G., and Moussignac, R. L. (2002) Resolvins: a family of bioactive products of omega-3 fatty acid transformation circuits initiated by aspirin treatment that counter proinflammation signals, *J Exp Med* 196, 1025-1037.
- [27] Serhan, C. N., Hamberg, M., and Samuelsson, B. (1984) Lipoxins: novel series of biologically active compounds formed from arachidonic acid in human leukocytes, *Proc Natl Acad Sci U S A* 81, 5335-5339.
- [28] Serhan, C. N. (2014) Pro-resolving lipid mediators are leads for resolution physiology, *Nature* 510, 92-101.
- [29] Archambault, A. S., Turcotte, C., Martin, C., Provost, V., Larose, M. C., Laprise, C., Chakir, J., Bissonnette, E., Laviolette, M., Bosse, Y., and Flamand, N. (2018) Comparison of eight 15-lipoxygenase (LO) inhibitors on the biosynthesis of 15-LO metabolites by human neutrophils and eosinophils, *PLoS One* 13, e0202424.
- [30] Wisastra, R., and Dekker, F. J. (2014) Inflammation, Cancer and Oxidative Lipoxygenase Activity are Intimately Linked, *Cancers (Basel)* 6, 1500-1521.
- [31] Carter, G. W., Young, P. R., Albert, D. H., Bouska, J., Dyer, R., Bell, R. L., Summers, J. B., and Brooks, D. W. (1991) 5-lipoxygenase inhibitory activity of zileuton, *J Pharmacol Exp Ther* 256, 929-937.
- [32] Wenzel, S. E., and Kamada, A. K. (1996) Zileuton: the first 5-lipoxygenase inhibitor for the treatment of asthma, *Ann Pharmacother* 30, 858-864.
- [33] Luci, D., Jameson, J. B., II, Yasgar, A., Diaz, G., Joshi, N., Kantz, A., Markham, K., Perry, S., Kuhn, N., Yeung, J., Schultz, L., Holinstat, M., Nadler, J., Taylor Fishwick, D. A., Jadhav, A., Simeonov, A., Holman, T. R., and Maloney, D. J. (2010) Discovery of ML355, a Potent and Selective Inhibitor of Human 12-Lipoxygenase, In *Probe Reports from the NIH Molecular Libraries Program*, Bethesda (MD).
- [34] Adili, R., Tourdot, B. E., Mast, K., Yeung, J., Freedman, J. C., Green, A., Luci, D. K., Jadhav, A., Simeonov, A., Maloney, D. J., Holman, T. R., and Holinstat, M. (2017) First Selective 12-LOX Inhibitor, ML355, Impairs Thrombus Formation and Vessel Occlusion In Vivo With Minimal Effects on Hemostasis, *Arteriosclerosis, thrombosis, and vascular biology* 37, 1828-1839.
- [35] Suzuki, H., Ueda, T., Juranek, I., Yamamoto, S., Katoh, T., Node, M., and Suzuki, T. (2000) Hinokitiol, a selective inhibitor of the platelet-type isozyme of arachidonate

12-lipoxygenase, *Biochemical and Biophysical Research Communications* 275, 885-889.

[36] Segraves, E. N., Shah, R. R., Segraves, N. L., Johnson, T. A., Whitman, S., Sui, J. K., Kenyon, V. A., Cichewicz, R. H., Crews, P., and Holman, T. R. (2004) Probing the activity differences of simple and complex brominated aryl compounds against 15 soybean, 15-human, and 12-human lipoxygenase, *J Med Chem* 47, 4060-4065.

[37] Vasquez-Martinez, Y., Ohri, R. V., Kenyon, V., Holman, T. R., and Sepulveda Boza, S. (2007) Structure-activity relationship studies of flavonoids as potent inhibitors of human platelet 12-hLO, reticulocyte 15-hLO-1, and prostate epithelial 15-hLO-2, *Bioorganic & Medicinal Chemistry* 15, 7408-7425.

[38] Rai, G., Joshi, N., Jung, J. E., Liu, Y., Schultz, L., Yasgar, A., Perry, S., Diaz, G., Zhang, Q., Kenyon, V., Jadhav, A., Simeonov, A., Lo, E. H., van Leyen, K., Maloney, D. J., and Holman, T. R. (2014) Potent and selective inhibitors of human reticulocyte 12/15-lipoxygenase as anti-stroke therapies, *J Med Chem* 57, 4035-4048.

[39] Liu, Y., Zheng, Y., Karatas, H., Wang, X., Foerch, C., Lo, E. H., and van Leyen, K. (2017) 12/15-Lipoxygenase Inhibition or Knockout Reduces Warfarin-Associated Hemorrhagic Transformation After Experimental Stroke, *Stroke* 48, 445-451.

[40] Yigitkanli, K., Zheng, Y., Pekcec, A., Lo, E. H., and van Leyen, K. (2017) Increased 12/15-Lipoxygenase Leads to Widespread Brain Injury Following Global Cerebral Ischemia, *Transl Stroke Res* 8, 194-202.

[41] Gregus, A. M., Buczynski, M. W., Dumlao, D. S., Norris, P. C., Rai, G., Simeonov, A., Maloney, D. J., Jadhav, A., Xu, Q., Wei, S. C., Fitzsimmons, B. L., Dennis, E. A., and Yaksh, T. L. (2018) Inhibition of spinal 15-LOX-1 attenuates TLR4-dependent, nonsteroidal anti-inflammatory drug-unresponsive hyperalgesia in male rats, *Pain* 159, 2620-2629.

[42] Eleftheriadis, N., Neochoritis, C. G., Leus, N. G., van der Wouden, P. E., Domling, A., and Dekker, F. J. (2015) Rational Development of a Potent 15-Lipoxygenase-1 Inhibitor with in Vitro and ex Vivo Anti-inflammatory Properties, *J Med Chem* 58, 7850-7862.

[43] Guo, H., Verhoek, I. C., Prins, G. G. H., van der Vlag, R., van der Wouden, P. E., van Merkerk, R., Quax, W. J., Olinga, P., Hirsch, A. K. H., and Dekker, F. J. (2019) Novel 15-Lipoxygenase-1 Inhibitor Protects Macrophages from Lipopolysaccharide Induced Cytotoxicity, *J Med Chem* 62, 4624-4637.

[44] Pelcman, B., Sanin, A., Nilsson, P., No, K., Schaal, W., Ohrman, S., Krog-Jensen,

- C., Forsell, P., Hallberg, A., Larhed, M., Boesen, T., Kromann, H., Vogensen, S. B., Groth, T., and Claesson, H. E. (2015) 3-Substituted pyrazoles and 4-substituted triazoles as inhibitors of human 15-lipoxygenase-1, *Bioorg Med Chem Lett* 25, 3024-3029.
- [45] Weinstein, D. S., Liu, W., Ngu, K., Langevine, C., Combs, D. W., Zhuang, S., Chen, C., Madsen, C. S., Harper, T. W., and Robl, J. A. (2007) Discovery of selective imidazole-based inhibitors of mammalian 15-lipoxygenase: highly potent against human enzyme within a cellular environment, *Bioorg Med Chem Lett* 17, 5115-5120.
- [46] Eleftheriadis, N., Poelman, H., Leus, N. G. J., Honrath, B., Neochoritis, C. G., Dolga, A., Domling, A., and Dekker, F. J. (2016) Design of a novel thiophene inhibitor of 15-lipoxygenase-1 with both anti-inflammatory and neuroprotective properties, *Eur J Med Chem* 122, 786-801.
- [47] Freedman, C., Tran, A., Tourdot, B. E., Kalyanaraman, C., Perry, S., Holinstat, M., Jacobson, M. P., and Holman, T. R. (2020) Biosynthesis of the Maresin Intermediate, 13S,14S-Epoxy-DHA, by Human 15-Lipoxygenase and 12-Lipoxygenase and Its Regulation through Negative Allosteric Modulators, *Biochemistry* 59, 1832-1844.
- [48] Tsai, W. C., Kalyanaraman, C., Yamaguchi, A., Holinstat, M., Jacobson, M. P., and Holman, T. R. (2021) In Vitro Biosynthetic Pathway Investigations of Neuroprotectin D1 (NPD1) and Protectin DX (PDX) by Human 12-Lipoxygenase, 15-Lipoxygenase-1, and 15-Lipoxygenase-2, *Biochemistry* 60, 1741-1754.
- [49] Wecksler, A. T., Jacquot, C., van der Donk, W. A., and Holman, T. R. (2009) Mechanistic Investigations of Human Reticulocyte 15- and Platelet 12-Lipoxygenases with Arachidonic Acid, *Biochemistry* 48, 6259-6267.
- [50] Wecksler, A. T., Kenyon, V., Deschamps, J. D., and Holman, T. R. (2008) Substrate specificity changes for human reticulocyte and epithelial 15-lipoxygenases reveal allosteric product regulation, *Biochemistry* 47, 7364-7375.
- [51] Meng, H., McClendon, C. L., Dai, Z., Li, K., Zhang, X., He, S., Shang, E., Liu, Y., and Lai, L. (2016) Discovery of Novel 15-Lipoxygenase Activators To Shift the Human Arachidonic Acid Metabolic Network toward Inflammation Resolution, *J Med Chem* 59, 4202-4209.
- [52] Lai, L., Liu, Y., Meng, H., and Hu, J. (2015) Hexahydroindazole 15-lipoxygenase activator and its application, (University, P., Ed.), Chin.
- [53] Meng, H., Dai, Z., Zhang, W., Liu, Y., and Lai, L. (2018) Molecular mechanism

of 15-lipoxygenase allosteric activation and inhibition, *Phys Chem Chem Phys* 20, 14785-14795.

[54] Shintoku, R., Takigawa, Y., Yamada, K., Kubota, C., Yoshimoto, Y., Takeuchi, T., Koshiishi, I., and Torii, S. (2017) Lipoxygenase-mediated generation of lipid peroxides enhances ferroptosis induced by erastin and RSL3, *Cancer Sci* 108, 2187-2194.

[55] Amagata, T. W., S.; Johnson, T.A.; Stessman, C.C.; Loo, C.P.; Lobkovsky, E.; Clardy, J.; Crews, P.; Holman, T.R. (2003) Exploring Sponge-Derived Terpenoids for Their Potency and Selectivity Against 12-Human, 15-Human, and 15-Soybean Lipoxygenases, *J. Nat. Prod* 66, 230-235.

[56] Robinson, S. J., Hoobler, E. K., Riener, M., Loveridge, S. T., Tenney, K., Valeriote, F. A., Holman, T. R., and Crews, P. (2009) Using enzyme assays to evaluate the structure and bioactivity of sponge-derived meroterpenes, *Journal of Natural Products* 72, 1857-1863.

[57] Smyrniotis, C. J., Barbour, S. R., Xia, Z., Hixon, M. S., and Holman, T. R. (2014) ATP allosterically activates the human 5-lipoxygenase molecular mechanism of arachidonic acid and 5(S)-hydroperoxy-6(E),8(Z),11(Z),14(Z)-eicosatetraenoic acid, *Biochemistry* 53, 4407-4419.

[58] Joshi, N., Hoobler, E. K., Perry, S., Diaz, G., Fox, B., and Holman, T. R. (2013) Kinetic and structural investigations into the allosteric and pH effect on the substrate specificity of human epithelial 15-lipoxygenase-2, *Biochemistry* 52, 8026-8035.

[59] Khalaf, A. A., El-Shafei, A. K., and El-Sayed, A. M. (1982) Synthesis of Some New Bicyclic Pyrazoline Derivatives, *J. Heterocyclic Chem.* 19, 609-612.

[60] Carroll, J., Jonsson, E. N., Ebel, R., Hartman, M. S., Holman, T. R., and Crews, P. (2001) Probing sponge-derived terpenoids for human 15-lipoxygenase inhibitors, *J Org Chem* 66, 6847-6851.

[61] Reinhart, G. D. (2004) Quantitative analysis and interpretation of allosteric behavior, *Methods Enzymol* 380, 187-203.

Chapter 4

STRUCTURAL BASIS FOR ALTERED POSITIONAL SPECIFICITY OF 15-LIPOXYGENASE 1 WITH 5S-HETE AND 7S-HDHA AND THE IMPLICATIONS FOR THE BIOSYNTHESIS OF RESOLVIN E₄

4.1 Abstract

Human 15-lipoxygenases (LOX) are critical enzymes in the inflammatory process, producing various pro-resolution molecules, such as lipoxins and resolvins, but the exact role each of the two 15-LOXs in these biosynthetic pathways remains elusive. Previously, it was observed that h15-LOX-1 reacted with 5S-HETE in a non-canonical manner, producing primarily the 5S,12S-diHETE product. To determine the active site constraints of h15-LOX-1 in achieving this reactivity, amino acids involved in the fatty acid binding were investigated. It was observed that R402L did not have a large effect on 5S-HETE catalysis, but F414 appeared to π - π stack with 5S-HETE, as seen with AA binding, indicating an aromatic interaction between a double bond of 5S-HETE and F414. Decreasing the size of F352 and I417 shifted oxygenation of 5S-HETE to C12, while increasing the size of these residues reversed the positional specificity of 5S-HETE to C15. Mutants at these locations demonstrated a similar effect with 7S-HDHA as the substrate, indicating that the depth of the active site regulates product specificity for both substrates. Together, these data indicate that of the three regions proposed to control positional specificity, π - π stacking and active site cavity depth are the primary determinants of positional specificity with 5S-HETE and h15-LOX-1. Finally, the altered reactivity of h15-LOX-1 was also observed with 5S-HEPE, producing 5S,12S-diHEPE instead of 5S,15S-diHEPE (aka resolvin E₄ (RvE₄)). However, h15-LOX-2 efficiently produces 5S,15S-diHEPE from 5S-HEPE. This result is important with respect to the biosynthesis of the RvE₄ since it obscures which LOX isozyme is involved in its

biosynthesis. Future work detailing the expression levels of the lipoxygenase isoforms in immune cells and selective inhibition during the inflammatory response will be required for a comprehensive understanding of RvE4 biosynthesis.

4.2 Introduction

Lipoxygenases (LOXs) are non-heme iron-containing dioxygenases that catalyze the hydroperoxidation of polyunsaturated acids (PUFA) containing a 1,4-pentadiene moiety^{1, 2} and play an important role in regulating the process of inflammation.^{3, 4} They can react with a variety of dietary fatty acids to form products broadly classified as oxylipins. Specialized-pro-resolving mediators (SPM) are a type of oxylipin that regulate the switch from a pro-inflammatory to a pro-resolving state^{5, 6}, with oxylipins derived from ω -3 fatty acids, such as eicosapentaenoic acid (EPA) and docosahexaenoic acid (DHA), having a larger role in pro-resolution than that of the ω -6 fatty acid, arachidonic acid (AA). LOXs can produce both pro-inflammatory mediators such as the leukotrienes, as well as anti-inflammatory SPM, such as the lipoxins, resolvins and maresins.⁷

The stereo- and regio-specificity of LOXs determine which oxylipin mediators a cell may produce, either on their own or in concert with other LOX isozymes expressed in neighboring cells through the process of transcellular biosynthesis.⁸ h15-LOX-1 is one of two 15-LOXs found in humans⁹. No crystal structure of h15-LOX-1 is available, so most studies to date have attempted to understand the stereo- and regio-specificity of the enzyme by comparison to the

structures of rabbit 15-LOX (r15-LOX) and human platelet 12-lipoxygenase (h12-LOX)¹⁰⁻¹¹. h15-LOX-1 shares 81% identity with r15-LOX (95% similarity), 65% identity to h12-LOX (88% similarity), but only 38% identity with h15-LOX-2 (72% similarity). In addition, if the critical active site residues are compared between h15-LOX-1 and h15-LOX-2, a low sequence identity of 47% is still observed.

15-LOXs principally catalyze the abstraction of a hydrogen from C13 of AA followed by insertion of dioxygen onto C15. The resulting molecule is 15S-hydroperoxy-5Z,8Z,11Z,13E-eicosatetraenoic acid (15S-HpETE), which can be reduced by glutathione peroxidases to 15S-hydroxy-5Z,8Z,11Z,13E-eicosatetraenoic acid (15S-HETE)¹²⁻¹³. The location of hydrogen abstraction depends on the depth of insertion of the methyl end of the substrate and which bis-allylic carbon is located proximal to the enzymes' active site iron. Generally, h15-LOX-1 abstracts the hydrogen atom from the ω -8 carbon, with oxygenation at the ω -6 carbon, with a smaller percentage of the ω -9 product also being made¹⁴. With AA and the ω -3 PUFA, EPA, the enzyme produces approximately 85% of the 15-product (ω -6) and 15% of the 12-product (ω -9). In contrast, h15-LOX-2 produces approximately 100% of the 15-oxylipin product with AA as substrate, giving it a more stringent criteria for product formation. However, placing a hydroxyl group on C5 of AA or C7 of DHA changes the product profile of h15-LOX-1 with these substrates¹⁵⁻¹⁷. For example, h15-LOX-1 shows a shift in the product profile when 5S-hydroxy-6E,8Z,11Z,14Z-eicosatetraenoic acid (5S-HETE) is the substrate, producing a 14:86 ratio of the ω -6 and ω -9 products. This indicates that the location of hydrogen abstraction is shifted

from C13 with AA to C10 with 5S-HETE. A similar shift in product profile emerges when h15-LOX-1 reacts with the DHA oxylipin, 7S-hydroxy-4Z,8E,10Z,13Z,16Z,19Z-docosahexaenoic acid (7S-HDHA). In this case, h15-LOX-1 reacts with DHA to produce 67% of the 17-product (ω -6) and 20% of the 14-product (ω -9) but reacts with 7S-HDHA to produce 10% of the 17-product (ω -6) and 90% of the 14-product (ω -9) (a ratio of 10:90 for the ω -6: ω -9 products), similar to that seen with 5S-HETE as the substrate¹⁷. In contrast, h15-LOX-2 produces almost 100% of the ω -6 di-oxygenated product¹⁵⁻¹⁷ with either 5S-HETE or 7S-HDHA as substrates.

Altered product specificity has important implications for the biosynthesis of SPM. The proposed biosynthetic routes of SPM, such as 5S,15S-6E,8Z,11Z,13E-dihydroxyeicosatetraenoic acid (5S,15S-diHETE), resolvin E4 (RvE₄, 5S,15S-dihydroxy-6E,8Z,11Z,13E,17Z-eicosapentaenoic acid, 5S,15S-diHEPE) and resolvin D5 (RvD₅, 7S,17S-dihydroxy-4Z,8E,10Z,13Z,15E,19Z-docosahexaenoic acid, 7S,17S-diHDHA), are based on the positional specificity of h15-LOX-1 with fatty acids, such as AA, EPA or DHA¹⁸⁻²⁰. However, the altered positional specificity of h15-LOX-1 with oxylipins suggests that h15-LOX-2 may be involved in the production of 5S,15S-diHETE, RvD₅ and RvE₄, due to its aforementioned higher fidelity. h15-LOX-1 instead produces 5S,12S-dihydroxy-6E,8Z,10E,14Z-eicosatetraenoic acid (5S,12S-diHETE), 5S,12S-dihydroxy-6E,8Z,10E,14Z,17Z-eicosapentaenoic acid (5S,12S-diHEPE), and 7S,14S-dihydroxy-4Z,8E,10Z,12E,16Z,19Z-docosahexaenoic acid (7S,14S-diHDHA) (**Figure 4.1**). Therefore, the *in vivo* biosynthetic routes of these molecules should be carefully

evaluated with the altered positional specificity of h15-LOX-1 and the higher fidelity of h15-LOX-2 in mind.

As stated above, the altered positional specificity of h15-LOX-1 is unusual, as it does not occur in other LOXs. h15-LOX-2, for example, shows strict regiospecificity. It produces approximately 100% the ω -6 product with AA, DHA, 5S-HETE and 7S-HDHA as the substrates^{15, 17, 21}. Similarly, h12-LOX produces approximately 100% of the ω -9 product from AA and greater than 90% of the ω -9 product from 5S-HETE. This suggests that distinct active site structural features of h15-LOX-1 lead to its altered positional specificity.

The structural basis for the stereo- and regio-specificity of h15-LOX-1 with AA has been investigated using site-directed mutagenesis of the active site. Three regions of the active site have been shown to be important for determining the positional specificity of h15-LOX-1 (**Figure 4.2**)²². Early work established that the aromatic ring of F414 forms a p-p stacking interaction with the substrate's Δ 11 double bond and that R402 interacts with the terminal carboxylate^{10, 23-26}. Sloane and coworkers also demonstrated that I417 and M418 help define the bottom of the active site cavity and that mutating these residues to smaller amino acids allowed the substrate to slide deeper into the active site, causing the enzyme to produce more 12-product (ω -9)¹⁰. Kuhn and coworkers expanded this work by showing that F352 further defines the active site and aids in maintaining C15 oxygenation over C12 oxygenation²⁷⁻³⁰. These studies lead to the fatty acid binding hypothesis, in which the specificity of the active site is defined by a few critical amino acids: I417 and M418

at the bottom of the active site, R402 at the active site entrance, and F414 and F352 in the middle of the active site³¹. These residues are positioned along in the boot-shaped active site cavity into which the substrate enters methyl-end first. This model is also observed with structural studies of h12-LOX, in which analogous mutations of conserved amino acids produced similar effects to those seen in h15-LOX-1, albeit with minimal arginine interaction at the entrance¹¹.

h15-LOX-1 primarily catalyzes the abstraction of the pro-S hydrogen from C13 of AA and C15 of DHA.³² To explain the altered positional specificity of h15-LOX-1 with 5S-HETE, 5S-hydroxy-6E,8Z,11Z,14Z,17Z-eicosapentaenoic acid (5S-HEPE) and 7S-HDHA, h15-LOX-1 must primarily abstract from C10 of AA/EPA and C12 of DHA. This implies deeper insertion of the substrate into the active site cavity for these two oxylipins (**Figure 4.2**). Molecular modeling has indicated that the alcohol of 5S-HETE and 7S-HDHA forms a hydrogen bond with the backbone carbonyl of I399 which positions the oxylipin substrates deeper in the active site compared with AA and DHA^{15, 17}. The proposed contribution of additional active site amino acids to substrate binding of 5S-HETE and 7S-HDHA indicates that the existing model of positional specificity in h15-LOX-1 may require additional refinement. The present study investigates whether the established residues which interact with AA also explain the structural basis for the altered positional specificity of h15-LOX-1 with 5S-HETE, 5S-HEPE, and 7S-HDHA and which LOX isozyme could be involved in the biosynthetic pathway for the production of the SPM, RvE4.

4.3 Methods

Expression and Purification of h15-LOX-1 and h15-LOX-2.

Overexpression and purification of his-tagged wild-type and mutant h15-LOX-1 (Accession ID: P16050) and h15-LOX-2 (Accession ID: O15296) was performed using cation exchange and nickel-affinity chromatography as previously described^{33, 34}. Overexpression and purification of wild-type h5-LOX was performed by ammonium-sulfate precipitation as previously described³⁵. The purity of h15-LOX-1 and h15-LOX-2 were assessed by SDS gel to be greater than 85%, and metal content was assessed on a Finnigan inductively-coupled plasma-mass spectrometer (ICP-MS), via comparison with iron standard solution. Cobalt-EDTA was used as an internal standard. The concentration of h5-LOX (Accession ID: P09917) in the ammonium-sulfate was determined as described before,^{15, 17} and due to the difficulty determining the iron content of crude ammonium sulfate-precipitated extracted enzyme, the metalation of h5-LOX was assumed to be 100%, indicating that the estimated kinetic parameters presented in this work are lower limits.

Site-directed Mutagenesis.

Amino acid numbering for h15-LOX-1 refers to the sequence with UniProt accession number P16050 without the 6XHis-tag and with the N-terminal methionine assigned as amino acid number one. The following mutations were introduced into h15-LOX-1: F352L, F352W, E398L, I399A, R402L, L407A, F414L, F414W, I417A, I417M, Q595L. Primers were designed using the Agilent Technologies (CA, USA) online primer-design tool found at:

(<http://www.genomics.agilent.com/primerDesignProgram.jsp>) Mutations were

introduced with a QuikChange[®]II site-directed mutagenesis kit from Agilent Technologies using the included protocol. The mutations were confirmed by sequencing the LOX insert in the pFastBac1 shuttle vector (Eurofins Genomics, KY, USA).

Production and isolation of Oxylipins from h5-LOX

7S-hydroperoxy-4Z,8E,10Z,13Z,16Z,19Z-docosahexaenoic acid (7S-HpDHA) was synthesized by reaction of DHA (25-50 μ M) with h5-LOX. The reaction was carried out for 2 hours in 800 mL of 25mM HEPES, pH 7.5 containing 50mM NaCl, 100 μ M EDTA and 200 μ M ATP. The reaction was quenched with 0.5% glacial acetic acid, extracted 3 times with 1/3 volume dichloromethane and evaporated to dryness under N₂. The products purified isocratically via high performance liquid chromatography (HPLC) on a Higgins Haisil Semi-preparative (5 μ m, 250mm x 10mm) C18 column with 45:55 of 99.9% acetonitrile, 0.1% acetic acid and 99.9% water, 0.1% acetic acid. 7S-HDHA was synthesized as performed for 7S-HpDHA with trimethylphosphite added as a reductant prior to HPLC. The isolated products were assessed to be greater than 95% pure by LC-MS/MS. 5S-HpETE and 5S-hydroperoxy-6E,8Z,11Z,14Z,17Z-eicosapentaenoic acid (5S-HpEPE) were synthesized by reaction of AA and EPA, respectively, (25-50 μ M) with h5-LOX. The reactions were carried out for 1 hour in 1000 mL of 25mM HEPES, pH 7.5 containing 50mM NaCl, 100 μ M EDTA and 200 μ M ATP. The reactions were quenched with 0.5% glacial acetic acid, extracted 3 times with 1/3 volume dichloromethane and evaporated to dryness under N₂. 5S-HETE and 5S-HEPE were

synthesized as performed for 5S-HpETE and 5S-HpEPE with trimethylphosphite added as a reductant prior to HPLC. The products purified isocratically via high performance liquid chromatography (HPLC) on a Higgins Haisil Semi-preparative (5 μ m, 250mm x 10mm) C18 column with 45:55 of 99.9% acetonitrile, 0.1% acetic acid and 99.9% water, 0.1% acetic acid. The products were determined to be of the S configuration, as described previously.^{15, 36}

Steady State Kinetics of h15-LOX-1

h15-LOX-1 steady-state kinetic reactions were constantly stirred at ambient temperature, in a 1 cm² quartz cuvette containing 2 mL of 25 mM HEPES, pH 7.5 with substrate, such as AA, DHA, 5S-HETE, 5S-HpETE, 7S-HDHA, or 7S-HpDHA. Substrate concentrations were varied from 0.25 μ M to 10 μ M for AA or 0.5 μ M to 40 μ M for 5S-HETE and 5S-HpETE. DHA concentrations were varied from 0.25-10 μ M, 7S-HDHA concentrations were varied from 0.3-15 μ M, and 7S-HpDHA concentrations were varied from 0.3-20 μ M. Concentrations of AA and DHA were determined by measuring the amount of 15S-HpETE and 17S-hydroperoxy-4Z,7Z,10Z,13Z,15E,19Z-docosahexaenoic acid (17S-HpDHA), respectively, produced from complete reaction with soybean lipoxygenase-1 (sLO-1). Concentrations of 5S-HETE, 5S-HpETE, 7S-HDHA, and 7S-HpDHA were determined by measuring the absorbance at 234 nm. Reactions were initiated by the addition of h15-LOX-1 (~200-600 nM final concentration) and were monitored on a Perkin-Elmer Lambda 45 UV/VIS spectrophotometer. Product formation was determined by the increase in absorbance at 234 nm for 5S-HETE ($\epsilon_{234} = 27,000 \text{ M}^{-1}$

cm⁻¹), 270 nm for 5S,12S-diHETE ($\epsilon_{270} = 40,000 \text{ M}^{-1} \text{ cm}^{-1}$), 254 nm for 5S,15S-diHETE ($\epsilon_{254} = 21,500 \text{ M}^{-1} \text{ cm}^{-1}$)³⁷, 234 nm for 7S-HpDHA ($\epsilon_{234} = 25,000 \text{ M}^{-1} \text{ cm}^{-1}$) and 270 nm for 7S,14S-diHDHA ($\epsilon_{270} = 40,000 \text{ M}^{-1} \text{ cm}^{-1}$)^{38, 39}. 5S,15S-diHDHA and 7S,17S-diHDHA have an absorbance max of 245 nm, however, due to overlap with the substrate peak at 234 nm formation of this product was measured at 254 nm using an extinction coefficient of 21,500 M⁻¹ cm⁻¹ to adjust for the decreased rate of absorbance change at this peak shoulder⁴⁰. KaleidaGraph (Synergy) was used to fit initial rates (at less than 20% turnover), as well as the second order derivatives (k_{cat}/K_M) to the Michaelis-Menten equation for the calculation of kinetic parameters.

Product Analysis of LOX reactions with AA, DHA, 5S-HETE, 5S-HEPE and 7S-HDHA

Reactions were carried out in 2 mL of 25 mM HEPES, pH 7.5 with stirring at ambient temperature. Reactions with AA and DHA contained 10 μM substrate and ~200 nM h15-LOX-1. Those with 5S-HETE, 5S-HEPE, 7S-HDHA and contained 20 μM substrate and ~550 nM h15-LOX-1, due to their low reactivity. Reactions were monitored via UV-vis spectrophotometer and quenched at 50% turnover with 0.5% glacial acetic acid. Each quenched reaction was extracted with 6 mL of DCM and reduced with trimethylphosphite. The samples were then evaporated under a stream of N₂ to dryness and reconstituted in 50 μL of methanol containing 3 μM 13-HODE as an internal standard. Control reactions without enzymes were also conducted and used for background subtraction, ensuring oxylipin degradation products were removed from analysis. Reactions were analyzed in the same manner mentioned

above. MS² was performed in a targeted manner with a mass list containing the following m/z ratios ± 0.5 : 317.2 (HEPE), 319.2 (HETE), 333.2 (diHEPE), 335.2 (diHETE) 343.4 (HDHA), 359.4 (diHDHA). Products were identified by matching retention times, UV spectra, and fragmentation patterns to known standards, or in the cases where MS standards were not available, structures were deduced from comparison with known and theoretical fragments. A representative trace of the reaction of AA with h15-LOX-1 demonstrates the relative purity of the oxylipin products and the negative control (Figure S4.1 in the Supporting Information).

4.4 Results and Discussion

The docking model proposed for AA binding in the active site of h15-LOX-1 postulates three regions of the active site to be important for determining the positional specificity which interact with the head, middle and base of the fatty acid (**Figure 4.3**). The key residues outlined in **Figure 4.3** are in h15-LOX-1 are R402, L407, F414, I417 and F352. To determine if 5S-HETE binds in a similar fashion to AA, we created a series of mutants to investigate the binding constraints of 5S-HETE and assayed their kinetic and product profiles.

Binding to substrate carboxylate: R402

Positively charged amino acids can play a role in binding the carboxylate of fatty acids⁴¹. R402, located near the entrance to the active site cavity, is conserved in both h12-LOX and h15-LOX-1 and is proposed to interact with the carboxylic acid moiety of AA²³. This interaction is thought to stabilize the substrate fatty acid in the

active site with the methyl end orientated towards the bottom of the active site pocket. To test whether this model can be applied to 5S-HETE, R402 was replaced with leucine in h15-LOX-1. However, only marginal change was observed in the steady-state Michaelis-Menten kinetics of 5S-HETE with R402L compared with the wild-type enzyme (**Table 4.1**). While this mutation slightly lowered the kinetic parameters for AA, it is observed that the k_{cat} is approximately 3-fold greater for R402L over that of wild-type with 5S-HETE as the substrate, which is unexpected. Considering that Arg is larger than Leu, it is possible that the smaller Leu allows for a more rapid product release of the larger 5S-HETE. The product profile showed that the percentage of 5S-HETE oxygenated by R402L at C12 did not change (within error). In total, the data indicate that R402L does not significantly impact 5S-HETE catalysis or positioning, relative to AA (**Table 4.2**). It should be noted that in the current work, the product profile of our R402L mutant with AA was similar to previously published work²³, however the kinetic parameters of R402L were not. The mutant, R402L, demonstrated a comparable k_{cat} with AA to that of the wild-type enzyme, however the k_{cat}/K_M was only 3-fold lower than wild-type (**Table 4.1**), which is smaller than the 7-fold change seen previously²³. This smaller change is consistent with recent studies on h12-LOX, which demonstrated negligible kinetic effects with the R402L mutant¹¹. The smaller kinetic effect for R402L than previously reported could be due to differences in the experimental design. The prior kinetic work used 13-HpODE, a known allosteric effector⁴², detergents and high concentrations of fatty acid substrate.

These conditions could lead to substrate inhibition and hence affect the kinetic parameters.

Narrow midpoint of active site cavity: L407

L546 is thought to define the bend point of the L-shaped active site cavity of soybean 15-LOX (s15-LOX), based on docking of AA into the crystal structure of s15-LOX^{23, 43}. Sequence alignment shows that this leucine is conserved in the majority of lipoxygenases and is homologous to L407 in humans²³. Substituting a smaller amino acid at this location in h12-LOX resulted in a loss of activity and a shift to greater oxygenation at C15, by widening the active site across from the catalytic iron¹¹. To test whether L407 influences the positioning of AA or 5S-HETE within the active site, L407A was generated. For AA, the k_{cat} and k_{cat}/K_M values decreased approximately 5-fold compared to wild-type, but for 5S-HETE, the values decreased even less (**Table 4.3**). The greater decrease in kinetic values for AA than that of 5S-HETE possibly suggests that the larger 5S-OH of 5S-HETE is filling the missing space of the L407A mutant, thus diminishing the mutational effect. When reacting with AA and 5S-HETE, L407A produces more C12 products with AA than wild-type, but similar product ratios for 5S-HETE (**Table 4.4**). These product profile data are similar to the kinetic data in that L407A affects the positioning of AA more than that of 5S-HETE, supporting the hypothesis that the larger 5S-HETE is better positioned for catalysis in the L407A active site.

Π -stacking interactions with substrate double bonds: F414

It has previously been determined that the $\Delta 11$ double bond of AA is

positioned in the active site of h15-LOX-1 to form π - π stacking interactions with F414²³. This interaction is also observed in h12-LOX with F414, and could be considered a common structural feature in hLOX biochemistry¹¹. To test whether F414 of h15-LOX-1 would also interact with 5S-HETE, the catalysis and product profile was investigated. Both the k_{cat} and k_{cat}/K_M values for F414I with 5S-HETE decreased over 15-fold compared to wild-type (**Table 4.5**), but the products generated from the reaction with 5S-HETE showed no change relative to wild-type (**Table 4.6**). Mutation of this residue to tryptophan, F414W, restored the wild-type activity of the enzyme for 5S-HETE, with both k_{cat} and k_{cat}/K_M nearly returning to their wild-type values. The recovery of activity with the addition of the aromatic tryptophan for the catalysis of 5S-HETE is similar to what was seen previously with AA and indicates that there are also π - π stacking interactions between 5S-HETE and F414. For comparison, we confirmed the previously established interaction of F414 and AA (**Table 4.5**)²³. Interestingly, F414W caused more oxygenation to occur at C15 for both AA and 5S-HETE. This is consistent with the “dip-stick” substrate binding model where the larger tryptophan prohibits the deeper entry of the substrate, relative to phenylalanine, and thus increases the production of the 15-product.

Depth of the of active site cavity: I417 and F352

Previous work indicated that F353 contributed to the positional specificity in s15-LOX by affecting the depth of the active site⁴⁴. This hypothesis was extended to the sequence equivalent residue in h15-LOX-1 with work on chimeric mutants, which showed a similar role for F352²⁷. I417 has also been implicated in binding the methyl

end of the substrate because of its position at the bottom of the active site in h12-LOX^{11, 45} and h15-LOX-1²⁴. Decreasing the residue size of either F352 or I417 in h15-LOX-1 increases the cavity size and thus increases oxygenation at C12 due to AA positioning deeper in the active site, as seen in previous work¹⁰. To extend this work and determine if the active site depth influences the reactivity of 5S-HETE, kinetics were investigated with smaller amino acids at positions 352 and 417. Compared to wild-type, the k_{cat} and k_{cat}/K_M values for I417A and F352L with both AA and 5S-HETE were approximately the same as wild-type (**Table 4.7**). This is remarkable considering that the oxygenation of AA at C12 increases dramatically for both I417A and F352L (**Table 4.8**), indicating a shift in the positioning of AA deeper in the active site pocket due to the smaller active site residues, but only a small change in rate is observed. With respect to 5S-HETE, oxygenation of C12 is already the major product, thus enlarging the active site has only a slight change in both the kinetics and product profile because 5S-HETE is already positioned deep in the active site.

With the smaller residues at 417 and 352 allowing the substrate to bind deeper into the active site, it was hypothesized that larger residues near the bottom of the active site would have the opposite effect by restricting substrate binding and thereby shifting positional specificity from C12 to C15. For I417M, the product profile for both AA and 5S-HETE were unchanged relative to wild-type, indicating that the positioning of the two substrates has not changed significantly with this mutant (**Table 4.8, Figure 4.4**). Interestingly, the kinetic values for both AA and 5S-HETE

increase with I417M. Considering that the product profiles for both of these substrates is similar to that of wild-type enzyme, it is difficult to explain this result by sterics, so possibly the active site dynamics are affected.

For F352W, the percent of C15 product increased for both AA and 5S-HETE relative to wild-type and I417M, indicating that F352W has a greater decrease in active site volume (**Table 4.8, Figure 4.5**). The effect of F352W is larger for 5S-HETE than that of AA, with the C15 percent increasing from 14% to 69%, possibly indicating that 5S-HETE binds deeper into the pocket than AA and thus the reduced active site volume has a larger effect. The kinetic data reflect this hypothesis with the k_{cat}/K_M of 5S-HETE decreasing 3-fold, while the value for AA increases 1.5-fold, indicating a larger change in 5S-HETE positioning in the active site than that of AA (**Table 4.7**).

Depth of active site with DHA and 7S-HDHA

The dip-stick model of substrate binding by h15-LOX-1 posits that the depth of the active site is a primary determinant for how far the methyl end of a substrate can insert. For 5S-HETE, its position in the active site of h15-LOX-1 is deeper than that of AA and thus the 5S,12S-diHETE product is primarily synthesized. 7S-HDHA shows an analogous change in positional specificity, with h15-LOX-1 producing the non-canonical product, 7S,14S-diHDHA, instead of 7S,17S-diHDHA¹⁷. 7S-HDHA and 5S-HETE are structurally similar in that the C7 and C5 alcohols are both located on the w-16 carbon relative to the methyl end of the substrate and h15-LOX-1 oxygenates at their w-9 positions, C14 and C12, respectively. Since h15-LOX-1

shows similar shifts in product profile with both 7S-HDHA and 5S-HETE, it is likely that they are bound in the active site in a similar fashion^{15, 17}. Consequently, it is likely that amino acid mutations changing the depth of the active site cavity will affect 7S-HDHA similarly to that of 5S-HETE.

To investigate this hypothesis, the positional specificity of h15-LOX-1 with both DHA and 7S-HDHA were assayed with I417A, I417M, F352L and F352W. h15-LOX-1 reacting with DHA produced a mixture of primarily the 14- and 17-oxylipins, as seen previously (**Table 4.9**).⁴⁶ When reacting with I417A, DHA displayed the expected shift to more oxygenation at C14 and less oxygenation at C17 relative to wt 12-LOX, as the substrate was able to position deeper in the active site relative to the iron (**Table 4.9**.)

The reaction of DHA with I417M demonstrated a small shift to increased oxygenation at C17, resulting from the slightly bulkier methionine residue. The reaction between F352L and DHA showed the expected decrease in oxygenation at C17, however instead of an increase at C14, a large increase in oxygenation at C20 occurred. It is unclear why this product increased, but it may indicate a change in the overall substrate orientation due to folding of the substrate methyl end so that it is positioned less deep in the active site. When reacting with DHA, F352W produced 79% of the 17-product, compared to 65% with wild-type, demonstrating that the bulkier tryptophan substitution produces the largest shift in product profile, similar to the results with AA (**Table 4.8**).

The product profile with 7S-HDHA as the substrate shows similar results as that with DHA as the substrate, with smaller substitutions allowing for deeper entry of 7S-HDHA into the active site (**Table 4.9**). The smaller amino acids of F352L and I417A both increase the amount of oxygenation occurring on C17, from 90% in wild-type to 97% with I417A and 100% with F352L. Substituting larger amino acids in these positions had the expected opposite effect. The reaction with I417M decreased oxygenation at C17 from 90% in wild-type to 64 % in the mutant. The reaction of F352W decreased oxygenation at C17 to only 6%, a near complete reversal of the altered positional specificity seen with 7S-HDHA and the wild-type enzyme.

When comparing the product profile of 5S-HETE (**Table 4.8**) and 7S-HDHA (**Table 4.9**), I417M has a much larger effect on 7S-HDHA, which may indicate that the larger size of 7S-HDHA compared with 5S-HETE, makes it more sensitive to the small change in active site depth brought about by I417M. In total, these data indicate that the shift in positional specificity is related to the size of the amino acids at the bottom of the active site for 7S-HDHA, consistent with the results obtained for 5S-HETE and indicates a similar mode of binding between 5S-HETE and 7S-HDHA.

Coordination of alcohol group of 5S-HETE/7S-HDHA through hydrogen bonding with the carbonyl backbone of I399

Molecular dynamic simulations coupled with computational docking revealed a possible intermolecular bond in the active site of h15-LOX-1 with the hydroxyl group of 5S-HETE/7S-HDHA^{15, 17}. The interaction observed was a hydrogen bond with the backbone carbonyl of I399. The positioning of this carbonyl hydrogen bond in the active site, relative to the coordinating iron and oxygen channel, is proposed to

hold the substrate in a manner that makes enzymatic hydrogen abstraction more likely at the w-9 carbon than the w-6 carbon. To test this hypothesis, the I399A mutant was reacted with 5S-HETE, with the hope that the side chain would affect the hydrogen bond to the backbone carbonyl, however, the reactivity and product profile of I399A were comparable to that of wild-type (data not shown). This is an inconclusive result and we are currently pursuing another line of inquiry in order to determine the structural requirements for the non-canonical activity of h15-LOX-1.

***In Vitro* Biosynthesis of Resolvin E₄ (5S,15S-diHEPE)**

Previous work has proposed that the biosynthesis of RvE₄ is accomplished by h15-LOX-1 reacting with EPA to produce 15S-HpEPE, which is then further oxidized by h5-LOX to yield the 5S,15S-diHEPE product (RvE₄)¹⁸. However, past *in vitro* experiments have shown w-6 oxylipins to be extremely poor substrates for h5-LOX^{15, 17}, which raises questions regarding the proposed biosynthetic pathway of RvE₄. To investigate this further, *in vitro* reactions with h15-LOX-1 and h15-LOX-2 in the presence of 5S-HEPE were carried out. Product profile analysis of the h15-LOX-1 products revealed a shift in positional specificity, similar to that seen with the other w-6 oxylipins, with more 5S,12S-diHEPE being generated than 5S,15S-diHEPE, 78% and 22%, respectively (**Table 4.10**). However, h15-LOX-2 produced mostly 5S,15S-diHEPE (93%, **Table 4.10**), supporting our previous work that h15-LOX-2 primarily generates the 5S,15S dioxylin product and, thus, may be the primary source of RvE₄. This was previously observed by Kutzner et al. when h5-LOX and h15-LOX-2 were added to a buffer containing EPA.¹⁶

Regarding the relative rates of catalysis for RvE₄, 5S-HEPE (10 μM) was reacted with h15-LOX-2 and 15S-HEPE (10 μM) with h5-LOX (**Table 4.11**). The data indicates that h15-LOX-2 is a 40-fold faster catalyst than h5-LOX when reacting with their secondary substrates, although they have comparable rates with AA and EPA as substrates, at 10 μM. Given the relative kinetic capabilities of h5-LOX with 15S-HETE and h15-LOX-2 with 5S-HETE^{15, 17, 47, 48}, h15-LOX-2 appears to be the faster catalyst for the final step in RvE₄ generation. However, considering that in vivo, the level of substrate could be lower than 10 μM and that the cell contains 5-LOX activating protein (FLAP) and other cellular components, we cannot discount a change in relative LOX isozyme reactivity due to the cellular milieu.

4.5 Conclusion

The fatty acid docking mode developed to explain the positional specificity of h15-LOX-1 (ALOX15) reactivity with AA²³ includes 5 principle residues: R402, L407, F414, I417 and F352. Of these five, three are conserved in the mouse ortholog, ALOX15 (residues 402, 407, 414, 69% identity to human ALOX15) but only two are conserved in h15-LOX-2 (ALOX15B, residues 352, 407, 38% identity to human ALOX15). These results are intriguing since the gene sequence of mouse ALOX15 is more similar to human ALOX15, but it primarily produces 12-HETE. However, the gene sequence of human ALOX15B is less similar to human ALOX15, but it primarily produces 15-HETE. These data illustrate the observation that the sequence similarity between genes is not as important as specific residues in the active site.

In the current work, the established AA docking model for h15-LOX-1 only partially explains the altered positional specificity of h15-LOX-1 with 5S-HETE and 7S-HDHA. R402L did not have a large effect on 5S-HETE catalysis, indicating that this interaction with the substrate carboxylate is not important for 5S-HETE positioning, as previously seen for h12-LOX and AA¹¹. F414 appears to π - π stack with 5S-HETE, as seen with AA binding, indicating an interaction between a double bond of 5S-HETE and F414. Further evidence of the importance of steric interactions at the bottom of the active site cavity comes from mutagenesis of F352 and I417, which plays the largest roles in 5S-HETE positioning. Decreasing the size of the amino acids in these locations shifted oxygenation of 5S-HETE to C12, while increasing the size of these residues reversed the positional specificity of h15-LOX-1 with 5S-HETE to C15, with F352 having a larger impact than I417. Mutants at these locations demonstrated a similar effect with 7S-HDHA, indicating that both substrates interact with the bottom of the active site. Together, these data indicate that of the three regions proposed to control positional specificity of h15-LOX-1, π - π stacking and active site cavity depth are the primary determinants of positional specificity with 5S-HETE and 7S-HDHA, similar to what was observed with AA as the substrate. Mutation of I399 did not support our hypothesis that its carbonyl backbone hydrogen bonded with the ω -16 alcohol. However, we have recently determined that unsaturation and length of the oxylipin substrate affects the product profile, undermining our I399 carbonyl hypothesis. We are currently investigating this line of inquiry to identify the structural property which accounts for the non-

canonical product profile of h15-LOX-1. Furthermore, experimentation by Saam et al.⁴⁹ with murine 12/15 lipoxygenase and Klinman and coworkers^{50, 51} with soybean 15-lipoxygenase has provided compelling evidence for the presence of a dynamic oxygen channel linking the enzyme surface to the active site of lipoxygenases. The change in positional specificity of h15-LOX-1 when reacting with 5S-HETE and 7S-HDHA could also be affected by changes in the oxygen channel with oxylipin binding, which we are currently investigating.

Finally, the altered reactivity of h15-LOX-1 with 5S-HEPE suggests that the biosynthesis of RvE₄ may not proceed through h15-LOX-1. The above *in vitro* reaction rates and product profiles suggest that the biosynthetic pathway for RvE₄ production could be initiated with h5-LOX biosynthesizing 5S-HEPE from EPA, followed by h15-LOX-2 producing 5S,15S-diHEPE (i.e., RvE₄). It should be mentioned that 5,15-oxylipin has been observed in a variety of human cell lines,^{52, 53} indicating important roles for h5-LOX and h15-LOX, but the order of biosynthetic steps and the specific identity of the h15-LOX isozyme remains unclear. Recently, Mainka et al. demonstrated that 5,15-oxylipin production was a primary product when 15-oxylipin was given to polymorphonuclear leukocytes (PMNL) and that h5-LOX was involved, with the presence of FLAP being critical.⁵⁴ Therefore, it could be that the lowered *in vitro* activity of h5-LOX observed in our work is due to the dissimilar environment relative to the cellular milieu. However, the role of h15-LOX-1 remains unclear. Due to the cellular mixture of the PMNLs, Mainka et al. could not identify if h15-LOX-1 or h15-LOX-2 were the active partner in the biosynthesis of

the 5,15-oxylipin, adding further obscurity to their biosynthetic pathway. Therefore, we are currently investigating the expression levels of the LOX isoforms in immune cells and their inhibition by specific LOX inhibitors during the inflammatory response to determine which LOX is involved in the production of RvE₄ and the order of the biosynthetic steps.

4.6 Figures and Tables

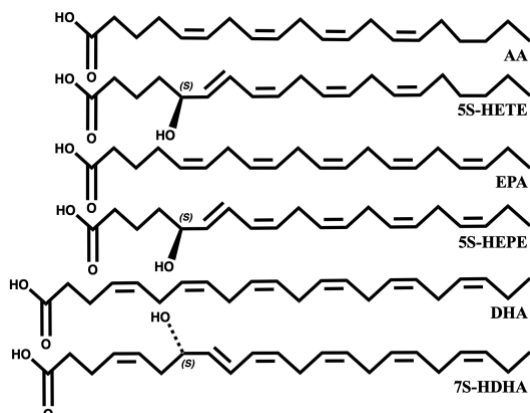


Figure 4.1 Structures of AA, EPA, DHA and their primary h5-LOX oxylipin

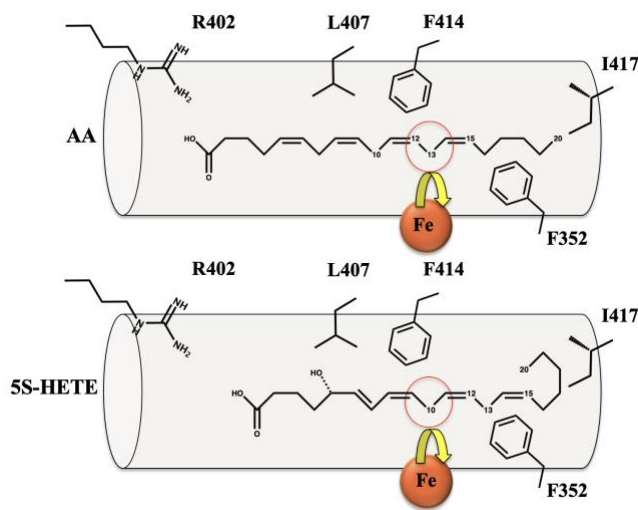


Figure 4.2 Model of the active site of h15-LOX-1, showing amino acid residues hypothesized to influence positional specificity with AA. The top figure depicts positioning of AA, while the bottom depicts positioning of 5S-HETE. h15-LOX-1 primarily abstracts a hydrogen from C13 of AA and C10 of 5S-HETE, which indicates that the two substrates must be positioned differently in the active site relative to the catalytic iron. The hydrogen bond between the alcohol of 5S-HETE and the carbonyl of I399 is not shown.

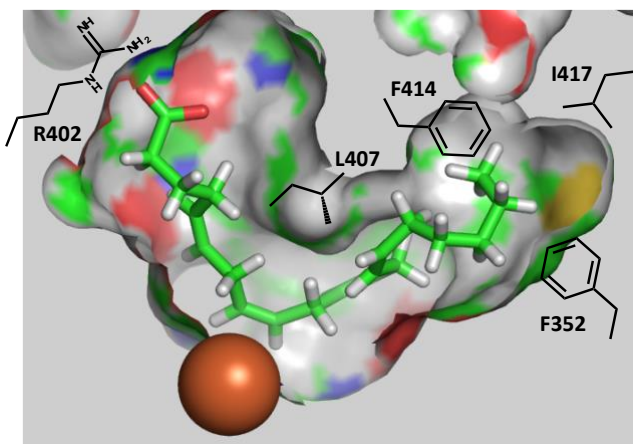


Figure 4.3 Model of the active site of h15-LOX-1 showing L-shaped binding cavity, position of catalytic iron in orange and AA in green at middle. Amino acids shown to play a role in positional specificity of AA are highlighted: R402, L407, F414, I417, F352.

	AA			5S-HETE		
	K_M	k_{cat}	k_{cat}/K_M	K_M	k_{cat}	k_{cat}/K_M
wild-type	5.1 ± 0.3	10 ± 1	2.1 ± 0.3	4.9 ± 0.6	1.1 ± 0.4	0.22 ± 0.08
R402	9.8	7.2	0.73	6.3	3.6 ± 0.1	0.55
L	± 1.5	± 0.5	± 0.13	± 0.6		± 0.06

Table 4.1 Steady state kinetics of wild-type and R402L h15-LOX-1 with AA and 5S-HETE substrates. K_M is in units of μM , k_{cat} is in units of $\text{sec}^{-1}\mu\text{M}^{-1}$, k_{cat}/K_M is in units of $\text{sec}^{-1}\mu\text{M}^{-1}$.

	AA		5S-HETE	
	% C15	% C12	% C15	% C12
wild-type	85 ±4	15 ±4	14 ±6	86 ±6
R402L	73 ±6	27 ±6	8 ±2	92 ±2

Table 4.2 Product profile of wild-type and R402L h15-LOX-1 with AA and 5S-HETE. The percent of the carbon which is being oxidized is presented (i.e., %C15 is percent oxidation on C15 of the substrate).

	AA			5S-HETE		
	K_M	k_{cat}	k_{cat}/K	K_M	k_{cat}	k_{cat}/K_M
wild-type	5.1 ±0.3	10 ±1	2.1 ±0.3	4.9 ± 0.6	1.1 ±0.4	0.22 ±0.08
L407A	4.9 ±1.2	2.0 ±0.4	0.41 ±0.08	7.9 ± 1.4	0.7 ±0.1	0.09 ±0.02

Table 4.3 Steady state kinetics of wild-type and L407A h15-LOX-1 with AA and 5S-HETE. K_M is in units of μM , k_{cat} is in units of $\text{sec}^{-1}\mu\text{M}^{-1}$, k_{cat}/K_M is in units of $\text{sec}^{-1}\mu\text{M}^{-1}$.

	AA		5S-HETE	
	% C15	% C12	% C15	% C12
wild-type	85 ±4	15 ±4	14 ±6	86 ±6
L407A	67 ±7	33 ±7	9 ±2	91 ±2

Table 4.4 Product profiling of wild-type and L407A h15-LOX-1 with AA and 5S-HETE. The percent of the carbon which is being oxidized is presented (i.e., %C15 is percent oxidation on C15 of the substrate).

	AA			5S-HETE		
	K_M	k_{cat}	k_{cat}/K	K_M	k_{cat}	k_{cat}/K_M
Wild-type	5.1 ± 0.3	10 ± 1	2.1 ± 0.3	4.9 \pm 0.6	1.1 ± 0.4	0.22 ± 0.08
F414I	6.6 ± 0.9	1.2 \pm 0.4	0.18 ± 0.03	4.7 \pm 0.7	0.073 ± 0.03	0.013 \pm 0.006
F414W	6.8 ± 0.5	12 ± 1	1.8 ± 0.1	4.2 \pm 0.6	0.95 \pm 0.4	0.23 \pm 0.09

Table 4.5 Steady state kinetics of wild-type, F414I and F414W h15-LOX-1 with AA and 5S-HETE. K_M is in units of μM , k_{cat} is in units of $\text{sec}^{-1}\mu\text{M}^{-1}$, k_{cat}/K_M is in units of $\text{sec}^{-1}\mu\text{M}^{-1}$.

	AA		5S-HETE	
	% C15	% C12	% C15	% C12
Wild-type	85 \pm 4	15 \pm 4	14 \pm 6	86 \pm 6
F414I	82 \pm 2	18 \pm 2	12 \pm 2	88 \pm 2
F414W	95 \pm 1	5 \pm 1	32 \pm 2	68 \pm 2

Table 4.6 Product profiling of wild-type, F414I and F414W h15-LOX-1 with AA and 5S-HETE. The percent of the carbon which is being oxidized is presented (i.e., %C15 is percent oxidation on C15 of the substrate).

	AA			5S-HETE		
	K_M	k_{cat}	k_{cat}/K_M	K_M	k_{cat}	k_{cat}/K_M
wild-type	5.1 ±0.3	10 ±1	2.1 ±0.3	4.9 ±0.6	1.1 ±0.4	0.22 ±0.08
I417A	3.9 ±1.5	5.1 ±1.8	1.3 ±0.5	3.7 ±1.5	0.5 ±0.2	0.14 ±0.06
I417M	1.9 ±0.3	8.0 ±0.5	4.2 ±0.4	3.5 ±0.4	3.8 ±0.2	1.1 ±0.2
F352L	4.3 ±2	8.4 ±3	1.9 ±0.8	4.4 ±2	0.91 ±0.3	0.21 ±0.08
F352W	3.5 ±0.9	11 ±1	3.1 ±0.6	20 ±5	1.3 ±0.2	0.065 ±0.01

Table 4.7 Steady state kinetics of wild-type and various mutants of h15-LOX-1 with AA and 5S-HETE. K_M is in units of μM , k_{cat} is in units of $\text{sec}^{-1}\mu\text{M}^{-1}$, k_{cat}/K_M is in units of $\text{sec}^{-1}\mu\text{M}^{-1}$.

	AA		5S-HETE	
	% C15	% C12	% C15	% C12
wild-type	85 ± 4	15 ± 4	14 ± 6	86 ± 6
I417A	22 ± 2	71 ± 2	3 ± 1	97 ± 1
I417M	87 ± 2	13 ± 2	16 ± 2	84 ± 2
F352L	16 ± 3	81 ± 3	5 ± 2	95 ± 2
F352W	96 ± 2	4 ± 2	69 ± 6	31 ± 6

Table 4.8 Product profiling of wild-type and various mutants of h15-LOX-1 with AA and 5S-HETE. The percent of the carbon which is being oxidized is presented (i.e., %C15 is percent oxidation on C15 of the substrate, i.e. AA and 5S-HETE).

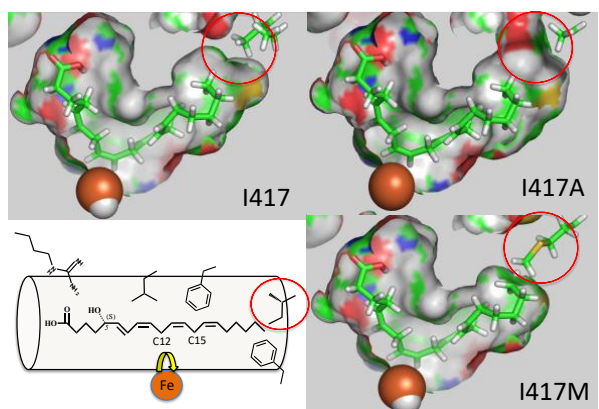


Figure 4.4 Model of the active site of h15-LOX-1 showing position of I417 and the effects that various amino acid mutations have on the size of the active site. I417A creates more space at the bottom of the active site, while I417M creates less space.

	DHA				7S-HDHA			
	% C20	% C17	% C14	% C11	% C20	% C17	% C14	% C11
wild-type	6 ±2	65 ±4	22 ±5	6 ±1	-	10 ±6	90 ±6	0
I417A	2 ±2	55 ±8	40 ±8	2 ±2	-	-	97 ±1	3 ±1
I417M	2 ±1	73 ±2	24 ±1	-	-	36 ±2	64 ±2	-
F352L	29 ±3	47 ±3	23 ±3	-	-	-	100	-
F352W	7 ±2	79 ±6	10 ±3	-	-	94 ±1	6 ±1	-

Table 4.9 Product profiling of wild-type and various mutants of h15-LOX-1 with DHA and 7S-HDHA. The percent of the carbon which is being oxidized is presented (i.e., %C11 is percent oxidation on C11 of the substrate). K_M is in units of μM , k_{cat} is in units of $\text{sec}^{-1}\mu\text{M}^{-1}$, k_{cat}/K_M is in units of $\text{sec}^{-1}\mu\text{M}^{-1}$.

	EPA		5S-HEPE	
	% C15	% C12	% C15	% C12
h15-LOX-1	87 ± 2	13 ± 2	22 ± 1	78 ± 1
h15-LOX-2	100	0	93 ± 3	7 ± 3

Table 4.10 In vitro Product profile of h15-LOX-1 and h15-LOX-2 reacting with EPA and 5S-HEPE. The percent of the carbon which is being oxidized is presented (i.e., %C15 is percent oxidation on C15 of the substrate).

Enzyme	Substrate	V_{max} (mol/sec ⁻¹ /mol ⁻¹)
h5-LOX*	AA	0.15 ± 0.03
h5-LOX*	EPA	0.14 ± 0.01
h5-LOX*	15S-HEPE	0.0037 ± 0.0006
h15-LOX-2	AA	0.24 ± 0.04
h15-LOX-2	EPA	0.26 ± 0.03
h15-LOX-2	5S-HEPE	0.17 ± 0.03

Table 4.11 V_{max} comparison of h5-LOX and h15-LOX-2 with secondary substrates. *The ammonium sulfate-precipitated h5-LOX protein concentration was estimated from SDS-PAGE as previously published (Perry et al., 2020), such that protein concentrations between the LOXs was maintained. [ENREF 1](#)

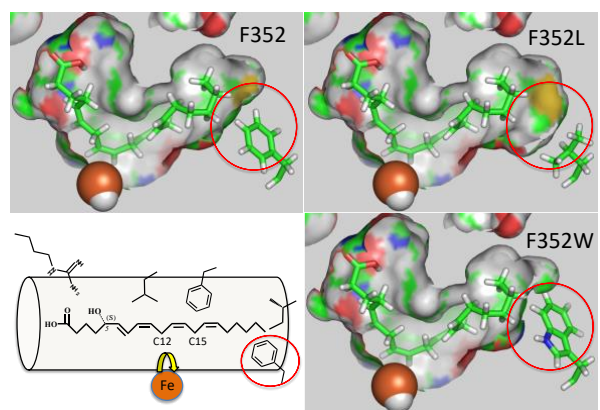


Figure 4.5 Model of the active site of h15-LOX-1 showing position of F352 and the effects that various amino acid mutations have on the size of the active site. F352L creates more space at the bottom of the active site, while F352W creates less space.

Figure S4.1

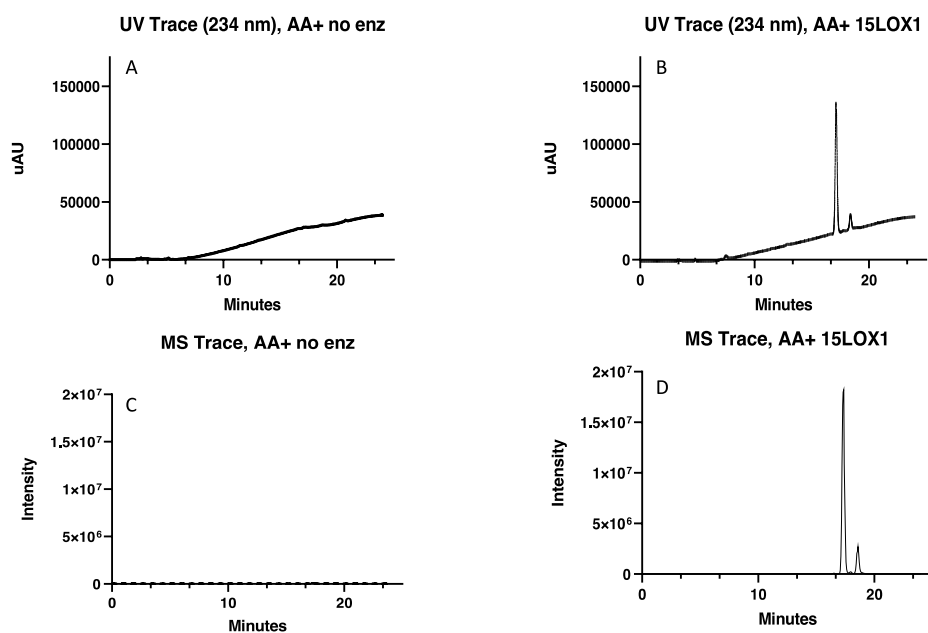


Figure S4.1 LC-MS/MS chromatograms. A, UV chromatogram at 234 nm of the control reaction (no enzyme + AA). B, UV chromatogram at 234 nm of the h15-LOX-1 + AA reaction. C, MS² TIC chromatogram of the control reaction. D, MS² TIC chromatogram of the h15-LOX-1 + AA reaction. Baseline drift at 234 nm is due to ACN gradient. MS² mass filter was set to 319.2 +/- 0.5.

4.7 References

- [1] Brash, A. R. (1999) Lipoxygenases: Occurrence, Functions, Catalysis and Acquisition of Substrate, *J. Biol. Chem.* 274, 23679-23682.
- [2] Kuhn, H., Saam, J., Eibach, S., Holzhutter, H. G., Ivanov, I., and Walther, M. (2005) Structural biology of mammalian lipoxygenases: enzymatic consequences of targeted alterations of the protein structure, *Biochem Biophys Res Commun* 338, 93-101.
- [3] Mashima, K., Suzuki, S., Mori, T., Shimizu, T., Yamada, S., Hirose, S., Okamoto, S., and Suzuki, N. (2015) Chronic lymphocytic inflammation with pontine perivascular enhancement responsive to steroids (CLIPPERS) after treatment for Hodgkin's lymphoma, *Int J Hematol* 102, 709-712.
- [4] Funk, C. D. (2006) Lipoxygenase pathways as mediators of early inflammatory events in atherosclerosis, *Arteriosclerosis, thrombosis, and vascular biology* 26, 1204-1206.
- [5] Serhan, C. N. (2007) Resolution phase of inflammation: novel endogenous anti-inflammatory and proresolving lipid mediators and pathways, *Annual review of immunology* 25, 101-137.
- [6] Serhan, C. N. (2010) Novel lipid mediators and resolution mechanisms in acute inflammation: to resolve or not?, *Am J Pathol* 177, 1576-1591.
- [7] Wisastra, R., and Dekker, F. J. (2014) Inflammation, Cancer and Oxidative Lipoxygenase Activity are Intimately Linked, *Cancers (Basel)* 6, 1500-1521.
- [8] Fabre, J. E., Goulet, J. L., Riche, E., Nguyen, M., Coggins, K., Offenbacher, S., and Koller, B. H. (2002) Transcellular biosynthesis contributes to the production of leukotrienes during inflammatory responses in vivo, *J Clin Invest* 109, 1373-1380.
- [9] Brash, A. R., Boeglin, W. E., and Chang, M. S. (1997) Discovery of a second 15S-lipoxygenase in humans, *Proc Natl Acad Sci U S A* 94, 6148-6152.
- [10] Sloane, D., Leung, R., Craik, C., and Sigal, E. (1991) A Primary Determinant for Lipoxygenase Positional Specificity, *Nature* 354, 149-152.
- [11] Aleem, A. M., Tsai, W. C., Tena, J., Alvarez, G., Deschamps, J., Kalyanaraman, C., Jacobson, M. P., and Holman, T. (2019) Probing the Electrostatic and Steric Requirements for Substrate Binding in Human Platelet-Type 12-Lipoxygenase, *Biochemistry* 58, 848-857.

- [12] Kuhn, H., Banthiya, S., and van Leyen, K. (2015) Mammalian lipoxygenases and their biological relevance, *Biochim Biophys Acta* 1851, 308-330.
- [13] Bryant, R. W., Bailey, J. M., Schewe, T., and Rapoport, S. M. (1982) Positional specificity of a reticulocyte lipoxygenase. Conversion of arachidonic acid to 15-S-hydroperoxy-eicosatetraenoic acid, *J Biol Chem* 257, 6050-6055.
- [14] Kuhn, H., Wiesner, R., Schewe, T., and Rapoport, S. M. (1983) Reticulocyte lipoxygenase exhibits both n-6 and n-9 activities, *Febs Lett* 153, 353-356.
- [15] Perry, S. C., Horn, T., Tourdot, B. E., Yamaguchi, A., Kalyanaraman, C., Conrad, W. S., Akinkugbe, O., Holinstat, M., Jacobson, M. P., and Holman, T. R. (2020) Role of Human 15-Lipoxygenase-2 in the Biosynthesis of the Lipoxin Intermediate, 5S,15S-diHpETE, Implicated with the Altered Positional Specificity of Human 15-Lipoxygenase-1, *Biochemistry* 59, 4118-4130.
- [16] Kutzner, L., Goloshchapova, K., Rund, K. M., Jubermann, M., Blum, M., Rothe, M., Kirsch, S. F., Schunck, W. H., Kuhn, H., and Schebb, N. H. (2020) Human lipoxygenase isoforms form complex patterns of double and triple oxygenated compounds from eicosapentaenoic acid, *Biochim Biophys Acta Mol Cell Biol Lipids* 1865, 158806.
- [17] Perry, S. C., Kalyanaraman, C., Tourdot, B. E., Conrad, W. S., Akinkugbe, O., Freedman, J. C., Holinstat, M., Jacobson, M. P., and Holman, T. R. (2020) 15-Lipoxygenase-1 biosynthesis of 7S,14S-diHDHA implicates 15-lipoxygenase-2 in biosynthesis of resolvin D5, *J Lipid Res* 61, 1087-1103.
- [18] Libreros, S., Shay, A. E., Nshimiyimana, R., Fichtner, D., Martin, M. J., Wourms, N., and Serhan, C. N. (2020) A New E-Series Resolvin: RvE4 Stereochemistry and Function in Efferocytosis of Inflammation-Resolution, *Front Immunol* 11, 631319.
- [19] Hong, S., Gronert, K., Devchand, P. R., Moussignac, R. L., and Serhan, C. N. (2003) Novel docosatrienes and 17S-resolvins generated from docosahexaenoic acid in murine brain, human blood, and glial cells. Autacoids in anti-inflammation, *J Biol Chem* 278, 14677-14687.
- [20] Green, F. A. (1990) Transformations of 5-HETE by activated keratinocyte 15-lipoxygenase and the activation mechanism, *Lipids* 25, 618-623.
- [21] Green, A. R., Barbour, S., Horn, T., Carlos, J., Raskatov, J. A., and Holman, T. R. (2016) Strict Regiospecificity of Human Epithelial 15-Lipoxygenase-2 Delineates Its Transcellular Synthesis Potential, *Biochemistry* 55, 2832-2840.

- [22] Ivanov, I., Kuhn, H., and Heydeck, D. (2015) Structural and functional biology of arachidonic acid 15-lipoxygenase-1 (ALOX15), *Gene* 573, 1-32.
- [23] Gan, Q.-F., Browner, M. F., Sloane, D. L., and Sigal, E. (1996) Defining the arachidonic acid binding site of human 15-lipoxygenase, *J. Biol. Chem.* 271, 25412 - 25418.
- [24] Sloane, D., Leung, R., Barnett, J., Craik, C., and Sigal, E. (1995) Conversion of Human 15-Lipoxygenase to an Efficient 12-Lipoxygenase - The Side-Chain Geometry of Amino Acids 417 and 418 Determine Positional Specificity, *Prot Eng* 8, 275-282.
- [25] Sloane, D. L., Leung, R., Barnett, J., Craik, C. S., and Sigal, E. (1995) Conversion of Human 15-Lipoxygenase to an Efficient 12-Lipoxygenase - The Side-Chain Geometry of Amino Acids 417 and 418 Determine Positional Specificity, *Prot. Eng.* 8, 275-282.
- [26] Sloane, D. L., and Sigal, E. (1994) On the positional specificity of 15-lipoxygenase, *Ann NY Acad Sci* 744, 99-106.
- [27] Borngraber, S., Kuban, R. J., Anton, M., and Kuhn, H. (1996) Phenylalanine 353 is a primary determinant for the positional specificity of mammalian 15-lipoxygenases, *J Mol Biol* 264, 1145-1153.
- [28] Borngraber, S., Browner, M., Gillmor, S., Gerth, C., Anton, M., Fletterick, R., and Kuhn, H. (1999) Shape and specificity in mammalian 15-lipoxygenase active site - The functional, interplay of sequence determinants for the reaction specificity, *J. Biol. Chem.* 274, 37345-37350.
- [29] Kuhn, H. (2000) Structural basis for the positional specificity of lipoxygenases, *Prostaglandins & other lipid mediators* 62, 255-270.
- [30] Walther, M., Ivanov, I., Myagkova, G., and Kuhn, H. (2001) Alterations of lipoxygenase specificity by targeted substrate modification and site-directed mutagenesis, *Chem Biol* 8, 779-790.
- [31] Vogel, R., Jansen, C., Roffeis, J., Reddanna, P., Forsell, P., Claesson, H. E., Kuhn, H., and Walther, M. (2010) Applicability of the triad concept for the positional specificity of mammalian lipoxygenases, *J Biol Chem* 285, 5369-5376.
- [32] Snodgrass, R. G., and Brune, B. (2019) Regulation and Functions of 15-Lipoxygenases in Human Macrophages, *Front Pharmacol* 10, 719.
- [33] Vasquez-Martinez, Y., Ohri, R. V., Kenyon, V., Holman, T. R., and Sepulveda-Boza, S. (2007) Structure-activity relationship studies of flavonoids as potent inhibitors

of human platelet 12-hLO, reticulocyte 15-hLO-1, and prostate epithelial 15-hLO-2, *Bioorganic & Medicinal Chemistry* 15, 7408-7425.

[34] Amagata, T., Whitman, S., Johnson, T. A., Stessman, C. C., Loo, C. P., Lobkovsky, E., Clardy, J., Crews, P., and Holman, T. R. (2003) Exploring sponge-derived terpenoids for their potency and selectivity against 12-human, 15-human, and 15-soybean lipoxygenases, *J Nat Prod* 66, 230-235.

[35] Robinson, S. J., Hoobler, E. K., Riener, M., Loveridge, S. T., Tenney, K., Valeriote, F. A., Holman, T. R., and Crews, P. (2009) Using enzyme assays to evaluate the structure and bioactivity of sponge-derived meroterpenes, *Journal of Natural Products* 72, 1857-1863.

[36] Perry, S. C., Kalyanaraman, C., Tourdot, B. E., Conrad, W. S., Akinkugbe, O., Freedman, J. C., Holinstat, M., Jacobson, M. P., and Holman, T. R. (2020) 15-Lipoxygenase-1 biosynthesis of 7S,14S-diHDHA implicates 15-Lipoxygenase-2 in biosynthesis of resolvin D5, *J Lipid Res*.

[37] Maas, R. L., and Brash, A. R. (1983) Evidence for a lipoxygenase mechanism in the biosynthesis of epoxide and dihydroxy leukotrienes from 15(S)-hydroperoxyicosatetraenoic acid by human platelets and porcine leukocytes, *Proc Natl Acad Sci U S A* 80, 2884-2888.

[38] Serhan, C. N., Dalli, J., Karamnov, S., Choi, A., Park, C. K., Xu, Z. Z., Ji, R. R., Zhu, M., and Petasis, N. A. (2012) Macrophage proresolving mediator maresin 1 stimulates tissue regeneration and controls pain, *Faseb Journal* 26, 1755-1765.

[39] Butovich, I. A. (2006) A one-step method of 10,17-dihydro(pero)xydocosahexa-4Z,7Z,11E,13Z,15E,19Z-enoic acid synthesis by soybean lipoxygenase, *J Lipid Res* 47, 854-863.

[40] Green, A. R., Freedman, C., Tena, J., Tourdot, B. E., Liu, B., Holinstat, M., and Holman, T. R. (2018) 5 S,15 S-Dihydroperoxyeicosatetraenoic Acid (5,15-diHpETE) as a Lipoxin Intermediate: Reactivity and Kinetics with Human Leukocyte 5-Lipoxygenase, Platelet 12-Lipoxygenase, and Reticulocyte 15-Lipoxygenase-1, *Biochemistry* 57, 6726-6734.

[41] Banaszak, L., Winter, N., Xu, Z., Bernlohr, D. A., Cowan, S., and Jones, T. A. (1994) Lipid-binding proteins: a family of fatty acid and retinoid transport proteins, *Adv Protein Chem* 45, 89-151.

[42] Wecksler, A. T., Kenyon, V., Deschamps, J. D., and Holman, T. R. (2008) Substrate specificity changes for human reticulocyte and epithelial 15-lipoxygenases reveal allosteric product regulation, *Biochemistry* 47, 7364-7375.

- [43] Minor, W., Steczko, J., Boguslaw, S., Otwinowski, Z., Bolin, J. T., Walter, R., and Axelrod, B. (1996) Crystal Structure of Soybean Lipoxygenase L-1 at 1.4 Å Resolution, *Biochemistry* 35, 10687-10701.
- [44] Prigge, S. T., Boyington, J. C., Gaffney, B. J., and Amzel, L. M. (1996) Structure Conservation in Lipoxygenases - Structural Analysis of Soybean Lipoxygenase-1 and Modeling of Human Lipoxygenases, *Proteins* 24, 275-291.
- [45] Chen, X. S., and Funk, C. D. (1993) Structure-function properties of human platelet 12-lipoxygenase: chimeric enzyme and in vitro mutagenesis studies, *FASEB J* 7, 694-701.
- [46] Kutzner, L., Goloshchapova, K., Heydeck, D., Stehling, S., Kuhn, H., and Schebb, N. H. (2017) Mammalian ALOX15 orthologs exhibit pronounced dual positional specificity with docosahexaenoic acid, *Biochim Biophys Acta Mol Cell Biol Lipids* 1862, 666-675.
- [47] Freedman, C., Tran, A., Tourdot, B. E., Kalyanaraman, C., Perry, S., Holinstat, M., Jacobson, M. P., and Holman, T. R. (2020) Biosynthesis of the Maresin Intermediate, 13S,14S-Epoxy-DHA, by Human 15-Lipoxygenase and 12-Lipoxygenase and Its Regulation through Negative Allosteric Modulators, *Biochemistry* 59, 1832-1844.
- [48] Tsai, W. C., Gilbert, N. C., Ohler, A., Armstrong, M., Perry, S., Kalyanaraman, C., Yasgar, A., Rai, G., Simeonov, A., Jadhav, A., Standley, M., Lee, H. W., Crews, P., Iavarone, A. T., Jacobson, M. P., Neau, D. B., Offenbacher, A. R., Newcomer, M., and Holman, T. R. (2021) Kinetic and structural investigations of novel inhibitors of human epithelial 15-lipoxygenase-2, *Bioorg Med Chem* 46, 116349.
- [49] Saam, J., Ivanov, I., Walther, M., Holzhutter, H. G., and Kuhn, H. (2007) Molecular dioxygen enters the active site of 12/15-lipoxygenase via dynamic oxygen access channels, *Proc Natl Acad Sci U S A* 104, 13319-13324.
- [50] Knapp, M. J., and Klinman, J. P. (2003) Kinetic Studies of Oxygen Reactivity in Soybean Lipoxygenase-1, *Biochemistry* 42, 11466-11475.
- [51] Collazo, L., and Klinman, J. P. (2016) Control of the Position of Oxygen Delivery in Soybean Lipoxygenase-1 by Amino Acid Side Chains within a Gas Migration Channel, *J Biol Chem* 291, 9052-9059.
- [52] Morita, E., Schroder, J. M., and Christophers, E. (1990) Identification of a novel and highly potent eosinophil chemotactic lipid in human eosinophils treated with arachidonic acid, *J Immunol* 144, 1893-1900.

[53] Turk, J., Maas, R. L., Brash, A. R., Roberts, L. J., 2nd, and Oates, J. A. (1982) Arachidonic acid 15-lipoxygenase products from human eosinophils, *J Biol Chem* 257, 7068-7076.

[54] Mainka, M., George, S., Angioni, C., Ebert, R., Goebel, T., Kampschulte, N., Krommes, A., Weigert, A., Thomas, D., Schebb, N. H., Steinhilber, D., and Kahnt, A. S. (2022) On the biosynthesis of specialized pro-resolving mediators in human neutrophils and the influence of cell integrity, *Biochim Biophys Acta Mol Cell Biol Lipids* 1867, 159093.